Insights into the function of NWMN_0364/Pvr of *Staphylococcus aureus,* revealing a virulence regulatory protein

Von der Fakultät für Lebenswissenschaften

der Technischen Universität Carolo-Wilhelmina zu Braunschweig

zur Erlangung des Grades

einer Doktorin der Naturwissenschaften

(Dr. rer. nat.)

genehmigte

D i s s e r t a t i o n

von Julia Bosselmann
aus Recklinghausen

1. Referentin: Prof. Dr. Susanne Engelmann
2. Referent: Prof. Dr. Wulf Blankenfeldt
eingereicht am: 26.01.2021
mündliche Prüfung (Disputation) am: 27.07.2021

Druckjahr 2021

Vorveröffentlichungen der Dissertation

Teilergebnisse aus dieser Arbeit wurden mit Genehmigung der Fakultät für Lebenswissenschaften, vertreten durch die Mentorin der Arbeit, in folgenden Beiträgen vorab veröffentlicht:

Tagungsbeiträge

Bosselmann J., Kucklick M. & Engelmann S.: Functional characterization of a lipid anchored protein in *Staphylococcus aureus* (Poster). Jahrestagung der Vereinigung für Allgemeine und Angewandte Mikrobiologie (VAAM), Wolfsburg (2018).

Bosselmann J., Kucklick M. & Engelmann S.: Functional characterization of a lipid anchored protein in *Staphylococcus aureus* (Talk). Jahrestagung der Vereinigung für Allgemeine und Angewandte Mikrobiologie (VAAM), Mainz (2019).

Bosselmann J., Kucklick M., Ihling C., Sinz A. & Engelmann S.: Identification of NWMN_0364, a novel virulence regulatory protein relevant for SaeRS activation in *Staphylococcus aureus* (Talk). Jahrestagung der Vereinigung für Allgemeine und Angewandte Mikrobiologie (VAAM), Leipzig (2020).

Der traurigste Aspekt derzeit ist, dass die Wissenschaft schneller Wissen sammelt, als die Gesellschaft Weisheit.

Isaac Asimov

Content

Tables

Figures

Abbreviations

Agr	Assessory gen regulator
bp	base pair
CDI	1,1′-carbonyldiimidazole
CFU	Colony forming unit
ddH_2O	double-distilled water
DNA	Deoxyribonucleic acid
DTT	Dithiothreitol
dNTP	desoxyribonucleotide triphosphate
DSBU	disuccinimidyl dibutyric urea
EDTA	Ethylenediaminetetraacetic acid
FDR	false discovery rate
GFP	Green Fluorescent Protein
GTP	guanosine triphosphate
IgG	Immunoglobulin G
IPTG	Isopropyl β- d-1-thiogalactopyranoside
kDa	kilo Dalton
LB	lysogenic broth
MOI	multiplicity of infection
MRSA	Methicillin resistant Staphylococcus aureus
MSSA	Methicillin sensitive Staphylococcus aureus
OD	optical density
PBS	phosphate buffered saline
PCR	Polymerase chain reaction
RNA	Ribonucleic acid
rpm	revolution per min
RR	Response Regulator
RSD	relative standard deviation
RT	room temperature

SA medium	Staphylococcal synthetic medium
SaeRS	*S. aureus* exoprotein expression system
SK	Sensor Kinase
TCS	two component system
TLR2	Toll Like Receptor 2
TSB	Tryptic soy broth
v/v	volume per volume
v/w	volume per weight
w/w	weight per weight
X-Gal	5-Bromo-4-chloro-3-indolyl β-D-galactopyranoside
XL-MS	chemical cross-linking mass spectrometry

Summary

Staphylococcus aureus is a human commensal bacterium whose lifestyle can become pathogenic, especially in immunocompromised patients, which can lead to skin infections, pneumonia, endocarditis, etc. Additionally, the ability of *S. aureus* to form biofilms and the increasing incidence of antibiotic resistant variants cause serious problems not only in hospitals. Therefore, it is essential to understand its adaptation to and interaction with the human host and its immune system.

The function of the hypothetical protein NWMN_0364 was totally unclear at the beginning of this study. This protein is composed of four domains: a signal sequence and a lipobox required for transport and membrane anchoring as well as two PepSY domains (N- and C-terminal) dominating the structure of the protein and probably influencing its function. In order to get more insights into the matter of virulence, a deletion mutant of NWMN_0364 in the *S. aureus* Newman strain was tested for its virulence ability by means of an infection assay, where human macrophages were infected with Newman wild type or mutant strain. Here, the results showed that the mutant strain was only able to kill 60% of all macrophages, while the wild type was able to kill about 95%. In order to find the reason for the reduced virulence, extracellular proteins of both strains were examined with a proteomic approach. This method revealed that many virulence factors regulated by the two-component system SaeRS were reduced in the deletion mutant. SaeRS is one of the major virulence regulatory systems in *S. aureus*. It directly controls the expression of more than 25 virulence factors. Moreover, SaeP, the negative regulator of SaeRS, was also less abundant in the mutant. The connection of NWMN_0364 to SaeRS is verified by transcriptional analyses that reveal significantly reduced transcript levels of the *sae* operon, which encodes proteins of the SaeRS system as well as of SaeR-regulated genes in the Δ*0364* mutant. In order to exclude strain-specific effects, the transcriptional analyses were also performed for the wild type and mutant in the *S. aureus* COL strain. The experiment shows similar results compared to the Newman strain. Interestingly, a co-immunoprecipitation experiment *in vivo* gives first hints about an interaction between NWMN_0364 and SaeP. Using recombinant proteins of SaeP and NWMN_0364, a direct interaction between both proteins is verified under *in vitro* conditions. Additionally, cross-linking experiments reveal that only the C-terminal PepSY domain of NWMN_0364 interacts with SaeP. Nevertheless, a second proteome analysis in synthetical medium reveals that many additional proteins significantly changed in the mutant strain, which cannot be explained by an effect of NWMN_0364 on the SaeRS system. The reduced WalHI proteins in particular, which belong to the WalKR two-component

system that is important for cell wall biosynthesis, and the reduced WalKR-regulated proteins indicate an effect on the WalKR system in the mutant strain. Additionally, the interaction assays reveal a possible interaction partner of NWMN_0364 among substrate binding proteins of ABC transporter. So far, these indications of a connection of NWMN_0364 to a cell wall effect have not been confirmed in other experiments.

Subsequently, a hypothesis of the function of NWMN_0364 was created based on the experimental results of this study. NWMN_0364 is important for virulence activation by binding to SaeP and thereby activating the SaeRS system, and maybe has additional functions connected to the cell wall. Based on these findings, the protein NWMN_0364 was renamed into “PepSY containing, virulence regulating protein” (Pvr).

Zusammenfassung

Staphylococcus aureus ist ein Kommensalbakterium des Menschen, dessen Lebensstil insbesondere bei immungeschwächten Patienten zur Pathogenität wechseln kann und dann zu Hautinfektionen, Pneumonien, Endokarditis usw führt. Zudem verursacht die Fähigkeit von *S. aureus* Biofilme zu bilden und das zunehmende Vorkommen antibiotikaresistenter Varianten schwerwiegende Probleme nicht nur in Krankenhäusern. Daher ist es wichtig, die Anpassung an und die Interaktion des Bakteriums mit dem menschlichen Wirt und seinem Immunsystem zu verstehen.

Die Funktion des hypothetischen Proteins NWMN_0364 war zu Beginn dieser Studie völlig unbekannt. Dieses Protein besteht aus vier Domänen: Signalsequenz und Lipobox sind für den Transport und die Membranverankerung erforderlich, während zwei PepSY-Domänen (N- und C-terminal) die Struktur des Proteins dominieren und wahrscheinlich dessen Funktion beeinflussen. Es gab nur Hinweise, die auf eine Zellwand oder Virulenzfunktion hinwiesen. Um mehr Einblicke in die Frage der Virulenz zu erhalten, wurde eine Deletionsmutante von NWMN_0364 im Newman Stamm mit Hilfe eines Infektionsassay auf ihre Virulenzfähigkeit getestet. Hierbei wurden menschliche Makrophagen mit dem Newman Wildtyp- oder Mutantenstamm infiziert. Hier zeigten die Ergebnisse, dass der Mutantenstamm nur 60% aller Makrophagen abtöten konnte, während der Wild Typ etwa 95% abtötete. Um den Grund für die verringerte Virulenz zu finden, wurden extrazelluläre Proteine beider Stämme mit einem proteomischen Ansatz untersucht. Diese Methode ergab, dass viele Virulenzfaktoren, die durch das Zweikomponentensystem SaeRS reguliert werden, in der Deletionsmutante reduziert waren. SaeRS ist eines der wichtigsten Virulenzregulationssysteme bei *S. aureus*. Es steuert direkt die Expression von mehr als 25 Virulenzfaktoren. Darüber hinaus war SaeP, der negative Regulator von SaeRS, auch weniger abundant in der Mutante. Diese mögliche Verbindung von NWMN_0364 mit SaeRS wurde durch Transkriptionsanalysen verifiziert, die signifikant reduzierte Transkriptionsniveaus des *sae*-Operons, welches Proteine des SaeRS-Systems codiert, sowie von SaeR-regulierten Genen in der Δ*0364*-Mutante zeigten. Zusätzlich wurden die Transkriptionsanalysen auch für den Wild Typ und die Mutante im *S. aureus* COL-Stamm durchgeführt, um stammspezifische Effekte auszuschließen. Die Ergebnisse zeigten ein ähnliches Verhalten im Vergleich zu dem zuvor verwendeten Newman-Stamm. Interessanterweise ergab ein Co-Immunpräzipitationsexperiment *in vivo* Hinweise auf eine Interaktion zwischen NWMN_0364 und SaeP. Um diese Interaktion zu bestätigen, wurden rekombinante Proteine von SaeP und NWMN_0364 verwendet, die *in vitro* eine Interaktion

zeigten. Unter Verwendung von Cross-linkingexperimenten zeigte NWMN_0364, dass es hauptsächlich mit der C-terminale PepSY-Domäne an SaeP bindet.

Eine zweite Proteomanalyse in synthetischem Medium ergab jedoch, dass sich viele zusätzliche Proteine im Mutantenstamm signifikant verändert haben, was nicht durch eine Wirkung von NWMN_0364 auf das SaeRS-System erklärt werden kann. Insbesondere die reduzierten WalHI-Proteine, die zum WalKR-Zweikomponentensystem gehören, das für die Zellwandbiosynthese wichtig ist, und die reduzierten WalKR-regulierten Proteine zeigten eine mögliche Wirkung auf das WalKR-Systems im Mutantenstamm. Zusätzlich zeigten die Interaktionsasssays einen möglichen Interaktionspartner von NWMN_0364 unter den Substratbindungsproteinen der ABC-Transporter. Bisher wurden diese Hinweise auf eine Verbindung von NWMN_0364 mit einem Zellwandeffekt in anderen Experimenten nicht bestätigt.

Zusammengenommen wurde eine Hypothese der Funktion von NWMN_0364 basierend auf den experimentellen Ergebnissen dieser Studie erstellt. NWMN_0364 ist wichtig für die Virulenzaktivierung durch Bindung an SaeP und damit Aktivierung des SaeRS-Systems und hat möglicherweise zusätzliche Funktionen, die mit der Zellwand zusammenhängen. Basierend auf diesen Befunden wurde das Protein NWMN_0364 in „PepSY containing, virulence regulating protein“ (Pvr) umbenannt.

1 Introduction

1.1 *Staphylococcus aureus*

Staphylococci first appeared in history when Alexander Ogston isolated the bacteria from a wound infection in 1880 and named it *Staphylococcus* two years later [1] [2]. The name *Staphylococcus aureus* was then introduced in 1884, when Rosenbach separated the genus into *aureus* and *albus.* Later on, different species were separated from *Staphylococcus aureus* based on various criteria, like the coagulase test which came up in 1939 [3] [4]. Nowadays, *S. aureus* is characterised as a Gram-positive coccoid bacterium with a G+C content of about 30–40%. It is a facultative anaerobic bacterium, meaning it can use oxygen or alternative electron acceptors for respiration, but it can also ferment carbohydrates in absence of electron acceptors. Additionally, it possesses a broad-ranged metabolism including the glycolytic pathway, the pentose phosphate pathway, and the tricarboxylic acid (TCA) cycle. The intermediates of these three pathways are needed to synthesise all macromolecules necessary in a cell, giving the bacterium high flexibility. Glucose is the carbon source of choice, but in its absence, *S. aureus* is able to use a variety of other carbon sources like glycerol, lactose, sucrose, or mannitol. It possesses 15 phosphotransferase systems (PTS) to import carbohydrates into the cell. All these metabolic possibilities enable the bacterium to adapt to different environmental niches. In addition, it can persist extreme situations like dryness, pH fluctuations, or high salt concentrations of about 7–10% [5] [6]. All these metabolic possibilities and resistances allow *S. aureus* to survive and replicate in its natural habitat, the human body, at different sites.

1.2 Colonisation and Infection

S. aureus colonises the human body but also a variety of animal species. In humans, the prioritised habitats of *S. aureus* are the anterior nares. Here, it can live as a commensal bacterium without harming its host. Up to 80% of the human population can be carrier of this bacterium. In this context, 15–20% are persistent carriers while the other 60% only occasionally carry *S. aureus* [7] [8] [9]. However, *S. aureus* also is the cause of a variety of infections, and the commensal colonisation can be a risk to develop an infection. Nevertheless, patients with infections from its own colonisation strain show significantly lower mortality rates [10] [11].

There is a wide variation in diseases that are caused by *S. aureus*. The most common diseases are skin and soft tissue infections. Furthermore, bone infections including osteomyelitis, pulmonary infections like pneumonia, blood stream infections, and infective endocarditis can be caused by *S. aureus*. Last but not least, it can also cause toxin-mediated diseases. In this case, the secreted toxins, like the TSST-1 and other superantigens, trigger T-cells proliferation, leading to an extreme overproduction of pro-inflammatory cytokines, which results in symptoms like high fever, hypotension, and even organ failure. These toxins act systemically even if the bacteria reside at the site of infection. Indeed, the bacteria do not even need to be inside the body itself. The toxin can be ingested orally due to food poisoning [12] [13].

S. aureus has also developed resistances against the most common antibiotics used for infection treatment. Already in the 1940s, a few years after the introduction of penicillin, resistant strains were isolated [14]. The same happened in 1960, when Knox introduced methicillin, which was called BRL 1241 or celbenin at that time, as an effective antibiotic against penicillin-resistant staphylococci. Only one year later, first methicillin-resistant strains were isolated [15] [16]. Nowadays, these strains are called methicillin-resistant *S. aureus* (MRSA). MRSA strains isolated from patients in 2018 possess a wide and diverse range of resistances against antibiotics like erythromycin, vancomycin, ciprofloxacin, tetracycline, gentamycin, and many more [17]. These resistances complicate the treatment of the bacterial infection. Moreover, between 1976 and 2007, the numbers of MRSA strains in Germany increased from 1.4% of all *S. aureus* infections to 20.3%. Since then, the MRSA numbers have been declining, with the lowest abundance at 13.3% in 2018. However, when only invasive infections were considered (isolates from blood and liquor), the MRSA abundance was even lower, with 7.6% in 2018. Here, it was below the European mean which is at 16.9% [17] [18].

1.3 *Staphylococcus aureus* and the Human Immune System

The interplay between *S. aureus* and the human immune system is a complex relationship, and the outcome often depends on the individual immune status. As described before, *S. aureus* mostly colonises the nose or skin without inducing infections. The skin is a strong physical barrier that is not easy to overcome and also displays antimicrobial activity by producing antimicrobial peptides like the human β-defensin 3 [19]. Nevertheless, skin lesions or damages are possibilities for *S. aureus* to enter the human body. Here, it is able to colonise the extracellular matrix. In this context, *S. aureus* surface proteins are important,

like clumping factors A and B, the iron surface determinant A, Fibronectin binding proteins A and B, or the collagen binding protein [20].

As soon as the bacteria enter the human body, they are confronted with the immune system. The immune system can roughly be divided into the innate and the adapted immune system. The innate immune system is the first and unspecific response to the pathogen. In the course of this, the most important cells are neutrophils, dendritic cells, and macrophages, of which tissue resident macrophages drive the initial inflammatory response. Macrophages recognise the bacteria by a variety of pattern recognition receptors. These receptors sense structures of bacteria, like lipoproteins or peptidoglycan. One of the more prominent pattern recognition receptors is the Toll-like receptor 2. Upon binding, the receptor leads to a signalling cascade over MyD88 and finally to the activation of NF-κB. NF-κB is a transcriptional regulator that activates the transcription of many cytokines and chemokines. These are released with the main goal to activate the immune response. In the process, antimicrobial peptides are produced and new immune cells are generated and recruited to the site of infection [21] [22] [23] [24] in order to kill the bacteria. Here, the complement system plays a crucial role by marking the bacteria and guiding the immune cells. This system is composed of many proteins that form a proteolytic cascade starting from the bacterial surface and leading to the cleavage of the complement factors C3 and C5 into C3a, C3b, C5a, and C5b. In the course of this, the b cleavage products bind to the bacterial surface and mark them, while the a products are released and can be sensed by immune cells, like neutrophils or macrophages. Besides, the complement system can also lead to the direct lysis of bacterial cells without recruiting immune cells. This is done by the formation of membrane penetrating pores, called the membrane attack complex [25].

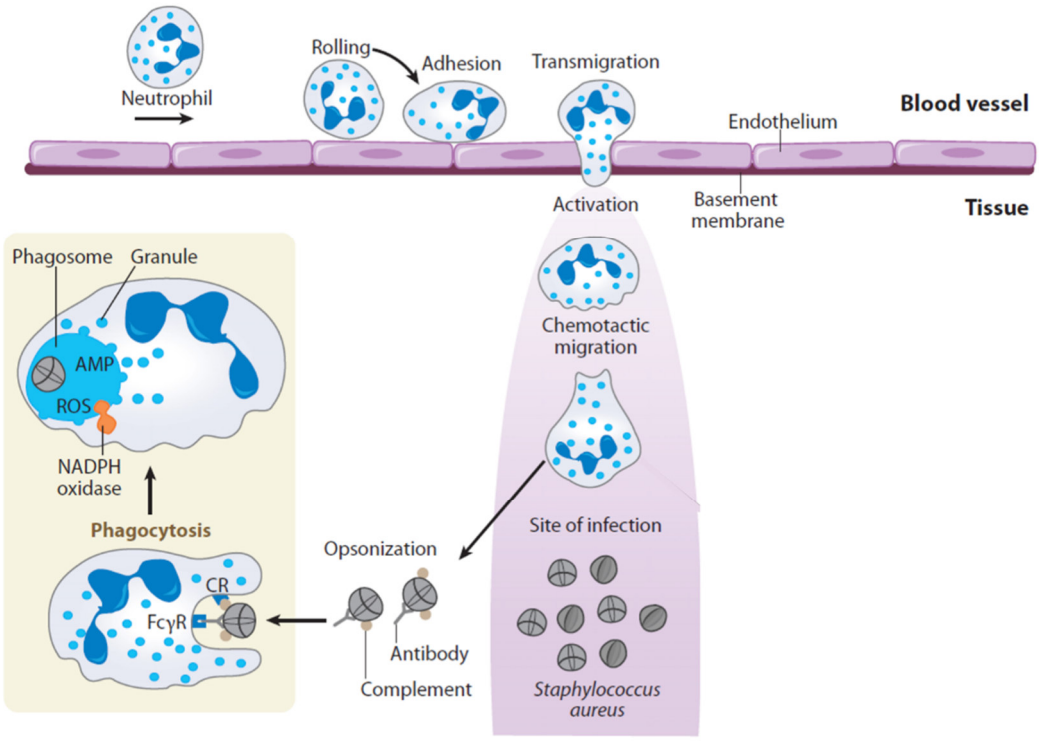

Figure 1 Neutrophil recruitment to the site of infection and phagocytosis.
Neutrophils slow down and adhere to the endothelium in the blood vessel by receptor binding mechanisms. Then, they transmigrate to the site of infection and engulf bacteria marked by antibodies or complement factors. They detect marked bacteria by receptors (CR and FcγR). ROS: reactive oxygen species, AMP: antimicrobial peptides. Adapted from Spaan *et al. [26]*

S. aureus has developed an impressive number of virulence factors to circumvent the immune system. In order to interfere with the complement system, it possesses the chemotaxis inhibitory protein (CHIPS) that binds to the C5a receptors on the immune cells and thus prevents binding of the C5a factors. Moreover, the *Staphylococcus* complement inhibitor (SCIN) blocks the complement system by stabilising the C3 convertase of the proteolytic cascade so that C3b cannot be formed anymore [27] [28]. Another site of action of *S. aureus* virulence factors is the recruitment of immune cells from the blood stream to the site of infection (Fig. 1). Among others, *S. aureus* expresses the staphylococcal superantigen-like 5 that inhibits the PSGL-1 receptor that is needed for neutrophil rolling. This rolling is essential for slowing down the neutrophils before leaving the blood vessel. Additionally, the extracellular adherence protein (Eap) is able to block the ICAM-1 receptor on endothelial cells in the blood vessel. This receptor is essential for neutrophils to leave the blood vessel and enter the infected tissue [29] [30]. Another strategy to undergo the innate immune system is the production of toxins. *S. aureus* produces different types of toxins, such as exfoliative toxins, superantigens, and pore forming toxins. Pore forming toxins are able to integrate into the membrane of diverse cell types, like endothelial cell,

neutrophils, or macrophages, and form pores which consequently lead to cell lysis. Among the pore forming toxins are α-, β-, and γ-haemolysins as well as leukotoxins and phenol-soluble modulins. The most prominent example is the α-haemolysin (Hla). Hla is a monomeric toxin that forms a β-barrel pore in the membrane of macrophages, lymphocyte subpopulations, and erythrocytes by binding to the ADAM10 receptor on the eukaryotic cell surface, and thereby induces cell lysis [31] [32] [33].

Even though *S. aureus* has a wide range of virulence factors affecting the immune system, it is not able to fully suppress the immune system. After reaching the infection site, professional phagocytes, such as neutrophils, macrophages, and dendritic cells, recognise the bacteria by the b cleavage products of the complement system as well as by antibodies, both bound to the bacterial surface. They engulf the bacteria and form phagolysosomes by fusion of the phagosome with the lysosomes. In this phagolysosome, the pathogens are attacked by various mechanisms. First, granule contents are released into the phagolysosome, including antimicrobial peptides and proteolytic enzymes like lysozyme, having bacteriostatic and bactericidal effects. Second, reactive oxygen species (ROS) are produced, such as superoxide and hydrogen peroxide. Hydrogen peroxide can be further processed by the myeloperoxidase to hypochlorous acid. Third, the phagolysosome is acidified by V-ATPases, and lastly, concentrations of divalent metal ions such as Fe^{2+}, Mn^{2+}, or Zn^{2+}, essential for bacterial survival, can be drastically reduced. On the other hand, macrophages are also able to use Cu^{2+} and Zn^{2+} in high concentrations to intoxicate the pathogens in the phagosome [34] [35] [36] [37] [38] [39].

Phagocytosis is a big issue which pathogenic bacteria have to deal with. Thus, *S. aureus* has developed several strategies to evade and survive phagocytosis. In order to undergo the recognition by professional phagocytes, *S. aureus* possesses protein A on the cell surface which is able to bind the Fc part of the human IgG and thus presents these molecules in a wrong orientation on the cell surface. In addition, the superantigen-like 10 or the staphylococcal immunoglobulin G binding protein (Sbi) may also interfere with antibody recognition [40] [41] [42]. In the phagolysosome, the pigment staphyloxanthin is produced, and due to its antioxidant activity, it protects *S. aureus* from ROS. In addition, the catalase is able to convert hydrogen peroxide to water and oxygen. Furthermore, to escape the activity of antimicrobial peptides (AMP), *S. aureus* expresses proteases, like aureolysin, which inactivates AMPs by cleavage as shown for cathelicidin LL-37. *S. aureus* does not only protect itself in the phagolysosome, but it is also able to proliferate in and escape from the phagolysosome by secreting several toxins. For instance, leucocidin AB is expressed in the

phagosome, leading to the appearance of pores in the phagosomal membrane [43] [44] [45] [46].

1.4 Virulence Regulatory Systems of *S. aureus*

A balanced expression of virulence genes when facing the immune system is essential for *S. aureus* to survive in the human host. Therefore, *S. aureus* has evolved a complex virulence regulatory network including several virulence regulators, each regulating virulence factors differentially. In order to facilitate a fine-tuned expression of virulence factors, the virulence regulators cross-regulate each other (Fig. 2). The major virulence regulators are the alternative sigma factor B, the SarA family of DNA binding proteins, and the two-component regulatory systems SaeRS and Agr [47].

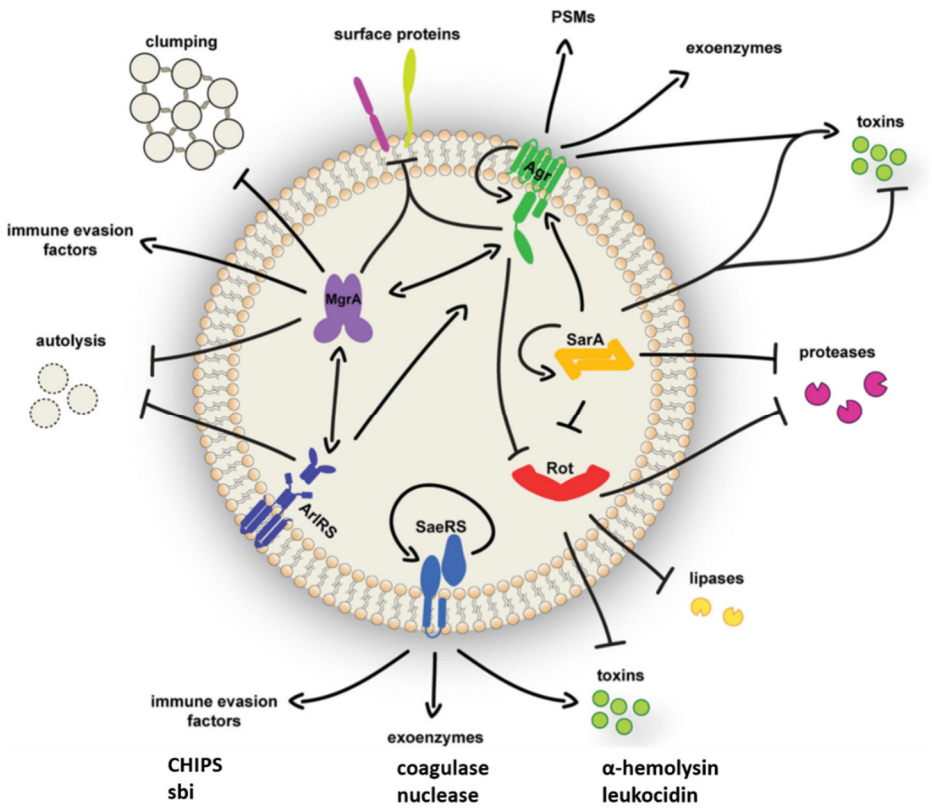

Figure 2 Virulence regulatory network of the six major virulence regulatory systems in *S. aureus*. These are SaeRS, Agr, MgrA, SarA, Rot, ArlRS. The arrows indicate the influence between the regulatory systems and the influence on virulence. Adapted from Jenul and Horswill, 2018 *[47]*

SigB

SigB is an alternative sigma factor that can be activated in diverse stress situations. It binds to the RNA polymerase to direct it to the promoter sequence of specific genes. Consequently, the transcription of these genes is activated. In *S. aureus*, SigB is active in case of alkaline stress, heat shock, and stationary growth [48] [49] [50]. Genes that are regulated by SigB encode proteins having functions in cell envelope composition, membrane transport, and virulence. In addition, SigB negatively influences the expression of toxins and proteases, whereas it positively influences that of cell surface proteins. These effects might be mediated via the Agr quorum sensing system [49] [51]. SigB is highly upregulated upon internalisation into epithelial cells and essential for intracellular replication of *S. aureus*. Moreover, it has been shown that SigB is important for long-term persistence in endothelial cells and for establishing an infection in an osteomyelitis model [52] [53].

SarA family

The Sar family has been identified as a group of DNA-binding proteins of which many are involved in the transcriptional regulation of virulence associated genes; these are SarA, SarR, SarS, SarU, SarV, SarX, SarZ, MgrA, and Rot.

SarA is the most prominent member of this family and influences the expression of extracellular and cell wall-associated proteins. Furthermore, it represses the expression of protein A and proteases, which leads to stabilisation fibronectin binding proteins [54] [55]. SarA regulates virulence gene expression on different levels. First, it possesses a helix-turn-helix motif that is able to bind specific DNA motifs whereby it regulates the transcription of virulence genes. In addition, it also regulates the transcription of virulence regulatory systems like Agr or ArlRS. Second, SarA is able to regulate on the post-transcriptional level by a direct interaction with mRNA. In the process, the mRNA is stabilised, and translational activity is significantly increased [56] [57] [58].

SarR is a SarA homologue and inhibits *sarA* expression by binding to the *sarA* promoter [59].

MgrA (multiple gene regulator) is a global transcriptional regulator that influences the expression of about 355 genes. Among them is a wide range of virulence genes encoding toxins or surface-associated proteins. Moreover, MgrA controls the expression of efflux pumps and autolysins and thus affects antibiotic resistance of *S. aureus*. Like SarA, MgrA positively regulates the expression of the Agr system. Notably, MgrA is able to sense reactive oxygen species. These reactive oxygen species lead to an oxidation of a cysteine residue,

resulting in a release of MgrA from DNA and an expression of antibiotic resistance-related genes [60] [61] [62].

Rot (repressor of toxins) is a SarA homologue that represses the expression of genes coding for toxins and lipases. At the same time, it activates genes encoding cell-surface proteins. It is mainly active during exponential growth and repressed by SarA and Agr during post-exponential growth. Moreover, it has been demonstrated that Rot interacts with SaeR, the response regulator of the SaeRS system. Here, both proteins form a complex that is able to activate the expression of *ssl* (enterotoxin-like toxin) genes [63] [64] [65] [66].

1.5 Two-component Regulatory Systems

Another group of virulence regulators is found among the two-component systems. Bacteria initially developed these two-component systems to adapt to environmental changes, like nutrient limitation, pH fluctuations, oxygen supply, or the presence of antimicrobial peptides. These systems are able to initiate a response, including genetic regulation, after sensing external signals.

These external signals are recognised by a sensor histidine kinase, in most cases an integral membrane protein that owns a cytoplasmic autokinase domain. Upon stimulation, the autokinase domain is phosphorylated on a histidine residue by ATP hydrolysis. Subsequently, the phosphate residue is transferred to an aspartic residue of a response regulator [67] [68]. Response regulators possess DNA-binding domains, and the most common output of an activated two-component system is the genetic regulation of specific genes [69].

The response regulator is the main target of phosphorylation by the sensor kinase, although there are sensor kinases that phosphorylate other targets next to its response regulator. For instance, in *E. coli*, the sensor kinase ArcB phosphorylates σ^s, which is part of the RNA polymerase, and this phosphorylation leads to the proteolysis of σ^s. In addition, ArcB also phosphorylates its response regulator ArcA which then binds to the promoter of many genes, including the σ^s encoding gene, and represses its transcription [70].

The described signalling pathway from signal detection over sensor kinase to response regulator resulting in gene regulation is the classical pathway of a two-component system. Additionally, many variations of this pathway occur among bacteria. For example, the hybrid two-component system has the same signalling way as the classical two-component system, but there is only one protein that fulfils the tasks of both the sensor kinase and the

response regulator. Moreover, a phosphorelay two-component system possesses intermediates that carry the phosphoryl group from the sensor kinase to the response regulator. These intermediates are domains of the sensor kinase or additional proteins, and their number varies between different two-component systems and bacterial species [71] [72].

In most *S. aureus* strains, 16 two-component systems have been identified so far. These two-component systems are important for diverse conditions, like oxygen sensing, cell wall stress, haem sensing, ion transport, or virulence regulation. The most important component systems that are involved in *S. aureus* virulence are Agr, SaeRS, WalKR, ArlRS, and SrrAB.

Agr

The Agr system (accessory gene regulator) is a prominent virulence regulatory system that senses cell density. In most cases, Agr activates the expression of toxins and proteases, while it downregulates surface proteins like protein A. Besides virulence regulation, it also influences metabolic pathways like the carbohydrate and amino acid metabolism. Among all influenced genes upon Agr activation, most are downregulated, but a few are upregulated, like the phenol-soluble modulins and also the *agrBDCA* operon [73].

Agr consist of the proteins AgrA, AgrB, AgrC, and AgrD, which are encoded in one operon *agrBDCA*. AgrA and AgrC form a classical two-component system, in which AgrC is the sensor kinase that phosphorylates the response regulator AgrA upon activation. The main target of AgrA is the gene for RNAIII, which is activated by AgrA. RNAIII is a regulatory RNA that influences gene expression at the post-transcriptional level. It affects the mRNA stability or translational activity of its target genes [74] [75].

Agr senses cell density via extracellular concentrations of an autoinducer peptide. *S. aureus* autoinducer peptides are peptides with an average of eight amino acids in length forming a thiolactone macrocycle structure. Autoinducer peptides in *S. aureus* are produced as propeptides encoded by *agrD* that are further processed and transported to the cell surface by AgrB, where the last processing step occurs by the SpsB, a type I signal peptidase, leading to the release of the autoinducer peptide [76] [77] [78].

Furthermore, there is an interplay between Agr and other virulence regulatory proteins. The activation of toxins by Agr is due to an inhibition of the repressor of toxins (Rot) by Agr. Besides, two other virulence-related two-component systems, ArlRS and SrrAB, influence Agr. While ArlRS has positive effects on Agr transcription, SrrAB has a negative effect. Moreover, the alternative sigma factor B also negatively regulates the Agr system. Another

group of transcriptional regulators that affect Agr is the SarA family. Here, the members either have positive effects on Agr activity, like SarA, SarU, SarZ, or MgrA, or they have negative effects, like SarX or SarT [76].

WalKR

A two-component regulatory system that is also connected to virulence is the WalKR system. Besides virulence, it is essential in cell wall stress situations. In 1999, Martin *et al.* first identified it to be an essential two-component system that appeared to be important for cell permeability [79].

WalKR is encoded in an operon consisting of four genes: *walR, walK, walH*, and *walI.* The proteins WalH and WalI are important for the activation of the TCS by binding to the sensor kinase WalK. This is mediated via transmembrane helices. Moreover, WalK possesses four PAS domains which have been described to be important for ligand binding. One ligand is Zn^{2+} that binds to the cytoplasmic PAS domains leading to conformational change of the kinase domain and its activation. The kinase domain is then able to phosphorylate the response regulator WalR, which binds DNA and activates expression of its target genes [80] [81].

WalKR is the only TCS that is essential for growth of *S. aureus* [82]. This system positively regulates the transcription of genes coding for proteins involved in cell wall metabolism, like LytM, IsaA, or AtlA, in protein secretion, like SecD, SecF, or in uptake of amino acids. A WalKR depletion mutant is characterised by a thickened cell wall and defects in cell division. Additionally, the resistance to lysostaphin has increased. This points towards a cell wall effect, as the endopeptidase lysostaphin cleaves the polyglycine bonds in the peptidoglycan layer. Besides, this system affects virulence by inducing biofilm formation and activating the virulence regulatory system SaeRS [83] [84] [85] [86].

1.6 *S. aureus* Exoprotein Expression System (SaeRS)

The *S. aureus* exoprotein expression system (SaeRS) is a two-component system that mainly focuses on virulence gene regulation. This system was first identified by Giraudo *et al.* in 1994, when they screened a transposon library and found a Tn551 mutant with diminished levels of exoproteins. Further analyses showed that it activates expression of toxins like α-haemolysin or leukocidins. However, it is also important for the expression of immune evasion proteins like coagulase, chemotaxis inhibitory protein (CHIPS), or staphylococcal

IgG binding protein (sbi) [87] [88]. The expression of virulence factors by SaeRS is essential for the survival of *S. aureus* in its host and the development of infections. In mouse infection models, SaeRS is important for development of skin infections, osteomyelitis, necrotising pneumonia, and bacteraemia. For the human system, mainly cell line experiments or experiments with primary cells offer information about the relevance of SaeRS. For example, SaeRS is essential for the escape of *S. aureus* from human macrophages [89] [90] [91] [92].

The Sae regulatory system consists of four proteins, SaeS, SaeR, SaeQ, and SaeP, which are encoded in the *sae* operon. The transcription of the *sae* operon is initiated at two distinct promoters, P1 and P3 (Fig. 3). While the initiation at P3 provides a basal transcription of *saeS* and *saeR,* the initiation at the P1 promoter is dependent on SaeR binding and results in the transcription of all four *sae* genes [93].

The sensor kinase SaeS contains two transmembrane helices, a HAMP, and a kinase domain. The two transmembrane domains and a linker peptide of nine amino acids connecting both transmembrane domains are essential for signal perception [94] [95]. There are at least three variants of SaeS in *S. aureus*. The first variant, $SaeS^{SK}$, occurs in the strains MW2, Mu50, and USA600 and has two substitution mutations (N227S and E268K) which do not affect the activity of the protein. The second variant, $SaeS^{SKT}$, has a third substitution in addition to the two described before (S351T), and this is present in the strains ST30 and ST36. With this additional substitution, the activity of SaeS changes the virulence gene expression from highest in the stationary growth phase towards highest during exponential growth [96] [97]. The third polymorphism was identified in the strain Newman and is called $SaeS^{P}$ (L18P). This substitution in the first transmembrane helix leads to a constantly active kinase domain, which in turn leads to a constant expression of virulence factors [98].

SaeR is the response regulator that is phosphorylated by the kinase domain of SaeS (SaeR-P) at position Asp51. This phosphorylation is required for the ability of SaeR to bind to DNA via its C-terminal helix-turn-helix motif. The perfect DNA binding site for SaeR-P is a repetitive nucleotide sequence $GTTAAN_6GTTAA$ which is present in the promoter region of regulated virulence genes, either as a single copy, as found in the promoter region of *hla, hlg*, and *sbi*, or as a double copy, as found in the promoter region of *coa*, *chp*, or *sae*. This facilitates the dose-dependent expression of different genes by SaeR [99] [100] [93] [101].

SaeQ is a membrane protein with three predicted transmembrane domains, and SaeP is a lipoprotein. Both proteins interact with the sensor kinase SaeS and thereby inhibit the signal transduction (Fig. 3). This inhibition is probably due to an activation of the phosphatase activity of SaeS leading to a dephosphorylation of the response regulator SaeR [102]. The negative effect of SaePQ on SaeRS mediated virulence regulation has also been shown in *in vivo* experiments [103].

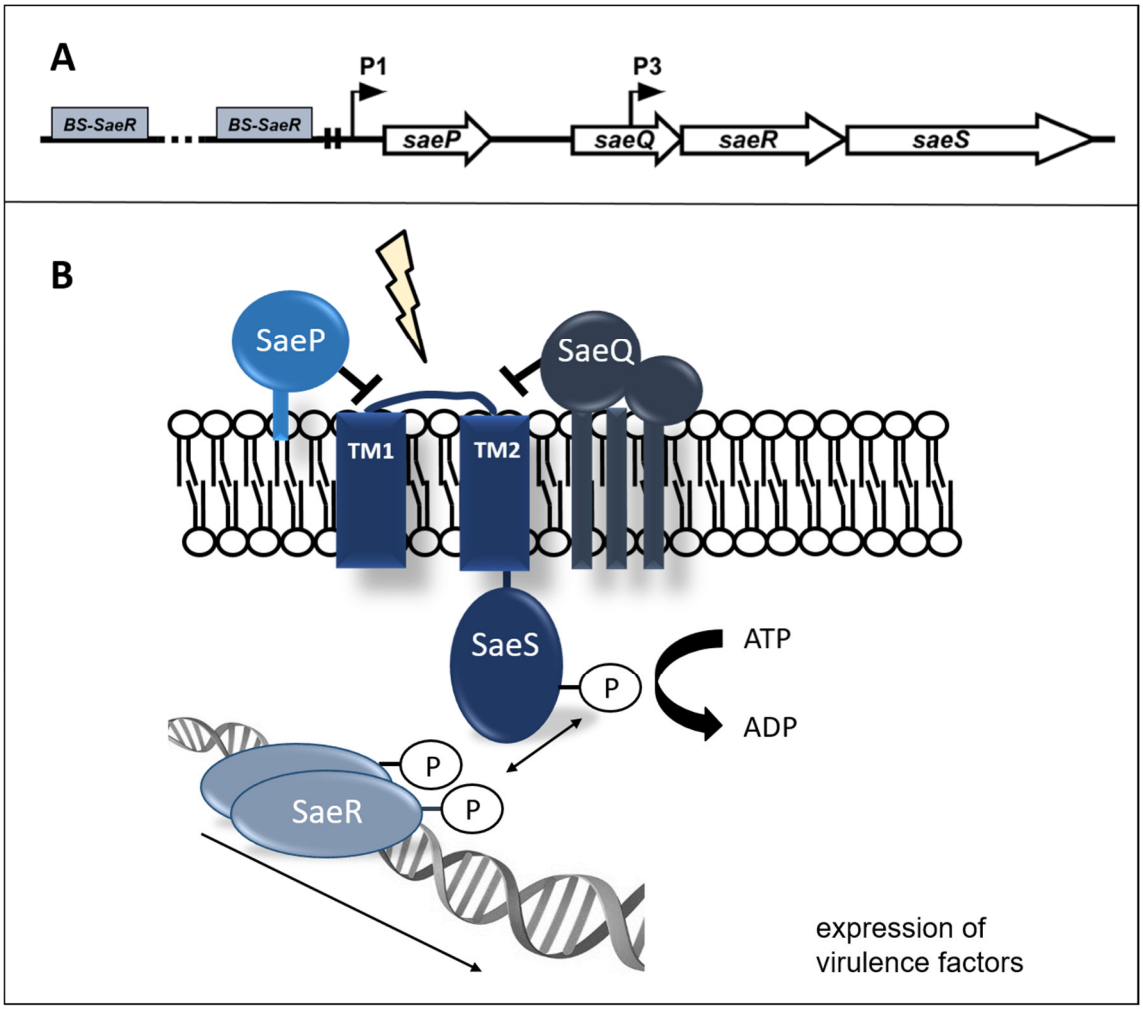

Figure 3: **Overview of the SaeRS system**.
A: *sae* operon with the four genes *saeP, saeQ, saeR,* and *saeS*. P1 and P3 are promoters. BS- SaeR: Binding sites for a phosphorylated SaeR to activate transcription from promoter P1. Adapted from Liu *et al. [95]*.
B: function of the four proteins SaeP, SaeQ, SaeR, and SaeS. The yellow arrow indicates an activation signal, upon which the histidine kinase SaeS is autophosphorylated (P) under ATP hydrolysis. The phosphorylation is transferred to the response regulator SaeR. SaeR binds to DNA and activates gene expression of many virulence factors and also of the *sae* operon. SaeP and SaeQ suppress the kinase activity of SaeS.

There has been great effort to study the signals the SaeRS system responds to. The main signals activating the SaeRS system are human neutrophil peptides 1, 2, and 3 (HNPs), which are antimicrobial and produced by human neutrophils in the phagolysosome. However, the response to HNPs is strain-specific. Whereas, for example, the *S. aureus* strains N315 and USA300 highly respond, the strains *S. aureus* COL and Newman do not respond to HNPs. A further signal for a SaeRS activation is hydrogen peroxide. In contrast, acidic pH or high salt concentrations negatively influence the activity of the SaeRS system. Moreover, the human skin fatty acid cis-6-hexadecenoic acid and also free fatty acids from *S. aureus* membranes inhibit the kinase activity of SaeS. Additional inhibitors are thymol, cerulenin, or flavone [104] [105] [106] [107] [108]. Furthermore, Fe, Cu, and Zn ions are known to suppress the SaeRS system, and Cu^{2+} and Zn^{2+} are able to inhibit the autokinase activity of the SaeS protein [109] [110].

The activity of the SaeRS system depends on the *S. aureus* cell density and nutrient supply. When growing in complex media, *saeRS* expression is increased during post-exponential growth. SaeRS activity is also adapted to nutrient supply via the transcriptional regulator CodY, which is a global transcriptional regulator and senses the concentration of branched-chain amino acids and GTP. The P1 promoter of the *sae* operon possesses a CodY binding site. In the presence of high nutrient availability, CodY binds to P1 and thereby prevents SaeR-P from binding and activating *sae* expression [97] [101] [111].

1.7 Surface-associated proteins

Virulence factors of *S. aureus* are mainly located extracellularly or are surface-associated. In a proteomic study, actually produced proteins of *S. aureus* have been identified that locate extracellularly or are surface-associated. Among them, virulence factors were found, but also proteins that do not have a described function [112]. These proteins without described function have a possibility to also influence the virulence of *S. aureus*, which is particularly true for those whose expressions are known to be regulated by a virulence regulatory system. For SaeRS, it is known that it regulates proteins with unknown function [113], and for SigB it is also known that it regulates proteins without known function. Among the proteins regulated by SigB, there is a surface-associated protein called NWMN_0364 [49]. This protein has an unknown function, but in 2018, it has been described as a putative lipoprotein by Graf *et al.,* and it is genetically conserved in 99% of 123 *S. aureus* genomes [114].

In general, lipoproteins are transported through the cytoplasmic membrane by the Sec translocation pathway to reach their destined localisation on the membrane surface. Here, they are directly connected with fatty acids. For this purpose, they possess a unique recognition sequence, called lipobox, where three conserved amino acids are followed by a cysteine at position +1 [(L/V/I)(A/S/T/G)(G/A)↓C] [115]. The cysteine residue is important for the connection of the protein to the lipid moiety. This lipid moiety is a diacylglyceryl group derived from a phosphatidylglycerol and is connected to the sulfhydryl group of the cysteine at position +1 in the signal sequence. This reaction is catalysed by the apolipoprotein diacylglyceryl transferase (Lgt) (Fig. 4) [116] [117]. In a second reaction, the signal peptide is removed by the activity of the lipoprotein signal peptidase (Lsp), which cleaves between the amino acid at position -1 and the cysteine at +1 [118] [119]. This results in a diacyl lipoprotein. In Gram-negative bacteria, a third enzyme, the apolipoprotein N-acyltransferase (Lnt), modifies the protein by adding a third fatty acid residue to the N-terminal amino group of cysteine to create a triacylated protein. In many Gram-negative bacteria, this is essential for the transfer of lipoproteins from the inner to the outer membrane [120] [121]. In Gram-positive bacteria, lipoproteins are localised at the outside of the cytoplasmic membrane, and for most species, an Lnt homologue is not described [122]. Although this is true for *S. aureus*, studies have demonstrated the existence of a triacyl lipoprotein (SitC). However, this acylated form is only present under certain environmental conditions. High temperatures, acidic pH values, or the stationary growth phase trigger the accumulation of the diacyl lipoprotein, while under neutral pH or during logarithmic growth, the triacylated variant is predominant [123] [124].

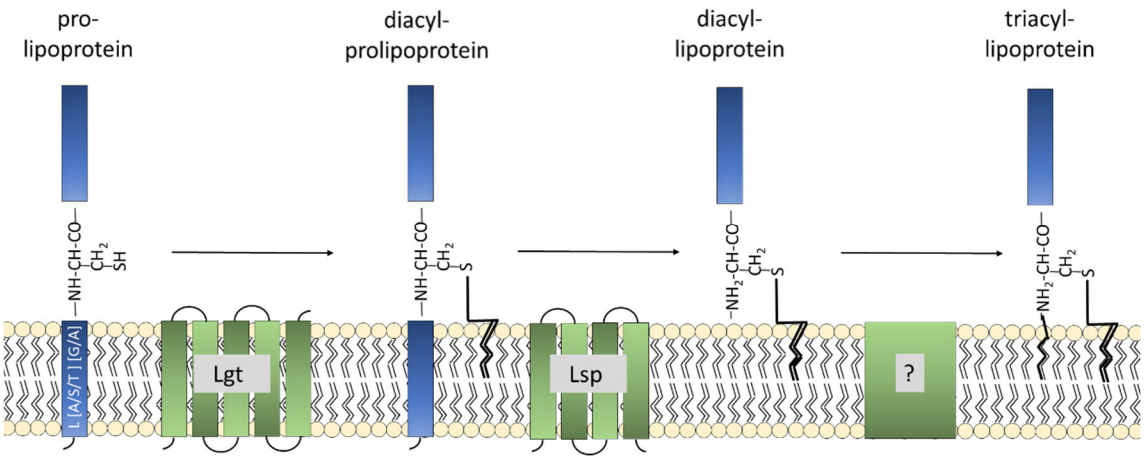

Figure 4: *S. aureus* lipoprotein synthesis
Blue: lipoproteins, green: enzymes involved in synthesis. Lgt recognizes the Lipobox and connects the cysteine with the lipid moiety. Lsp cleaves the signal sequence. In Gram-positive bacteria the enzyme that connects the Nitrogen of the cysteine with a lipid moiety is not known. Adapted from Angelika Gründling *[125]*

Overall, *S. aureus* possesses 70 lipoproteins on average, but the number varies between different strains. 40 proteins are conserved in almost all strains. Most lipoproteins are important for transport. This includes the transport of trace elements like Fe, Mn, Mo, Ni, and Zn, but also the transport of phosphates, amino acids, and peptides. A few other lipoproteins have various functions, but for 30–40% of all lipoproteins, the functions are still unknown, like it is the case for the function of NWMN_0364 [114] [126].

On the one hand, the localisation of NWMN_0364 on the membrane indicates a connection to virulence, and it has already been shown, that lipoproteins are an important trigger for the Toll-like receptor 2, which is present on the surface of immune cells like macrophages. The binding of lipoproteins to the Toll-like receptor 2 leads to a signalling cascade from MyD88 to the activation of the transcriptional regulator NF-κB, which results in an activation of the innate immune system [22] [23] [24]. The lipid moiety of the lipoprotein is essential for the Toll-like receptor 2 binding. In order to detect both diacyl and triacyl lipoproteins, the Toll-like receptor 2 forms complexes with other Toll-like receptors. The combination of the Toll-like receptor 2 and the Toll-like receptor 6 recognises diacyl lipoproteins, while the Toll-like receptor 2 and the Toll-like receptor 1 recognise triacyl lipoproteins [127].

Another hint that the NWMN_0364 function is connected to virulence, next to its localisation and the regulation by SigB, is that this protein is expressed under infective conditions. An unpublished pre-experiment of a mice antibody assay gave first hints that this protein is expressed in mice, as the mice produced an antibody response to NWMN_0364. Furthermore, a study with human patients supports the assumption that NWMN_0364 is expressed under infective conditions, as it showed that an antibody response to NWMN_0364 was observed in humans. This response in humans could be used as a marker to distinguish patients developing a sepsis from those who do not [128]. This promotes a possible connection of NWMN_0364 to virulence.

On the other hand, the localisation of NWMN_0364 indicates a connection to membrane and cell wall functions. Here, it has been shown that the WalKR system, which reacts to cell wall stress and positively regulates cell wall biosynthesis, negatively influences the transcription of *NWMN_0364* [58]. Another hint that connects NWMN_0364 to cell wall functions comes from a small protein called CwrA. This protein is highly upregulated when cell wall biosynthesis is blocked. Moreover, CwrA positively influences the gene transcription of *NWMN_0364* [129].

1.8 Aim of the Study

Finding the function of NWMN_0364 may help to extend the knowledge of the physiology and survival strategies of *S. aureus.* It could lead to more insights into the functions and possibilities of lipoproteins. Here, the functional possibilities that have been indicated by literature regarding cell wall and especially virulence could lead to a better understanding of how *S. aureus* interacts with or survives in the human host when the function of NWMN_0364 could be revealed.

The overall goal of this study was to determine the function of NWMN_0364. In order to achieve this goal, several strategies were designed. Here, the construction of a deletion mutant should be the basis for further analysis concerning the function using phenotypic analyses, like infection assays, and proteome analyses, including the examination of virulence factor accumulation. In addition, the determination of interacting proteins reveals a lot about protein function. Here, a recombinant protein as well as an *in-vivo* expressed protein containing a Strep-tag should be generated and used for interaction assays.

2 Material and Methods

2.1 Chemicals, Equipment and Software

2.1.1 Chemicals

Chemicals used in this study were purchased from Sigma Aldrich, Carl Roth, GE healthcare, Thermo Scientific or as described in Tab. 1.

Table 1 Chemicals used in this study

Name	**Manufacturer**
6x loading dye	Thermo Fisher Scientific (Leon-Rot, DE)
Aqua Phenol	Carl Roth GmbH (Karlsruhe, DE)
BCIP (5-Bromo-4-chloro-3-indolyl phosphate p-toluidine salt	Carl Roth GmbH (Karlsruhe, DE)
Blocking reagent	ROCHE (Mannheim, DE)
Bromphenolblue	Thermo Fisher Scientific (Leon-Rot, DE)
CDI (1,1′-carbonyldiimidazole)	Sigma Aldrich (Darmstadt, DE)
CDP-Star	ROCHE (Mannheim, DE)
Coomassie Brilliant Blue	Carl Roth GmbH (Karlsruhe, DE)
d-desthiobiotin	IBA GmbH (Göttingen, DE)
DIG RNA labeling Mix	ROCHE (Mannheim, DE)
dNTP set	Thermo Fisher Scientific (Leon-Rot, DE)
DSBU (disuccinimidyl dibutyric urea)	Thermo Fisher Scientific (Leon-Rot, DE)
Formamid (deionized)	Carl Roth GmbH (Karlsruhe, DE)
Gene Ruler 1kb	Thermo Fisher Scientific (Leon-Rot, DE)
HABA (2-(4-Hydroxyphenylazo)benzoic acid)	Sigma Aldrich (Darmstadt, DE)
IPTG (Isopropyl-β-D-thiogalactopyranosid)	Carl Roth GmbH (Karlsruhe, DE)
LiCl	Carl Roth GmbH (Karlsruhe, DE)
Methylene blue	Carl Roth GmbH (Karlsruhe, DE)
Na_3-citrate	Carl Roth GmbH (Karlsruhe, DE)
NBT (p-Nitrotetrazoliumblauchlorid)	Carl Roth GmbH (Karlsruhe, DE)
Page Ruler Prestained	Thermo Fisher Scientific (Leon-Rot, DE)
Paraformaldehyde	Carl Roth GmbH (Karlsruhe, DE)

RbCl	Applichem (Darmstadt, DE)
Roti-Gelstain	Carl Roth GmbH (Karlsruhe, DE)
Roti-Nanoquant	Carl Roth GmbH (Karlsruhe, DE)
Sheep blood, defibrinated	Thermo Fisher Scientific (Leon-Rot, DE)
Trichloracetic acid	Carl Roth GmbH (Karlsruhe, DE)
X-Gal	Carl Roth GmbH (Karlsruhe, DE)

2.1.2 Equipment

Equipment used in this study is listed in Tab. 2.

Table 2 Equipment and consumables

Name	**Manufacturer**
Amicon Ultra-4, centrifugal filter	Merck Millipore (Billerica, USA)
Äkta-Purifier	GE Healthcare (Chalfont St. Giles, GB)
Bio-Dot apparatus	BIO-RAD (Hercules, CA, USA)
CL-1000 Ultraviolet crosslinker-UVP	Thermo Fisher Scientific (Leon-Rot, DE)
FastPrep-24	MP Biomedicals (Eschwege, DE)
Genomic DNA Isolation Kit	Norgen (Thorold, Canada)
Gravity flow Strep-Tactin® Sepharose® column	IBA GmbH (Göttingen, DE)
HiLoad 16/60 Superdex 75 prep grade	GE Healthcare (Chalfont St. Giles, GB)
High pure plasmid isolation kit	ROCHE (Mannheim, DE)
Horizon 11.14 - electrophoresis	Thermo Fisher Scientific (Leon-Rot, DE)/ life technologies
LAS3000	Fujifilm (Neuss, DE)
LMW calibration kit	GE Healthcare (Chalfont St. Giles, GB)
LTQ Orbitrap Velos Pro mass spectrometer	Thermo Fisher Scientific (Leon-Rot, DE)
Mini PROTEAN Tetra Cell - electrophoresis	BIO-RAD (Hercules, CA, USA)
nanoAQUITY Ultra Performance Liquid Chromatography System	Waters Corporation (Milford, MA, USA)
NucleoSpin® Gel and PCR Clean-up kit	Machery-Nagel (Düren DE)
PVDF-membrane	Carl Roth GmbH (Karlsruhe, DE)
Ultrospec 2100pro	Biochrom (Cambridge, UK)

Zeta Probe Blotting membrane (nylon)	BIO-RAD (Hercules, CA, USA)
ZipTip Filter	Merck Millipore (Billerica, USA)

2.1.3 Software

Software used in this study is listed in Tab. 3.

Table 3 Software and online tools used in this study

Name	**Manufacturer**
AIDA-Advanced Image Data Analyzer	version 4.15., Raytest Isotopenmeßgeräte GmbH, Straubenhardt DE
GraphPad Prism	GraphPad Software, San Diego, California
LocateP	[130]
MaxQuant	Max Planck Institute of Biochemistry, Martinsried, Germany, www.maxquant.org, version 1.5.2.8
MUSCLE	[131]
Perseus	Max Planck Institute of Biochemistry, Martinsried, Germany, version 1.5.2.6
Pfam	[132]
UniProt	[133]

2.2 Oligonucleotides, Plasmids and Proteins

2.2.1 Enzymes and Proteins

Enzymes and proteins used in this study are described and purchased as listed in Tab. 4.

Table 4 Enzymes and proteins used in this study

Name	**Manufacturer**
Anti-rabbit IgG	Sigma Aldrich (Darmstadt, DE)
Anti-Digoxigenin antibody	ROCHE (Mannheim, DE)
*Bam*HI	Thermo Fisher Scientific (Leon-Rot, DE)
*Bsa*I	Thermo Fisher Scientific (Leon-Rot, DE)
*Dnase*I	Thermo Fisher Scientific (Leon-Rot, DE)

Go Taq G2 DNA polymerase	Promega (Mannheim, DE)
Lysostaphin	Ambi Products LLC (New York, USA)
Phusion Green High-Fidelity DNA Polymerase	Thermo Fisher Scientific (Leon-Rot, DE)
ProteinaseK	Sigma Aldrich (Darmstadt, DE)
Rabbit anti-SACOL0444	Anika Westphal, Greifswald 2013, produced by Pineda (Berlin, DE)
RNasin	Thermo Fisher Scientific (Leon-Rot, DE)
rSAP (shrip alkaline phosphatase)	New England Biolabs (Frankfurt/M, DE)
T4 DNA ligase	Thermo Fisher Scientific (Leon-Rot, DE)
T7 RNA polymerase	Thermo Fisher Scientific (Leon-Rot, DE)
Trypsin sequencing grade	Promega (Mannheim, DE)

2.2.2 Oligonucleotides

Oligonucleotides used in this study were purchased from life technologies / Thermo Fisher Scientific (Leon-Rot, DE) and are described in Tab. 5.

Table 5 oligonucleotides used in this study

Name	Sequence	Description
Construction of pMAD-0364		
P0364-01	GCGGATCCTGACGTTTATGCCGAAATCTACA	Upstream fragment (*BamHI*)
P0364-02	TATGACTAACTGACCATGGTCATGCGTTACTTTCGTTCGT	
P0364-03	TACCATGGTCAGTTAGTCACGTGTTGTGAGGGTTTATTTGC	Downstream fragment (*BamHI*)
P0364-04	GCGGATCCTGCGTTATTCTAAGTAGTACCCC	
Construction of pMAD-0364-strep		
P0364-05	TTATTTTTCGAACTGCGGGTGGCTCCAGTGATCTTGCTCACTCT	*0364-strep*
P0364-06	TGGAGCCACCCGCAGTTCGAAAAATAAAAAGATTCGTTGCATTA	
RNA analysis experiments		
PR_saes-01	GGGCATATCGAACGCCACTTGAGC	*saeS* + T7 RNA polymerase promoter
PR_saes-02	CTAATACGACTCACTATAGGGAGATTGTTGCGCGAGTTCATTAG	
PR_saep-01	GGGCTTTTTAGCAGCTGGTGCTGT	*saeP* + T7 RNA polymerase promoter
PR_saep-02	CTAATACGACTCACTATAGGGAGACGTAGTCAACCATTGCGATT	
PR_hlgc-01	CGTCGAGTGTTTTATGGGGCGTCAA	*hlgC* + T7 RNA polymerase promoter
PR_hlgc-02	CTAATACGACTCACTATAGGGAGAAATGGCATGAGTGACATCCA	

PR_sbi-01	AACATTACGCGAACACCCAGAACGTG	*sbi* + T7 RNA polymerase promoter
PR_sbi-02	CTAATACGACTCACTATAGGGAGATTGGCGCCACTTTCTTT	
Construction of pPR-IBA 1 derivates		
PP_saeP-01	GCCGGTCTCGAATGGGTAATTCTAATTCACAAG	*saeP* without signal sequence
PP_saeP-02	TATGGTCTCGGCGCTTTTTAATTTAGCGCCGC	
PP_0364-01	GCCGGTCTCGAATGGGCAATGATACTCCAAAAGATG	*0364* without signal sequence
PP_0364-02	TATGGTCTCGGCGCTGTGATCTTGCTCACTCTTTAAT	
PP_metQ1-01	GCCGAGGTCTCGAATGGACGACAAGAAAATAAC	*metQ1* without signal sequence
PP_metQ1-02	AATGGTCTCGGCGCTTTTAGCAGGAATAACTGCAC	
PP_tcyA-01	CCTAGGTCTCGAATGGACAAGGAAGCTAGTAAA	*tcyA* without signal sequence
PP_tcyA-02	AATGGTCTCGGCGCTTTTAGATTTAGAAACATCTT	
Plasmid primer		
Iba1-for	TAATACGACTCACTATAGGG	Control primer for pPR-IBA1
Iba1-rev	TAGTTATTGCTCAGCGGTGG	
pMAD-for	CCCAATATAATCATTTATCAACTCTTTTACACTTAAATTTCC	Control primer for pMAD
pMAD-rev	GCAACGCGGGCATCCCGATG	

2.2.3 Plasmids

Plasmids used in this study are listed in Tab. 6.

Table 6 Plasmids used in this study

Plasmid	Description	Reference/Source
Mutant construction		
pMAD	Shuttle vector for allelic replacement	[134]
pMAD-*Δ0364*		This study
pMAD-0364strep		This study
Protein expression in *E. coli*		
pPR-IBA1	*E. coli* expression vector for expression of Strep-tag fusion proteins (C-terminal), Amp^r	IBA GmbH, Göttingen, DE
pPR-IBA1-*0364*		This study
pPR-IBA1-*saeP*		This study

2.3 Organisms and Cultivation

2.3.1 Bacterial strains, Bacteriophages, eukaryotic cell lines

Bacterial strains, phages and eukaryotic cell lines used in this study are listed in Tab. 7.

Table 7 strains used in this study

Strain	Description	Reference/Source
Escherichia coli		
DH5α	F-φ80d*lac*Z Δ(*lac*ZYA-*arg*F) U169 *deo*R*sup*E44Δ*lac*U169 (f80*lac*ZDM15) *hsd*R17 *rec*A1 *end*A1 (rk- mk+) *sup*E44*gyr*A96 *thi*-1 *gyr*A69 *rel*A1	[135]
BL21 (DE3) pLysS	F- *omp*T *hsd*S *gal* (rb- mb+) DE3(Sam7 Δnin5 *lac*UV5-T7 Gen1)	[136]
Staphylococcus aureus		
COL	mec, high-Mc^r clinical isolate	[137]
COL *Δ0444*		
Newman	human clinical isolate	[138]
Newman *Δ0364*		This study
RN4220	Restriction negative strain	[139]
Bacteriophages		
Staphylococcus phage 80		[140]
Eukaryotic cell line		
THP-1		[141]

2.3.2 Antibiotics

Antibiotics used in this study are listed in Tab. 8.

Table 8 Antibiotics used in this study

Antibiotic	Solvent	Concentration	Manufacturer
Ampicillin	ddH_2O	100 µg/mL	Carl Roth GmbH (Karlsruhe, DE)
Chloramphenicol	Ethanol	10 or 20 µg/mL	Sigma Aldrich (Darmstadt, DE)
Erythromycin	Ethanol	10 µg/mL	Carl Roth GmbH (Karlsruhe, DE)
Gentamycin	ddH_2O	150 µg/mL	Carl Roth GmbH (Karlsruhe, DE)

2.3.3 Cultivation

For the general cultivation the following conditions were used. Necessary variations are described for the experiments separately.

Liquid cultures

Escherichia coli was cultivated in LB medium (Lennox, Carl Roth GmbH, Karlsruhe) at 37°C and 120 rpm.

S. aureus was cultivated in LB medium (Lennox, Carl Roth GmbH, Karlsruhe), TSB medium (Oxoid Limited, Basingstoke UK) or Staphylococcal synthetic medium (see 2.3.4). Generally at 37 °C and 120 rpm.

THP-1 cells were cultivated in RPMI 1640 medium (GIBCO/Thermo Scientific, St. Leon-Rot) containing 10% Fetal Bovine Serum (FCS) (GIBCO/Thermo Scientific, St. Leon-Rot) at 37°C and 5% CO_2.

Solid cultures

For the cultivation of bacterial strains on solid media, LB medium was supplemented with 1.5% agar (Carl Roth GmbH, Karlsruhe) and the cultures incubated at 37 °C.

2.3.4 Staphylococcal synthetic medium (SA)

The staphylococcal synthetic medium [142] is a well-defined minimal medium. It was always prepared freshly before usage from the components listed in Tab 9. All components were sterile filtrated except for citrate, glucose and MOPS which were autoclaved at 121°C for 10 min before usage. As a carbon source was either glucose or glycerol used.

Table 9 staphylococcal synthetic medium

Component	Ingredient	Stock concentration	Final concentration
Basal Medium	Na_2HPO_4	20 mM	10 mM
	KH_2PO_4	20 mM	10 mM
	NH_4Cl	18.6 mM	9.34 mM
	NaCl	17.1 mM	8.55 mM
	$MgSO_4$	1.74 mM	0.87 mM

Amino acids	L-Alanine	50 mM	1 mM
	L-Valin	50 mM	1 mM
	L-Leucine	50 mM	1 mM
	L-Isoleucine	50 mM	1 mM
	L-Aspartic acid	50 mM	1 mM
	L-Glutamic acid	50 mM	1 mM
	L-Arginine	50 mM	1 mM
	L-Lysine	50 mM	1 mM
	L-Proline	50 mM	1 mM
	L-Serine	50 mM	1 mM
	L-Threonine	50 mM	1 mM
	L-Cysteine	50 mM	1 mM
	L-Glycine	50 mM	1 mM
	L-Phenylalanine	25 mM	1 mM
	L-Trypthophan	25 mM	1 mM
	L-Histidine	25 mM	1 mM
Citrate	Tri-sodium citrate	1 M	0.14 mM
Vitamins	Cyanocobalamin	0.036 mM	0.036 µM
	4-aminobenzoic acid	0.29 mM	0.29 µM
	Biotin	0.04 mM	0.04 µM
	Nicotinic acid	0.81 mM	0.81 µM
	Ca-D-pantothenic acid	0.21 mM	0.21 µM
	Pyridoxamine dihydrochloride	0.62 mM	0.62 µM
	Thiamine chloride hydrochloride	0.29 mM	0.29 µM
	Riboflavine	0.26 mM	0.26 µM
Trace elements	$ZnCl_2$	0.51 mM	0.51 µM
	$MnCl_2$	0.5 mM	0.5 µM
	H_3BO_4	0.097 mM	0.097 µM
	$CoCl_2$	1.46 mM	1.46 µM
	$CuCl_2$	0.015 mM	0.015 µM
	$NiCl_2$	0.1 mM	0.1 µM
	Na_2MoO_4	0.148 mM	0.148 µM
	$FeCl_3$	0.83 mM	1.24 µM

Buffer	MOPS	1 M	40 mM
Carbon source	Glucose	20%	0.148% (8.2 mM)
	Glycerol	86%	0.150% (16.4 mM)

Glycerol stocks

Bacteria were grown in LB-Medium containing antibiotics for selection, overnight at 37°C with 120 rpm. The culture was diluted to an OD_{540nm} of 0.05 and grown until it reached an OD_{540nm} of 0.5. The culture was mixed with glycerol to a final concentration of 30%. Aliquots of 500 µL were stored at -80°C.

2.4 Cloning Methods

2.4.1 Genomic DNA isolation

Genomic DNA of *S. aureus* was isolated with the Bacterial Genomic DNA Isolation Kit (Norgen, Thorold, Canada) according to the manufacturer´s. Only the first step when the cell pellet was solved in Lysis buffer, Lysostaphin (0.1 µg/µL) was added and incubated for 60 min at 37°C. The purified DNA was stored at -20°C.

2.4.2 Plasmid DNA isolation

To isolate plasmid DNA, the High pure plasmid isolation kit (ROCHE, Mannheim, DE) was used and the manual instructions were followed when *E. coli* was used. In the case of *S. aureus,* the cell pellet of 4 mL cell culture was first suspended in suspension butter containing Lysostaphin (0.1 µg/µL) and proteinaseK (0.02 µg/µL). An incubation step at 37°C for 1 h slightly shaking was performed. After this the isolation was continued as described by the manual instructions. The plasmid DNA was stored at -20°C.

2.4.3 Polymerase chain reaction (PCR)

The polymerase chain reaction is the method of choice for the amplification of DNA fragments. Therefore, the Phusion High Fidelity DNA Polymerase (Thermo Scientific, St. Leon-Rot DE) was used with the following buffer condition and reaction program (Tab. 10, Tab. 11).

Table 10 PCR ingredients

Ingredients PCR mixture	**Concentration/Volume**
5 x Green phusion HF buffer	1 x
dNTPs	0.2 mM
Forward primer	0.2 µM
Reverse primer	0.2 µM
DNA Template	~100 ng
Phusion HF DNA Polymerase	0.4 Units
bidest H_2O	Ad 20 µL

Table 11 PCR protocol

	Temperature (°C)	Time	Cycles
Initial denaturing	98	2 min	1
Denaturing	98	30 sec	
Annealing	55 – 60	30 sec	35
Elongation	72	30 sec/1 kb	
Final Elongation	72	10 min	1

Colony PCR

The colony PCR was used to check the plasmid that was up taken by *E. coli* or *S. aureus.* For this reaction the GoTaq DNA Polymerase was used with the buffer conditions and program listed in Tab. 12 and Tab. 13. When *E. coli* was used for the PCR, colony material was used as a template and directly transferred into the PCR reaction mixture. In the case of *S. aureus*, according to a protocol from Richardson lab, colony material was solved in 100 µL Lysis Buffer (20 mM Tris, 3 mM $MgCl_2$, 0.5% Tween 20, 0.5% Igepal CA-630, 60 µg/mL proteinase K) and incubated at 55°C for 1 h. Then an incubation at 95°C for 10 min was followed by a short centrifugation step at 7000 x g for 5 min. 10 µL of the supernatant was used as a template for the PCR reaction.

Table 12 Colony PCR ingredients

Ingredients PCR mixture	**Concentration/Volume**
5 x Green GoTaq reaction buffer	1 x
dNTPs	0.2 mM
Forward primer	0.2 µM
Reverse primer	0.2 µM
DNA Template	Colony material
GoTaq DNA Polymerase	0.5 Units
bidest H_2O	Ad 25 µL

Table 13 Colony PCR protocol

	Temperature (°C)	Time	Cycles
Initial denaturing	95	5 min	1
Denaturing	95	30 sec	
Annealing	55 – 60	30 sec	35
Elongation	72	60 sec/1 kb	
Final Elongation	72	10 min	1

2.4.4 Agarose gel-electrophoresis

For the separation of DNA fragments concerning their size, the DNA was supplemented with 1 x loading dye (Thermo Scientific, St. Leon-Rot, DE) and run on a 1% TBE-agarose gel containing Roti- GelStain (Carl Roth GmbH, Karlsruhe, DE) in TBE buffer (90 mM Tris, 90 mM boric acid, 1 mM EDTA) at 120 V and 350 mA for 30-60 min. For the visualization, UV-light was used at 360 nm.

2.4.5 Purification of DNA

To purify DNA from agarose gels, the DNA bands were cut out of the gel and the NucleoSpin® Gel and PCR Clean-up kit (Machery-Nagel, Düren DE) was used and followed the manual instructions. The DNA was eluted in ddH_2O and stored at -20°C.

2.4.6 Restriction digest of DNA

For the digest of fragment DNA or plasmids, required enzymes (2.2.1) were purchased and applied as described by the company.

2.4.7 Dephosphorylation of plasmid DNA

To prevent a relegation the plasmid DNA, it was dephosphorylated after restriction digest. For this, the Shrimp Alkaline Phosphatase (rSAP) was used as described by the company.

2.4.8 Ligation

Ligation of digested DNA was performed using the T4-DNA-ligase in concentrations the company suggested. The following incubation was done at 16°C over night or at 22°C for several hours.

2.4.9 DNA-sequencing

After constructions of plasmids or mutants the DNA was send to Eurofins Genomics (Ebersberg, DE) or Microsynth Seqlab GmbH (Göttingen, DE) for the control of the DNA sequence.

2.5 Plasmid construction

Construction of the plasmid pMAD-*Δ0364*, deletion plasmid for the gene *NWMN_0364*

The 5' and the 3' flanking regions of the gene *NWMN_0364*, which are about 500 bp in size, were amplified by PCR using the primers p0364-01/p0364-02 and p0364-03/p0364-04 (see 2.2.2/Tab. 5) from *S. aureus* Newman genomic DNA. The primers p0364-01 and p0364-04 add a BamHI restriction site to the 5' end of the upstream fragment and to the 3' end of the downstream fragment. The primer p0364-02 and p0364-03 add a 17 base pair overhang to the amplified fragments allowing the fusion of the up- and the downstream fragments in a second PCR. The fused construct was inserted into the pMAD vector via the BamHI restriction site by digestion and ligation. After ligation, the plasmid was transformed into *E. coli* DH5α and positive colonies were selected on LB plates containing 100 µg/mL ampicillin. Colony PCR and sequencing of the plasmid was performed to check the accuracy of the construct.

Construction of the plasmid pMAD-*0364*strep

The 5' flanking region and the gene *NWMN_0364* without a stop codon were amplified using the primers P0364-01/P0364-05 (see 2.2.2/Tab. 5) from *S. aureus* Newman genomic DNA. The 3' flanking region of the gene *NWMN_0364* was amplified using the primers P0364-06/P0364-04 (see 2.2.2/Tab. 5). The primers P0364-01 and P0364-04 generate a *Bam*HI restriction site and the primers P0364-05 and P0364-06 add a sequence for a strep tag to the fragment, which was further used, in a second PCR, to connect the two DNA fragments. The fused fragment was then inserted into the pMAD vector by digestion and ligation. After ligation, the plasmid was transformed into *E. coli* DH5α and positive colonies were selected on LB plated containing 100 µg/mL ampicillin. Colony PCR and sequencing of the plasmid was performed to check the accuracy of the construct.

Construction of the plasmids pPR-IBA1-SaeP, pPR-IBA1-TcyA, pPR-IBA1-MetQ1, pPR-IBA1-NWMN_0364

The genes *saeP* (NWMN_0677), *tcyA* (NWMN_2313), *metQ1* (NWMN_0782) and *Pvr* (NWMN_0364) were amplified from *S. aureus* Newman genomic DNA without the signal sequence and without the stop codon, using the corresponding primers (see 2.2.2/Tab. 5). The primers generated a *Bsa*I restriction site, which was used for digestion and ligation into the pRB-IBA1 plasmid. After ligation, the plasmid was transformed into E. coli DH5α and positive colonies were selected on LB plated containing 100 µg/mL ampicillin. Colony PCR and sequencing of the plasmid was performed to check the accuracy of the construct.

2.6 Bacterial genetic manipulation techniques

2.6.1 Chemically competent *E. coli* cells

To generate chemically competent *E. coli,* bacteria were grown in LB-Medium (Lennox, Roth) containing possible relevant antibiotics, overnight at 37°C with 120 rpm. The culture was diluted to an OD_{540nm} of 0.05 in 100 mL and grown until it reached an OD_{540nm} of 0.8. The culture was harvested in 4 reaction tubes (50 mL) containing 25 mL each. A centrifugation step for 10 min at 3600 x g followed. The supernatant was discarded and pellet placed on ice. Respectively two pellets were resuspended in 20 mL Solution 1 (10 mM MOPS, pH 7, 10 mM RbCl). After another centrifugation step (10 min, 3600xg) each pellet was resuspended in 20 mL Solution 2 (100 mM MOPS, pH 6.5, 10 mM RbCl, 50 mM $CaCl_2$). The suspensions were again centrifuged (10 min, 3600 x g) and both pellets were resuspended in 5 mL Solution 2. 1.3 mL glycerol was added and aliquots were stored at -80°C.

2.6.2 DNA-Transformation in *E. coli*

To bring a plasmid into an *E. coli* DH5α or a BL21 DE3 pLyss cell, 50-200 ng of the target plasmid was mixed with 100 µL chemically competent cells and incubated for 10 min on ice. The mixture was then transferred to 43°C for 60 sec and afterwards on ice for 2 min. 800 µL LB medium was added and the cells incubated for 30-60 min at 37°C shaking. After a centrifugation step with 5000 x g, 5 min at RT the supernatant was reduced to 100 µL and the pellet resuspended. The suspension was plated on an LB plate containing the required amount of antibiotics. Incubation occurred at 37°C over night.

2.6.3 Electrocompetent *S. aureus* cells

To generate competent *S. aureus* RN4220 cells, which are able to uptake DNA, 200 mL culture in TSB medium was inoculated to an OD_{600nm} 0.05 and cultivated at 35°C, 120 rpm until OD_{600} 0.5/0.6. Then all steps were carried out on ice and all centrifugation steps were done at 2500 x g, 4°C for 5 min. After a first centrifugation, the pellet was dissolved in an ice-cold 0.5 M sucrose solution with a volume of 0.5 fold of the initial volume. Again a centrifugation was done and the pellet suspended in ice-cold 0.5 M sucrose solution with a volume of 0.25 fold of the starting volume. The solution was incubated for 2-4 hours on ice. After centrifugation the pellet was dissolved in ice-cold 0.5 M sucrose solution with a volume of 0.125 fold of the initial volume. The centrifugation step was done again and the pellet solved in 0.5 M ice-cold sucrose solution with a volume of 0.0625 fold of the starting volume. A last centrifugation step was done and the pellet dissolved in 20% sterile glycerol. The cells were stored until further use at -80°C.

2.6.4 Electroporation with *S. aureus*

To bring DNA into *S. aureus* RN4220, 50 µL electro competent cells were thawed on ice and mixed with 50-200 ng plasmid. After an incubation of 30 min on ice the suspension was given into an electroporation cuvette with an electrode distance of 1 mm. In an electroporation device the electric shock was performed by 1.5/2.0 kV, 100 Ω and 25 µFd. Directly afterwards 900 µL cold SOC-medium (2% (w/v) tryptone, 0.5% (w/v) yeast extract, 10 mM NaCl, 2.5 mM KCl, 10 mM $MgSO_4$, 10 mM $MgCl_2$, 20 mM Glucose, pH 7) was given to the cells and incubated at 37°C, shaking for 90 min. Furthermore, the solution was centrifuged at 5000 x g, 5 min, the supernatant reduced to 100 µL, the pellet dissolved and finally plated on LB plated containing required antibiotic.

2.6.5 Generation of phage lysate

To generate phages that carry the plasmid of interest, the *S. aureus* strain, harboring the plasmid, was cultivated overnight in 20 mL LB medium. Then 100 µL $CaCl_2$ was added to the culture to achieve a final concentration of 5mM and incubated for 5-30min. The Phages 80 (see 2.3.1 / Tab. 7) were diluted up to 10^{-4} in Phagebuffer (LB-medium with 5 mM $CaCl_2$). For each dilution, 0.3 mL bacterial culture was used. The bacteria were incubated at 52 °C for 2 min and afterwards mixed with the phages. After 15 min at room temperature 4mL

liquid soft agar (LB-medium with 0.6% agar; 52°C) containing 5 mM $CaCl_2$ was given to the phage-bacteria mix, vortexed and plated on blood agar plates (LB-medium, 1.5% agar, defibrinated sheep blood in 1:10 dilution). The incubation followed over night at 37°C. The plate with the highest dilution and a confluent lysis was used to gain the phage extract. Therefore, 2-4 mL Phagebuffer was given on the plate and mixed through the soft agar. The liquid was the transferred to a reaction tube, centrifuged at 6000 x g for 10 min and filtered through a 0.45 µm filter. The final lysate can be stored at 4°C.

2.6.6 Phage transduction

Phage transduction was used to insert plasmid DNA into an *S. aureus* strain of interest. Therefore, the strain was cultivated in 10 mL LB medium over night at 37°C shaking. Then 100 µL $CaCl_2$ was added to the culture to achieve a final concentration of 5 mM and incubated for 5-30 min. The Phages 80 were diluted up to 10^{-4} in Phagebuffer (LB-medium with 5 mM $CaCl_2$). For each dilution, 0.3 mL bacterial culture was used. The bacteria were incubated at 52°C for 2 min and afterwards mixed with the phages. After 15 min at room temperature, 3mL liquid soft agar (LB-medium with 0.6% agar; 52°C) containing 20 mM Na_3-citrate, was given to the phage-bacteria mix, vortexed and plated on agar plates containing an antibiotic for selection. The incubation followed over night at 37°C and colonies grew 24 – 48 h after phage transduction.

2.6.7 Generation of genomic mutations in *S. aureus*

To generate mutations in the genome of *S. aureus,* the thermosensitive shuttle vector pMAD was used as described by Arnaud *et al*. [134]. For an insertion of DNA, the DNA that has to be inserted as well as the genomic flanking regions (~500 bp) were cloned into the pMAD (see 2.5). In case of a deletion mutant, only the flanking regions (~500 bp) were inserted into the pMAD (see 2.5). The completed plasmid was introduced into the *S. aureus* RN4220 via electroporation and then transferred into the target strain by using phage transduction with the bacteriophage Phage ϕ80. Due to the thermosensitive origin of the pMAD, an integration of the plasmid into the genome via homologous recombination was forced by increasing the temperature. For it, 100 µL of a TSB overnight culture, grown at 37°C supplemented with erythromycin (10 µg/mL), were given into 10 mL TSB containing erythromycin (10 µg/mL). The culture was grown at 30°C for 1 hour and the directly transferred to 42°C for 7 hours. The culture was diluted and plated on LB-agar plates

containing erythromycin (10 µg/mL) and X-Gal (40 µg/mL). The plates were incubated overnight at 42°C. After a successful integration, the excision of the plasmid followed to generate the mutation. For this purpose, blue colonies were picked from the agar plates and inoculated in TSB medium containing erythromycin (10 µg/mL) and grown at 42°C overnight. 10 µL of this culture was used to set up a 10 mL culture in TSB medium without antibiotics. An incubation at 30°C for 7 hours followed. The culture was diluted and plated on LB-agar plates containing X-Gal (40 µg/mL). The plates were kept overnight at 42°C. White colonies, which were sensitive to erythromycin, were checked via PCR for the mutation. In addition, sequencing of the target genomic region was done to verify the mutation and exclude other unwanted mutations within this region.

2.7 RNA Methods

2.7.1 Culture sampling for RNA preparation

Bacterial strains were grown in desired medium to an optical density of choice. For harvest at least 10 OD units (1 OD unit = 1 mL of OD 1 or 2 mL of OD 0.5) were used. All steps were performed on ice. The cells were quickly mixed with ice-cold killing buffer (20 mM sodium azide, 20 mM Tris pH 7.5, 5 mM $MgCl_2$) in a ratio of 2:1. Furthermore, a centrifugation step at 10000 x g, 4°C for 5 min and a resuspension of the pellet in 1 mL killing buffer followed. After a second round of centrifugation at 12000 x g, 4°C for 5 min, the supernatant was removed and the pellet stored at -80°C.

2.7.2 RNA isolation

For the isolation of bacterial RNA, the acid-phenol method [143] was used with modifications described by Fuchs *et al.,* [144]. Thereby, cells were thawed, suspended in 500 µL suspension buffer (3 mM EDTA pH 8.0, 200 mM NaCl) and mixed with glass beads (ø0,1 mm) in a ratio of 1:1. Additionally, 500 µL PCl (aqua phenol, chloroform and isoamyl alcohol in a ratio of 25:24:1) were added. Disruption of the cells took place, with mechanical force, in a Fast Prep for 1 min at 6.5 m/s. The lysate was centrifuged at 12000 x g for 5 min at room temperature and the upper aqueous phase transferred to a new tube containing 500 µL PCl. The sample was shaken at 9.5 m/s for 5 min at room temperature and then centrifuged at 15000 x g, 5 min at room temperature. Again, the upper aqueous phase was transferred to a new tube containing 500 µL Cl (chloroform, isoamyl alcohol in a ratio of

24 : 1) and the sample was shaken at 9.5 m/s for 5 min at room temperature and then centrifuged at 15000 x g, 5 min at room temperature. This procedure was repeated, where the upper aqueous phase was transferred to a new tube containing 500 µL Cl (chloroform, isoamyl alcohol in a ratio of 24:1) and the sample was shaken at 9.5 m/s for 5 min at room temperature and then centrifuged at 15000 x g, 5 min at room temperature. Subsequently, the upper aqueous phase was mixed with 40 µl sodium acetate and 1ml ice-cold 98% ethanol. An incubation step overnight at -20°C followed to precipitate the RNA. After a centrifugation step at 15000 x g, 4 °C for 30 min the pellet was washed with 500 µl ice-cold 70% ethanol and centrifuged again at 15000 x g, 4°C for 10 min. Then the supernatant was removed and the pellet dried under the hood. Finally, the RNA was solved in 50 µl sterile ddH_2O overnight at 4°C. The concentration of the RNA was determined by using a Nano-photometer.

2.7.3 Generation and labelling of RNA probes

The generation of RNA probes requires a DNA template of 300 – 500 bp of the target gene connected to a promoter for the T7 RNA polymerase. Therefore, primers for the target gene with a sequence for the T7 promoter were used for the amplification of the DNA via Polymerase-chain- reaction. The PCR product was run on an agarose gel electrophoresis, DNA bands cut out and purified. From this purified DNA about 500 ng were mixed with 2 µL DIG RNA Labeling Mix (ROCHE, Mannheim, DE), 4 µL transcription buffer, 2 µL T7 RNA polymerase, 1 µL RNasin and filled with sterile ddH_2O up to 20 µL. After an incubation at 37 °C for 2 hours 2 µL DNase was added and incubated for another 15 min at 37°C. Finally, the reaction was stopped with 2 µL 0.2 M EDTA and the produced RNA precipitated with 2.5 µL 4 M LiCl and 75 µL ice-cold 96% EtOH for 30 min at -70°C. A centrifugation step at 12,000 x g, 4°C for 10 min followed. The supernatant was removed, the resulting pellet washed with 50 µL 70% EtOH and dried in a vacuum concentrator. Then, the pellet was solved in 50 µL DEPC-water for 30 min at 37°C.

2.7.4 Labelling efficiency test of RNA probes

The RNA probe was spotted in a serial dilution (1:10, 1:100, 1:1000, 1:10000) on a nylon membrane using 1 µL per spot. The membrane was UV-cross-linked (120 mJ/cm^2) and afterwards incubated for one min in buffer 1 (0.1 M maleic acid, 0.15 M NaCl) at room temperature. An incubation for 30 min at room temperature in buffer 2 (1% (w/v) blocking

reagent (ROCHE, Mannheim, DE), 0.1 M maleic acid, 0.15 M NaCl) followed. Then, the anti-dioxygenin antibody (ROCHE, Mannheim, DE) was diluted 1:10,000 in buffer 2 and incubated on the membrane for 30 min at room temperature. Two washing steps for each 15 min in buffer 1 followed. For the equilibration, buffer 3 (0.1 M Tris, 0.1 M NaCl pH 9.5) was given to membrane for 5 min at room temperature followed by the chemiluminescence substrate CDP-star diluted 1:200 in buffer 3. After a 5 min incubation, the signal was detected by using a chemiluminescence imager (LAS 3000, Fujfilm) at an exposure time of 10 min.

2.7.5 RNA Dot Blot Assay

For the determination of specific transcript intensities, the isolated RNA was diluted in 10 x SSC (1.5 M NaCl, 0.15 M Na-citrate) in a serial dilution of 1:2 each step starting from 1 µg / 100 µL. For the denaturation, the RNA was incubated at 65°C for 10 min and directly set back on ice. Then, 100 µL RNA solution were spotted on a nylon membrane (equilibrated before in ddH_2O and 20 x SSC (3 M NaCl, 0.3 M Na-citrate)) using a Bio-Dot apparatus. Furthermore, the membrane was UV-cross-linked (120 mJ/cm²) and stained with methylene blue (0.4 M sodium acetate pH 5.2, 0.1% (w/v) methylene blue, 2% (v/v) acetic acid) for 5 min at room temperature. De staining of the membrane was carried out with ddH_2O. Moreover, the membrane was incubated in hybridization buffer (5 x SSC (750 mM NaCl, 75 mM Na-citrate), 0.1% (w/v) N-lauroyl sarcosine, 7% (w/v) SDS, 1% (v/v) blocking reagent (ROCHE, Mannheim, DE), 50% (v/v) formamid (deionized)) at 68°C for 1 h. The RNA probe (diluted 1:1000 in hybridization buffer) was denaturated at 95 °C for 5 min and cooled down on ice for 5 min, before replacing the hybridization buffer on the membrane. The RNA hybridization took place over night at 68°C in a hybridization oven. To detect the RNA hybrids, the membrane was washed 2 times for 5 min with wash buffer 1 (2 x SSC (300 mM NaCl, 30 mM Na-citrate), 0.1% (w/v) SDS) at room temperature. This was followed by 2 washing steps at 65°C with washing buffer 2 (0.2 x SSC (30 mM NaCl, 3 mM Na-citrate), 0.1% (w/v) SDS) for 15 min. After an incubation for 1 min in buffer 1 (0.1 M maleic acid, 0.15 M NaCl), buffer 2 (1% blocking reagent in buffer 1) was given to the membrane for 30 min at room temperature. Moreover, the antibody anti-digoxigenin (ROCHE, Mannheim, DE) (diluted 1:10000 in buffer 2) was incubated on the membrane for 30 min at room temperature. Then, two washing steps in buffer 1 for 15 min each followed and afterwards the membrane was equilibrated for 5 min in buffer 2 (0.1 M Tris/HCl pH 9.5, 0.1 M NaCl). For the detection the chemiluminescence substrat CDP-star (ROCHE,

Mannheim, DE) was diluted 1:200 in buffer 3 and directly spread over the membrane. After an incubation for 5 min the signal was detected with an LAS-3000 imager (Fujifilm).

2.8 Protein Analysis

2.8.1 Preparation of extracellular proteins 1

The *S. aureus* strains of interest were cultivated to a defined optical density in TSB medium. The culture was harvested by centrifugation of 10000 x g at 4°C for 10 min. The supernatant was transferred to a new centrifugal tube and trichloracetic acid, solved in ddH_2O as a 100% (w/v) solution, was given to the supernatants in a final concentration of 10% (w/v). The incubation followed overnight at 4°C to precipitate the proteins from the supernatant. Afterwards, a centrifugation at 10000 x g, 4°C for 45 min was done. The pellet was solved in 2 x 1 mL 100% (v/v) ethanol with the help of an inoculation loop and transferred to a new 2 mL reaction tube. Washing steps followed with 2 x 100% ethanol (v/v), 1 x 70% ethanol (v/v) and 1 x 100% (v/v). In between, the centrifugation was done at 13000 x g, 4 °C for 5min. After washing the pellet was dried in a vacuum concentrator for 2-4 min using the program V-HV. The dried protein extract was solved in 300 µL Urea buffer (8 M urea, 2 M thiourea) by shaking at room temperature for 30 min. After centrifugation at 13000 x g, 20°C for 20 min the supernatant was stored at -20°C

2.8.2 Preparation of extracellular proteins 2

This method was used to prepare proteins from staphylococcal synthetically medium. The proteins were prepared as it was done in preparation of extracellular proteins 1 with following modifications: dried protein extracts were dissolved in 1 mL Urea buffer (8 M urea, 2 M thiourea) by shaking at room temperature for 30 min. After centrifugation at 13000 x g, 20°C for 20 min the supernatant was used for a second precipitation. Therefore, 4 mL ice cold (-20°C) 100% (v/v) acetone was given to the supernatant to achieve a final concentration of 80% (v/v) acetone. The incubation was performed at -20°C over night or for several hours at room temperature. The precipitated proteins were centrifuged at 13000 x g, 20°C for 15 min. The pellet was washed with 1 x 80% (v/v) acetone and 1 x 100% (v/v) acetone, the centrifuged in between was done at 13000 x g, 20°C for 5 min. Afterwards the pellet was air dried for 15 – 45 min and solved in 300 µL urea buffer (8 M

urea, 2 M thiourea) by shaking at room temperature for 20 min. The last centrifugation was done at 13000 x g, 20°C for 20 min and the supernatant stored at -20°C.

2.8.3 Determination of protein concentration

To determine the protein concentration Roti®-Nanoquant (Carl Roth, Karlsruhe, DE) was used and applied as the manufacturer recommended. Thereby, a standard curve was first generated using a mixture of BSA, trypsin inhibitor, ribonuclease and γ globulin as a standard in buffer conditions used in the experiments. Whenever the proteins were in urea buffer (8 M urea, 2 M thiourea), a maximum of 20 µL of this buffer was used and filled up with ddH_2O for measurement. The standard curve was then used to calculate the protein amount in the samples.

2.8.4 SDS PAGE (polyacrylamide gel electrophoresis)

Proteins can be separated due to their molecular weight and visualized by an SDS PAGE according to Laemmli [145]. The polyacrylamide gel consists of a stacking gel (5% acrylamide, 0.133% bisacrylamide, 125 mM Tris pH 6.8, 0.25% SDS (w/v), 0.075% ammonium persulfate, 0.075% TEMED) and a resolving gel (12 – 15% acrylamide, 0.32 – 0.4% bisacrylamide, 375 mM Tris pH 8.8, 0.25% SDS (w/v), 0.062% ammonium persulfate, 0.062% TEMED). The samples were loaded on the gel in a loading buffer (15% glycerol, 5% β-mercaptoethanol, 2.4% (w/v) SDS, 0.004% (w/v) bromophenol blue, 66 mM Tris, pH 6.8) and run at 120 V and 15 mA/per gel in an electrophoresis chamber in electrophoresis buffer (25 mM Tris, 200 mM glycine, 0.1% (w/v) SDS). As standard proteins, the low molecular weight standard (GE healthcare, Chalfont St. Giles, GB) was used. After running, the gel was incubated in fixing solution (40% (v/v) ethanol, 10% (v/v) acetic acid) for 1 hour. Staining of the proteins in the gel followed overnight in colloidal coomassie staining solution (20% methanol, 0.08% (w/v) coomassie, 600 mM ammonium sulfate, 0.85% ortho-phosphoric acid) and then destained with ddH_2O for 30-90 min.

2.8.5 Western blot

A Western blot gives the opportunity to detect and visualize a protein of interest on a membrane. First, the protein sample was run on a SDS-PAGE (see 2.8.4) on 12 or 15% gels until the sample dye reached the bottom of the gel. The gel was the used to blot the proteins

on a PVDF membrane. For that, the gel was incubated in chilled transfer buffer (25 mM Tris, 192 mM glycine, 15% (v/v) methanol, 0.04% (w/v) SDS, pH 8.3) for 15-30 min. Meanwhile, the PVDF membrane was activated for 15 sec in 100% methanol, then for 2 min in ddH_2O and finally for 5 min in transfer buffer. For blotting, a tank Blot (BioRad, Hercules, CA, USA) was used und assembled as described by the company. The tank was filled with transfer buffer und the blotting was performed for 1 hour at 100 V and 350 mA. Subsequent to the blotting, the membrane was transferred to a reaction box and washed 2 x for 5 min with TBST (50 mM Tris, 150 mM NaCl, pH 7.5, 0.05% (v/v) Tween20). Then, two washing steps for 5 min with TBS (50 mM Tris, 150 mM NaCl, pH 7.5) followed. The membrane was further blocked with TBS containing 5% (w/v) skim milk powder for 1 hour at room temperature. Again, the membrane was washed with TBST for 5 min and afterwards 2 x washed for 5 min with TBS. The antibody specific for the target protein was diluted in 15 mL TBS containing 1% skim milk powder and incubated over night at 4°C slightly rotating. Then, the membrane was washed three times with TBST for 5 min each and the second antibody (Anti-rabbit IgG, Sigma Aldrich, Darmstadt, DE) was added, diluted in TBS containing 2% (w/v) skim milk powder. After an incubation for 1 hour at room temperature, the antibody was washed off three times with TBST for 5 min each. Detection buffer (100 mM Tris pH 9.5, 100 mM NaCl, 5 mM $MgCl_2$) was given on the blot for 30 min at room temperature. Subsequently, 5 mL of the detection reagent (detection buffer, 0.033% (w/v) NBT, 0.017% (w/v) BCIP) was used on the membrane. When the signals became visible on the membrane, the reaction was stopped by adding ddH_2O

2.8.6 Melting curve of proteins

Melting curves were performed using 0.5 – 1 mg/mL protein and the Tycho NT6 (NanoTemper Technologies GmbH, München DE).

2.9 Proteomic methods

Identification and quantification of proteins via mass spectrometry is the goal of this method. To achieve this, the protein samples were loaded on a SDS PAGE (see 2.8.4). For total proteome measurements 30 µg of the protein solution were used while for interaction studies 3-4 µg. For interaction studies, the proteins samples were only run shortly into the gel due to the low protein amounts. The stained gels were scanned with a densitiometer and the exact protein amount on the gel determined by using the AIDA (Advanced Image Data

Analyzer) software. Afterwards the gel was cut into fractions that contained no more than 5 µg protein. For total proteome measurements a sample was cut into 6 fractions and for interaction studies one sample was cut in only one fraction. The fractions were further cut into small pieces of ~1 mm^2.

2.9.1 Tryptic *in-gel* digest of proteins

The tryptic *in-gel* digest was performed according to Toyofuku *et al.,* [146]. To remove the coomassie from the proteins, the gel pieces were incubated in a destaining solution (50% methanol, 50% 25 mM $(NH_4)HCO_3$ (pH 7,8 – 8,1)). This incubation occurred for 3 x 30 min, followed by and overnight incubation at 4°C. The fully destained gel pieces were then washed two times with roughly 150 µL 100 % acetonitrile and incubated until all pieces remained dehydrated. An incubation for 5 min in 50 mM $(NH_4)HCO_3$ followed. Dehydration in acetonitrile was performed in 150 µL and the rehydration was done for 5 min in 50 mM $(NH_4)HCO_3$. Then gel pieces were washed two times with 100% acetonitrile and incubated in roughly 130 µL DTT-solution (10 mM DTT in 50 mM $(NH_4)HCO_3$) for 30 min at 60°C. Afterwards, gel pieces were washed two times with 100 % acetonitrile and incubated until all pieces remained dehydrated. An incubation step in roughly 130 µL Iodoacetamide-solution (50 mM Iodoacetamide in 50 mM $(NH_4)HCO_3$) for 1 hour at room temperature in the dark followed. Gel pieces were washed with roughly 150 µL 100% acetonitrile and incubated until all pieces remained dehydrated. An incubation for 5 min in 50 mM $(NH_4)HCO_3$ followed. Again the dehydration in acetonitrile was performed in 150 µL and the rehydration was done for 5 min in 50 mM $(NH_4)HCO_3$. Then the gel pieces were washed two times with 100% acetonitrile and dried under the hood at room temperature. Trypsin (Promega, Mannheim, DE) was diluted in digestion solution (50 mM Tris, 1 mM $CaCl_2$, pH 7.6) to reach a trypsin/sample protein ratio of 1:10 (w/w) or 1:20 (w/w). An incubation followed for 12 hours at 37°C, slightly shaking.

2.9.2 Extraction of peptides from the gel

After tryptic *in-gel* digest, the peptides were extracted from the gel pieces [147]. During all steps the samples were kept at 4°C and all supernatants were collected in one tube. The gel pieces were first two times washed with roughly 120 µL 100% acetonitrile and incubated until all pieces remained dehydrated. Then the pieces were rehydrated in 150 µL 1% formic acid for 10 min, before another incubation step in acetonitrile was performed. Gel pieces

were covered with 150 µL 10% formic acid for 10 min. After this rehydration, the gel pieces were washed two times with 100% acetonitrile. In the end the collected supernatant was completely dried in a vacuum concentrator and stored at -20°C.

2.9.3 Desaltment of peptide samples

To remove salts in the sample, Zip Tip pipetting tips were used. First, dried peptide samples were solved in 20 µL wash solution (5% acetonitrile, 0.1% formic acid), shortly centrifuged and incubated at room temperature for 1 hour. Further, samples were vortexed and shortly centrifuged. The Zip Tip pipetting tip was bathed three times with 10 µL in wetting solution (50% acetonitrile) and washed two times with 10 µL in wash solution. Then, the Zip Tip was loaded with peptide solution by pipetting up and down 10 x 10 µL in the sample. The tip was washed three times with 10 µL wash solution and then eluted three times with 10 µL elution buffer (60% acetonitrile, 0.1% formic acid). The eluted peptides were dried in a vacuum concentrator.

2.9.4 Sample preparation for LC-MS/MS measurement

Before mass spectrometry measurement, each sample was solved in 16 µL buffer A (3% acetonitrile, 0.1% formic acid), shortly centrifuged and incubated at room temperature for 1 hour. An incubation for 5 min in an ultra-sonic bath (37 kHz, sweep, 100% power) followed. The sample was then centrifuged for 20 min, 109,000 x g at 22°C. The supernatant was transferred into glass vials.

2.9.5 LC-MS/MS-Analyses

For liquid chromatography – coupled tandem mass spectrometry (LC-MS/MS) analyses a nanoAQUITY Ultra Performance Liquid Chromatography System (Waters Corporation, Milford, MA, USA) was connected to an LTQ Orbitrap Velos Pro mass spectrometer (Thermo Fisher Scientific Inc). Peptides from each gel piece were solved in 3% acetonitrile and 0.1% formic acid. After centrifugation for 20 min at 109,000 x g, the supernatant was loaded onto a BEH C18 column, 130 Å, 1.7 µm, 75 µm x 250 mm at a flow rate of 0.35 µl min-1 (Waters Corporation). Elution of peptides from the column was performed using a 125 min gradient starting with 3.7% buffer B (80% acetonitrile and 0.1% formic acid) and 96.3% buffer A

(0.1% formic acid in Ultra-LC-MS-water): 0 to 30 min 3.7% B; 30 to 60 min 3.7 to 31.3% B; 60 to 100 min 31.3 to 62.5% B; 100 to 108 min 62.5 to 99% B; 108 to 113 min 99% B; 113 to 118 min 99 to 3.7% B; 118 to 125 min 3.7% B.

Primary MS scans were performed in the Fourier transformation mode scanning an m/z of 400-2000 with a resolution (full width at half maximum at m/z 400) of 60,000 and a lock mass of 445.12003. Primary ions were fragmented in a data-dependent collision induced dissociation mode for the 10 most abundant precursor ions with an exclusion time of 13 s and analysed by the LTQ ion trap. The following ionization parameters were applied: normalized collision energy: 35, activation Q: 0.25, activation time: 10 ms, isolation width: 2 m/z, charge state: ≥ +2. The signal to noise threshold was set to 2000.

2.9.6 Data analyses of LC-MS/MS measurement

MS/MS raw files were analysed using MaxQuant (Max Planck Institute of Biochemistry, Martinsried, Germany, www.maxquant.org, version 1.5.2.8) and the following parameters: peptide tolerance: 5 ppm; tolerance for fragment ions: 0.6 Da; variable modification: methionine oxidation, fixed modification: carbamidomethylation; a maximum of four modifications per peptide was allowed; the fixed false discovery rate (FDR) was set to 1% for peptides and proteins. All samples were searched against databases containing all protein sequences of *S. aureus* Newman extracted from NCBI (National Center for Biotechnology Information, 2016/09/06). MaxQuant supplied a decoy mode of reverted sequences and common contaminants. MS data filtering was done using the proteinGroups.txt output file of MaxQuant. For reliable identifications, only proteins with a minimum of two unique peptides were used and the intensities of all three replicates were sum up and the raw intensities ≤ 500.000 were set to zero. Moreover, the identified proteins must have at least two MS/MS scans in two different replicates. For statistical analysis, the software Perseus was used. Thereby, the intensities were taken for the base 2 logarithm, which followed up by the generation of z-scores. With these data a student's t-test was performed using the p-Value with a significance threshold at 0.05. To determine the fold change between wild type and mutant strain for each protein, the intensity mean of the mutant was divided by the intensity mean of the wild type. The received ratio was used for the base 2 logarithm.

2.10 Protein-Interaction techniques

2.10.1 Identification of protein-interaction partners under *in vivo* conditions

For the the target protein fused with a strep-tag was expressed in *S. aureus*. The following experiment was performed in three replicates. Here, bacteria were grown in culture media at 37°C, 120 rpm and when the desired optical density was reached paraformaldehyde was added to the culture in a final concentration of 0.6% (w/v). An incubation followed for 15 min, before glycine was given to the culture in a final concentration of 135 mM. A centrifugation of the culture was then performed at 8,000 x g, 4°C for 10 min. The extracellular proteins were prepared as described in preparation of extracellular proteins 2 (see 2.8.2) but solved in 1 mL urea buffer. To extract the target protein with bound interaction partner from the extracellular protein solution, the protein solutions was applied on affinity chromatography using the Gravity flow Strep-Tactin® Sepharose® columns (IBA GmbH, Göttingen). The protocol was performed as recommended by the manufacturer but instead of a Tris buffer, an ammonium bicarbonate buffer (100 mM NH_4HCO_3, 50 mM NaCl) was used. The eluted proteins were concentrated in a vacuum concentrator and run on a SDS-PAGE using equal volumes for each sample (~2-4 µg). Each sample on the gel was cut in one fraction, prepared according to the protocols (see) and measured with LC-MS/MS (see LC-MS/MS-Analyses).

For data analysis Max Quant was used (see MS/MS Data analyses). Only proteins were taken into account with a minimum of two unique peptides, at least two MS/MS scans in two different samples and raw intensity ≥ 166000. For each sample, relative intensities were determined, by dividing each protein raw intensity by the raw intensity of Pvr. For these relative raw intensities means and standard deviations were calculated. Standard deviations are presented in relation to the mean (relative standard deviation (RSD)).

2.10.2 Co-Immunoprecipitation assay

The protein extracts were generated from *S. aureus* Newman cells grown in three replicates in staphylococcal synthetic medium to an OD_{500} 2. Cells were treated with paraformaldehyde for 10 min at 37°C in a final concentration of 0.6%. This reaction was quenched using 0.135 mM glycine for 5 min. After centrifugation at 10,000 xg and washing in phosphate-buffered saline (PBS), the bacterial pellet was used for preparation of membrane proteins. For this purpose, the pellet was solved in Lysis buffer (20 mM Tris, 10

mM $MgCl_2$, 1 mM $CaCl_2$, pH 7.5) and cells disrupted in a FastPrep (MP Biomedicals) at 6.5 m/s for 3 x 30 sec. After centrifugation at 10,000 x g for 10 min, the supernatant was used for ultracentrifugation at 100,000 x g for 1 h at 4°C. The resulting pellet was solved in phosphate-buffered saline (PBS) containing 2% Triton X-100. After an incubation for 1 hour at 10°C, the solution was centrifuged and the supernatant used for Co-Immunoprecipitation. For this experiment, Protein A beads were purchased from BioRad (Sure Beads, Magnetic Beads) and 100 µL beads were loaded with 5.5 µg antibodies specific for NWMN_0364. The assay was performed as recommended by the manufacturer. The proteins were eluted by heating for 10 min at 70°C in loading dye and run on an SDS-PAGE (see SDS-PAGE) using equal volumes for each sample (~2-4 µg). Each sample on the gel was cut in one fraction, prepared according to the protocols (see) and measured with LC-MS/MS (see LC-MS/MS-Analyses).

For data analysis Max Quant was used (see MS/MS Data analyses). Only proteins were taken into account with a minimum of two unique peptides, at least two MS/MS scans in two different samples and raw intensity ≥ 166000. For each sample, relative intensities were determined, by dividing each protein raw intensity by the raw intensity of Pvr. For these relative raw intensities means and standard deviations were calculated. Standard deviations are presented in relation to the mean (relative standard deviation (RSD)).

2.10.3 Generation of recombinant Proteins

For the generation of recombinant proteins, the pPR-IBA1 expression plasmids with the corresponding genes were constructed (see 2.5) and transformed into *E. coli* BL21 (DE3) pLysS. Colonies were selected on LB containing 100 µg/mL ampicillin and 20 µg/mL chloramphenicol. Growing colonies were used for protein expression. LB medium was used and pre-cultures were set up overnight. From these, main cultures were set up to OD_{540} 0.05 and the cells were grown at 37°C until they reached OD_{540} ~0.8. Then, expression was induced by 1 mM IPTG. For 0364 and SaeP, the proteins were expressed at 25°C for 18 hours. For MetQ1 and TcyA, the proteins were expressed at 37°C for 4 hours. Furthermore, cell sampling was performed by centrifugation of the culture at 10000 x g for 10 min at 4°C. Then, the pellet was solved in Tris buffer (100 mM Tris, 50 mM NaCl, pH 8) and lysed using an ultrasonicator (Sonoplus HD 2070, Bandelin) at 90% power, 2 x 3 min with 5 cycles. After centrifugation at 10000 x g for 10 min at 4°C, the supernatant was used for affinity chromatography using the Gravity flow Strep-Tactin® Sepharose® columns (IBA GmbH, Göttingen). The protocol was used as recommended by the manufacturer, except for the

washing and eluting steps, where a HEPES buffer (20 mM HEPES, 50 mM NaCl, pH 7.5) was used. For further cleanup, a size exclusion chromatography was performed using a HiLoad 16/60 Superdex 75 prep grade (GE healthcare). Here, the proteins ran in HEPES buffer (20 mM HEPES, 50 mM NaCl, pH 7.5) with a flow setting of 1 mL/min. The elution was fractionated intro 1.8 mL fractions which were analyzed via SDS-PAGE.

2.10.4 Gel shift assay for proteins

To detect protein oligomerization and protein-protein interaction on a gel shift assay, 20 µM of each protein was used and mixed in HEPES buffer (20 mM HEPES, 50 mM NaCl, pH 7.5) with different additives. Incubation for 30 min at 37°C followed. Then, the proteins were fixed using paraformaldehyde at a final concentration of 0.6% for 5 min at room temperature. The reaction was quenched by adding glycine in a final concentration of 0.135 M. The samples were mixed with loading dye (250 mM Tris pH 6.8, 25% (w/v) glycerol, 5% (w/v) SDS, 0.05% (w/v) bromphenol blue) and the band pattern analyzed on a SDS-PAGE.

2.10.5 Chemical cross-linking/MS (XL-MS)

Chemical cross-linking, LC-MS/MS analysis, and data analysis were performed as described by Iacobucci *et al.* [148]. For XL-MS experiments, the concentration of the recombinant proteins Pvr and SaeP was set to 10 µM each and the amine-reactive MS-cleavable cross-linkers DSBU (disuccinimidyl dibutyric urea) [149] and CDI (1,1′-carbonyldiimidazole) [150] were used and purchased from Thermo Scientific (DSBU) and Sigma Aldrich/Merck (CDI). DSBU was applied at 0.2 mM and CDI at 1 mM final concentration. Initially, the proteins were mixed with each cross-linker separately in HEPES buffer (20 mM HEPES, 50 mM NaCl, pH 7.5), followed by the addition of 1 mM $ZnCl_2$, 0.05 mM $CuCl_2$ or both (1 mM $ZnCl_2$ and 0.05 mM $CuCl_2$). The cross-linking reactions were conducted at room temperature for 30 min and were quenched by adding NH_4HCO_3 to a final concentration of 20 mM.

After the cross-linking reaction, SDS-PAGE was performed and the cross-linked protein bands excised from the gel. Reduction of the proteins was performed with 10 mM DTT, followed by an alkylation with 55 mM iodoacetamide. For *in-gel* digestion, 0.25 µg trypsin (Promega) was added to each sample and digestion was conducted for 4 h at 37°C. The peptides were extracted according to [148] and the samples analyzed by LC/MS/MS.

Peptide digestion mixtures were separated on an Ultimate 3000 RSLC Nano-HPLC system (Thermo Fisher Scientific); precolumn: C8 reversed phase, Acclaim PepMap, 300 µm × 5 mm, 5 µm, 100 Å (Thermo Fisher Scientific); separation column: C18 reversed-phase, 50 cm µPAC-column (PharmaFluidics, Ghent, BEL). Peptide mixtures were washed on the precolumn with water containing 0.1% TFA for 15 min, before the peptides were separated on the separation column using gradients from 1% to 35% (40%) B (90 min), 35% (40%) to 85% B (5 min) followed by 85% B (5 min), with solvent A: 0.1% formic acid (FA) in water and solvent B: 0.08% FA in acetonitrile. The nano-HPLC system was directly coupled to a Fusion Tribrid Orbitrap mass spectrometer equipped with a Nanospray Flex Ion Source (Thermo Fisher Scientific, Bremen, DE). Data were acquired using the data-dependent MS/MS mode, i.e., each high-resolution full-scan in the Orbitrap (*m/z* 300 to 2000, R = 120,000) was followed by high-resolution product ion scans in the orbitrap (R = 15,000) within 5 s, starting with the most intense signal in the full-scan mass spectrum (isolation window 2 *m/z*). Fragmentation was performed by stepped HCD (29 ± 3 NCE). Dynamic exclusion (exclusion duration: 60 s, exclusion window: ±2 ppm) was enabled to allow detection of less abundant ions.

Cross-links were identified with MeroX (version 2.0) [151] using the following settings. Precursor precision: 5 ppm, Fragment ion precision: 15 ppm, lower mass limit: 1000 Da, upper mass limit: 8000 Da, ion type: a, b and y selected, RISEUP Mode: activated, max. missing ions: 2, losses: neutral loss of identified fragments, FDR cut off: 1%, Score cut off: 30, score settings: slow, precise scoring

2.10.6 Structural Modelling of Pvr

The structural modelling was done by Dr. Christian Tüting (Kastritis Laboratory for Biomolecular Research, University of Halle-Wittenberg)

For the generation of the initial model without signal peptide and Strep tag (residues 20 – 190), the I-TASSER webserver (https://zhanglab.ccmb.med.umich.edu/I-TASSER/) was used [152]. The best scored model was superimposed with the template model (PDB-ID 4EXR) and the bound sodium ion was merged into the model of Pvr. A final refinement was done with MODELLER (Version 9.22) using the refinement protocol, described in the manual (chapter 2.2.2), including VTFM and MD optimization [153]. Euclidean distances between Cα atoms were calculated using a local version of Xwalk (https://github.com/abxka/Xwalk) [154].

2.11 Macrophage-Infection assay

Counting of living THP-1 cells

Non-adherent cells

For the determination of the cell concentration of living THP-1 cells, cells were stained with trypan blue (0.5% in PBS) in a ratio of 1:2 (culture volume : trypan blue). The cell concentration was then determined with a Neubauer Improved counting chamber.

Adherent cells

Counting adherent cells in a well plate was done by removing the medium and adding 200 µL pre-warmed 0.05% Trypsin/EDTA (GIBCO/Thermo Scientific, St. Leon-Rot). After an incubation time of 10 min at 37°C and 5% CO_2 the reaction was stopped by adding 800 µL RPMI + 10% FCS medium. Then, pipetting the culture medium up and down loosens the cells. The cell solution was centrifuged at 100 x g for 5min and the supernatant discarded. The pellet was solved in 100 µL RPMI + 10% FCS medium. Then, the cells were stained with trypan blue (0.5% in PBS (136 mM NaCl, 2.68 mM KCl, 10 mM Na_2HPO_4, 1.76 mM KH_2PO_4, pH 7.4)) in a ratio of 1:2 (culture volume : trypan blue) and cell concentration was determined with a Neubauer Improved counting chamber.

Differentiation of macrophages

To observe the survival of macrophages followed by a *S. aureus* infection, the THP-1 cells were differentiated 36 to 48 hours prior to infection. For this purpose, cells were counted and a solution of 3 x 10^5 cells/mL in RPMI + 10% FCS medium was prepared. Then, PMA (Phorbol 12-myristate 13-acetate) was added in a final concentration of 200 nM. The cells were transferred into 12-well plates, at which 3 x 10^5 cells get into one well. After 24 hours the medium was removed and 1 mL RPMI + 10% FCS medium without phenol red added to each well.

Survival of macrophages

The bacterial strain that was tested for virulence was grown in SA-minimal medium containing glycerol as carbon source. Therefore, a pre-culture was set up in 20 mL and inoculated with material from a glycerol stocks. After a growth period of 10-12 hours at

37°C and 120 rpm, main cultures were set up to an OD_{500} of 0.075. When the bacterial culture reached OD_{500} 0.5, a defined amount of bacterial culture was used for the infection of THP-1 cells. Meanwhile, the differentiated cells were washed twice with PBS (136 mM NaCl, 2.68 mM KCl, 10 mM Na_2HPO_4, 1.76 mM KH_2PO_4, pH 7.4) before the bacteria were given on the cells. To achieve a defined amount of bacteria per mL, the bacterial culture was diluted in RPMI + 10% FCS medium without phenol red. After adding the bacteria to the cells, a centrifugation step followed at 100 x g for 10 min to descent the bacteria. An incubation took place at 37°C, 5% CO_2 for 45 min, afterwards the cells were washed twice with PBS and 1 mL RPMI + 10% FCS medium without phenol red containing 20 µg/mL lysostaphin and 150 µg/mL gentamycin was given on each well. The infected cells were incubated at 37°C and 5% CO_2. After defined time points, the survival of macrophages was determined by cell counting.

Bacterial uptake by macrophages

The infection of the macrophages was performed as described in survival of macrophages. But instead of counting the macrophages, after 1 hour the macrophages were washed with PBS twice and 100 µL 1% Triton-X-100 in PBS was given to the cells. After an incubation for 10 min at 37°C, 900 µL PBS was added and a serial dilution in LB medium set up. From these, 100 µL were then plated on LB agar plates and after incubation for 24 hours the colonies counted (CFU).

3 Results

3.1 Proteins with Two PepSY Domains like NWMN_0364 Are Connected to Extracellular or Cell Surface Functions

The goal of this study was to reveal the function of NWMN_0364. NWMN_0364 is a so far hypothetical protein with about 21 kDa in size. It has an architecture of four domains: a signal sequence for membrane transport (amino acids 1-20), a lipobox (LTAC) for membrane anchoring (amino acids 16-19), and two PepSY domains (amino acids 54-100 and 130-186) (Fig. 5).

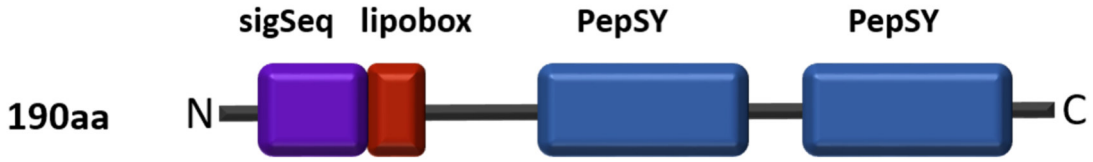

Figure 5 Domain architecture of the protein NWMN_0364
NWMN_0364 is 190 amino acid in size and possesses four sequence characteristics, a signal sequence (sigSeq) (amino acids 1-20), a lipobox (LATC) (amino acids 16-19) and two PepSY domains (amino acids54-100 and 130-186)

In 2004, the PepSY domain was identified as a characteristic domain of the propeptide of M4 peptidases by Yeats *et al.,* and it was assumed to have protease inhibitory functions [155]. Besides, there are proteins without peptidase function that harbour two PepSY domains, like NWMN_0364. Here, the function of the PepSY domains is still unclear, but the function of two proteins having two PepSY domains is associated with sporulation. These are SspA from *Streptomyces coelicolor*, a lipoprotein that is important for septum formation and spore maturation [156], and YpeB from *Bacillus subtilis* that is important for cortex hydrolysis during germination by inhibiting SleB, the lytic transglycosylase enzyme [157] [158].

The lack of knowledge regarding the function of the PepSY domain, especially of the PepSY domains that are not in combination with a peptidase, led to a closer analysis of these. Especially proteins with two PepSY domains, like NWMN_0364, were of interest.

The Pfam server displayed a PepSY family (PF03413) that contains 5648 sequence entries from 2659 species. These species mainly belong to bacteria and they are evenly distributed through the phyla *Firmicutes*, *Proteobacteria*, and *Actinobacteria*. Moreover, in the PepSY family, 114 different domain organisations are described, with the major domain

organisation being a protein with a single PepSY domain. This group contains 2045 sequence entries. The second largest domain organisation, containing 788 sequences, is a protein with two PepSY domains. These two groups are followed by organisations where a PepSY domain is in combination with other domains, often in association with transmembrane domains or peptidase domains [132]. In this study, the focus lies on the second largest group, and the UniParc database from UniProt was used to extract the 788 protein sequences of the proteins harbouring two PepSY domains [133]. Then, a localisation prediction followed using locateP [130]. For this purpose, the protein sequences were divided by their origin: from Gram-positive or Gram-negative bacteria. In the process, 75% of the proteins with two PepSY domains were found in Gram-positive bacteria and only 25% in Gram-negative bacteria. For Gram-negative bacteria, 70% of the proteins were located in the periplasm, followed by 20% outer membrane lipoproteins. For Gram-positive bacteria, three major groups appeared with 35% N-terminally anchored, 32% lipoproteins, and 29% secretory proteins (Fig. 6A). These data suggest that an architecture of two PepSY domains correlates with extracellular or cell surface-associated functions.

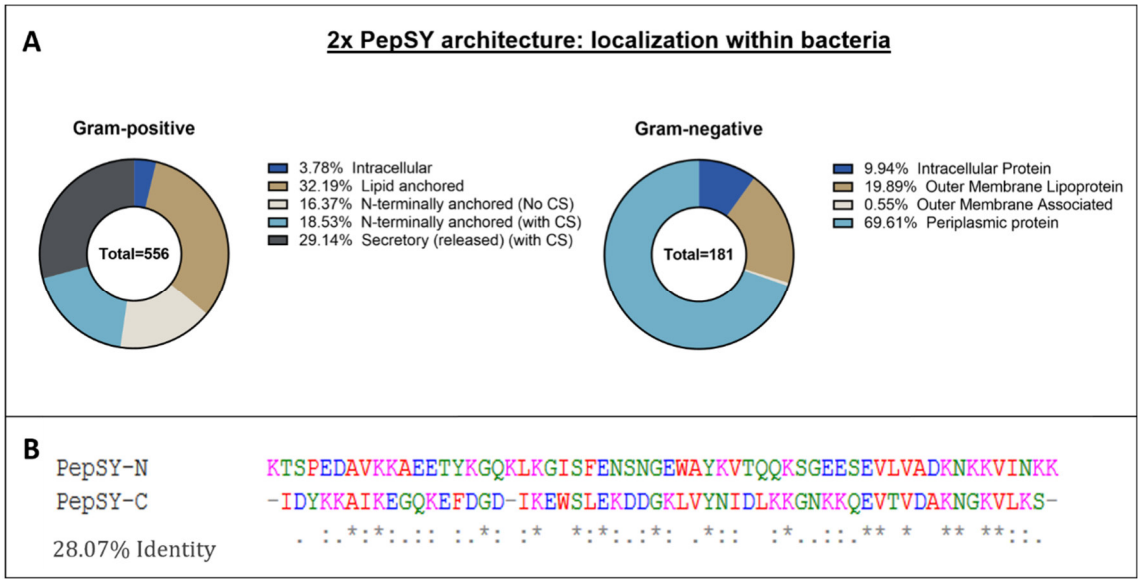

Figure 6 PepSY domain localisation in bacteria
(A) Localisation of proteins harbouring a two PepSY domain structure. The sequences entries from Pfam for proteins with two PepSY domains were downloaded using UniParc and localised using locateP. The localisations were divided into proteins from Gram-positive and proteins from Gram-negative bacteria. CS: cleavage site.
(B) Sequence alignment of the N-terminal PepSY domain (PepSY-N) and the C-terminal PepSY domain (PepSY-C) from NWMN_0364. Code: red: small and hydrophobic (including aromatic); blue: acidic; magenta: basic; green: hydroxyl + sulfhydryl + amine; *: conserved; :: strongly similar properties; .: weakly similar properties.

For a better overview, the PepSY domains of NWMN_0364 were aligned using the multiple sequence alignment tool (MUSCLE) [131]. Interestingly, the PepSY domains of NWMN_0364 are not an exact copy of each other, they only have an identity of 28.07%, having 16 conserved amino acids and 19 strongly similar amino acids (Fig. 6B).

3.2 Phenotypic Analysis of *S. aureus* Newman Δ*0364*

The determination of the function of NWMN_0364 is the main goal of this study. Without any knowledge of the function, a classical and efficient strategy is the generation of a deletion mutant and the resulting phenotypic observations. This can give hints regarding the biological role of NWMN_0364.

For functional analysis, a deletion mutant Δ*0364* was constructed in the *S. aureus* strain Newman (Fig. 7). Newman is a clinical isolate and an MSSA strain (methicillin sensitive). This strain is widely used as a model organism, especially regarding infection assays. In this study, a marker less deletion mutant was generated to limit side effects due to inserted marker genes. Therefore, the plasmid pMAD-Δ*0364* was constructed containing up- and down-stream fragments of NWMN_0364 without the gene itself (see 2.5). This was inserted into *S. aureus* Newman wild type via phage transduction. The bacteria used this plasmid to switch the nucleotide sequence of the NWMN_0364 locus with the sequence without NWMN_0364 from the plasmid via homologous recombination. The resulting mutant was verified by PCR and sequencing.

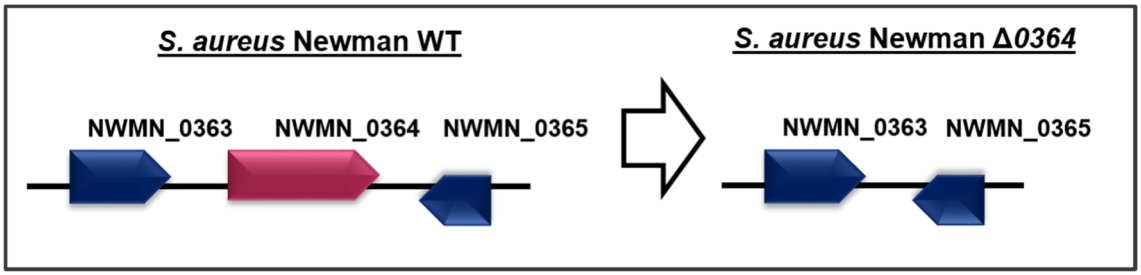

Figure 7 Genomic organisation of NWMN_0364
The depiction shows the original organisation of NWMN_0364 and its neighbour genes in *S. aureus* Newman WT (left) and the constructed *S. aureus* Newman Δ*0364* strain (right). The marker less deletion of the gene was generated using homologous recombination.

3.2.2 NWMN_0364 Is Not Essential for Bacterial Growth

The first hint at the function of a protein is the growth behaviour of the mutant compared to the wild type strain. A slower growth of a mutant indicates a defect in essential metabolism that is needed for bacterial fitness. Thus, growth experiments were performed in triplicates using *S. aureus* Newman Δ*0364* and *S. aureus* Newman wild type. The first experiment was done in a complex medium (TSB). Here, the growth behaviour of both strains was identical (Fig. 8A). Next, a synthetic medium (SA) with defined components and glucose as nutrient source was used to observe the growth behaviour. As a result, the Δ*0364* strain grew slightly faster compared to the wild type but reached the same final optical density (Fig. 8B). From these experiments, it can be concluded that NWMN_0364 is not involved in essential pathways, but further information regarding the function could not be obtained.

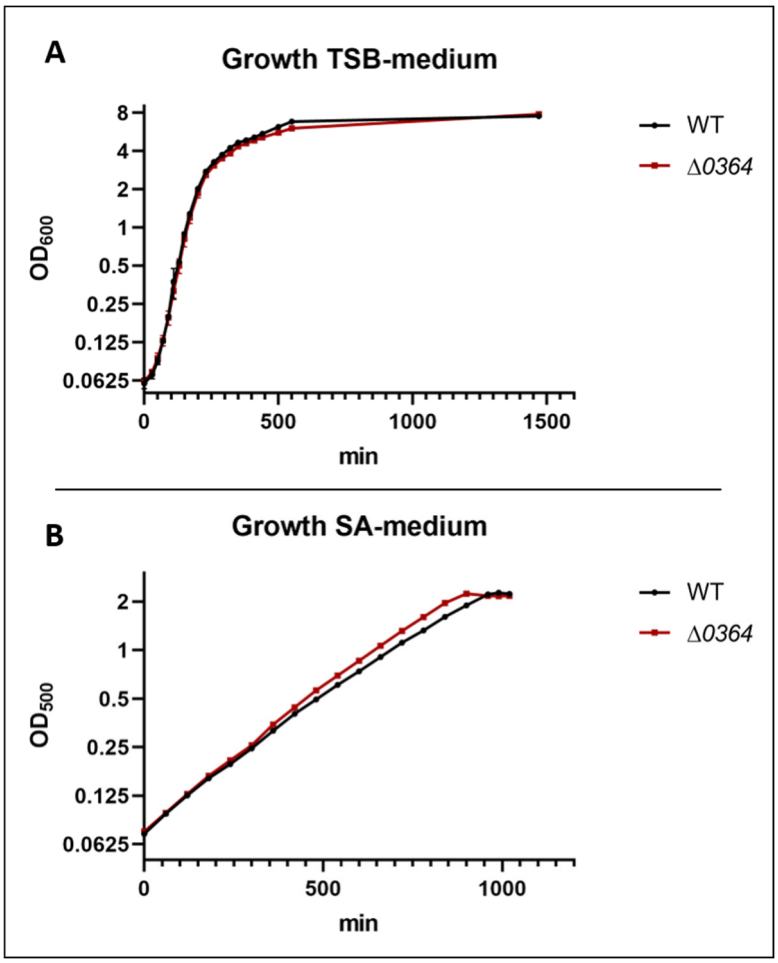

Figure 8 Growth phenotype of Δ*0364*
(A) *S. aureus* Newman WT and Δ*0364* were grown in Tryptic soy broth (TSB) at 37°C, 120rpm.
(B) *S. aureus* Newman WT and Δ*0364* were grown in staphylococcal synthetic medium (SA) at 37°C, 120rpm

3.2.3 NWMN_0364 Is Important for Virulence of *S. aureus* Newman

The topic of virulence is connected to NWMN_0364. In a study by Lawrence *et al.* (2014) [159], they found NWMN_0364 as one of the three best candidates for a vaccination in cattle because it induces high levels of IFN-γ in T-cells. Moreover, in a study with human patients having *S. aureus* infections with bloodstream invasion, NWMN_0364 was one of the eight best candidates to distinguish patients developing sepsis from those who did not. Patients with high IgG titres against NWMN_0364 less frequently developed sepsis symptoms than those with low IgG titres against NWMN_0364 [159] [128]. Hence, the presence of NWMN_0364 during human infections led to the question whether it is involved in the virulence of *S. aureus*. In order to determine its virulence ability, a macrophage infection assay was performed, using the human monocytic cell line THP-1. This cell line can be differentiated into macrophages and thus can be used for displaying human macrophage induced bacterial clearance and phagocytosis.

In this experiment, the main focus was on the ability of internalised *S. aureus* to kill macrophages. Therefore, macrophages were infected with *S. aureus* Newman WT and Newman Δ*0364*, and all extracellular bacteria that were not absorbed by the immune cells were removed by lysostaphin and antibiotics.

In order to observe the uptake of the bacteria by the THP-1 cells, one replicate was performed whereby infected macrophages were lysed after one hour of infection and the CFUs of the bacteria counted. Here, a multiplicity of infection (MOI) of 50 was set up. As a result, about 400 cells/mL could be counted for *S. aureus* Newman WT and 1100 cells/mL for *S. aureus* Newman Δ*0364,* but for both strains, a high standard deviation was calculated. Nevertheless, the results indicate that both strains were absorbed by macrophages (Fig. 9A).

Furthermore, a macrophage survival assay was performed in triplicates. Here, a MOI of 100 was set to have a good ability for the wild type strain to kill macrophages. After infection with the Newman WT and Δ*0364* strain, living macrophages were counted after 3, 12, 24, and 48 hours. Looking at the results, the wild type was able to kill most macrophages within 12 hours, and at the end of the experiment, after 48 hours, the macrophages had a survival rate of only 5%. In contrast to this, the Δ*0364* mutant was not as efficient as the wild type. After 48 hours of infection, 40% of the THP-1 macrophages were still alive (Fig. 9B). This experiment demonstrates that the *S. aureus* Newman Δ*0364* mutant strain is less virulent compared to the wild type strain.

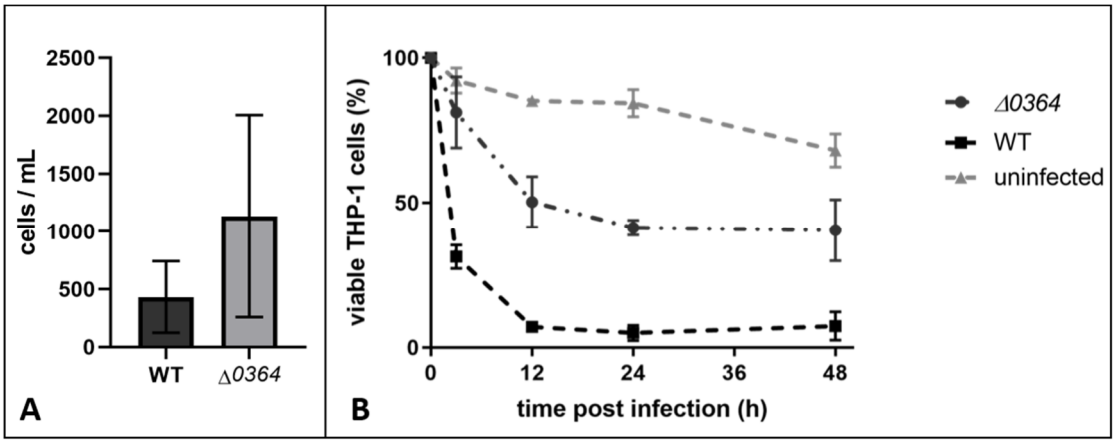

Figure 9 Decreased virulence in the Newman Δ*0364* strain
The depiction shows macrophage infection assays with human-derived macrophages (THP-1). The THP-1 were either infected with *S. aureus* Newman wild type or Δ*0364.* After infection, the extracellular bacteria were removed. Then the macrophages were either lysed and CFUs were counted (A) or living macrophages were counted (B).
(A) MOI of 50 in one replicate; the depiction shows the bacterial cells per mL derived from the lysed macrophages after one hour of infection.
(B) MOI of 100 in three replicates; 3, 12, 24, 36, and 48 hours after infection, living macrophages were counted.

3.2.4 NWMN_0364 Is Important for Accumulation of Virulence Factors

The infection assay shows that the Δ*0364* mutant strain is not able to kill macrophages as efficiently as the wild type, and the question arises what the differences between wild type and mutant are. During phagocytosis, *S. aureus* is strongly dependent on its fitness as well as virulence factors to survive the attack with antimicrobial peptides, pH shifts, and reactive oxygen species and subsequently lyse the macrophages [34]. Thus, in order to see if the mutant is equipped with virulence factors, as it is the case for the wild type, a proteome analysis was performed. The expression of virulence factors is dependent on different conditions, like bacterial density, pH, or nutrient supply. Therefore, two different media were chosen – a synthetic medium (SA) with glycerol as carbon source and a complex medium (TSB) – to cover different conditions under which virulence factors are produced. In both media, the proteome samples were taken at post-exponential growth phase to get high bacterial density. This was the case in SA at OD_{500} 2.5 and in TSB at OD_{600} 7 (Fig. 10). These experiments were performed in three biological replicates.

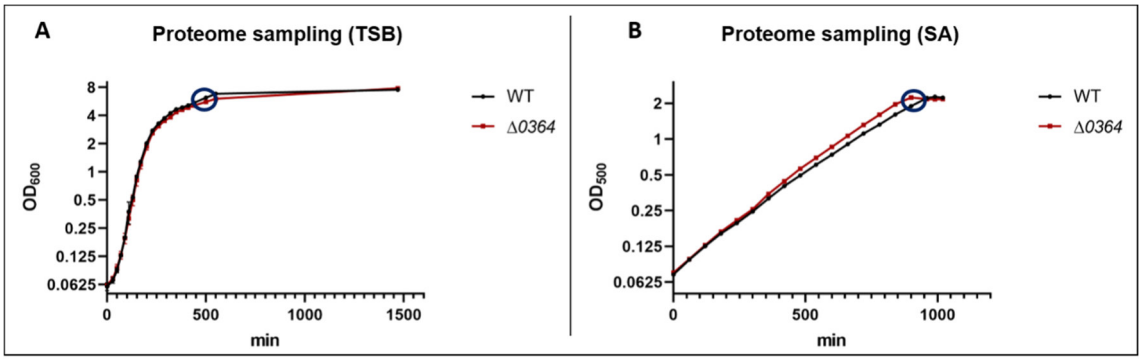

Figure 10 Proteome sampling
The depiction shows the time points and growth phases in which the samples for extracellular proteome analysis were taken. This is indicated by the circle. Extracellular proteins were prepared in triplicates from *S. aureus* Newman WT and *S. aureus* Newman Δ*0364*.
(A) Bacteria were grown until OD_{600}7 in TSB medium.
(B) Bacteria were grown until OD_{500} 2.5 in SA medium.

The extracellular proteins of both strains were prepared from the supernatant of cultures from both media, and the proteins were solved in the same volume at the end. Protein concentrations were determined, and these already displayed differences between the wild type and the mutant strain in each media. As the concentrations are dependent on the optical density of the harvested culture, only protein concentrations between WT and mutant of samples from the same medium can be compared. Accordingly, protein concentrations from TSB samples of the wild type samples were 12.7 µg/µL on average, while the concentrations of the mutant samples were 9.5 µg/µL on average. Similar observations have been made for samples coming from cultures grown in synthetic SA medium. Here, the average concentration for wild type samples was 1.2 µg/µL, while the average concentration for mutant samples was 0.61 µg/µL. These results suggest that, compared to the wild type strain, the mutant strains produce significantly lower amounts of extracellular proteins. Accordingly, for quantitative LC-MS/MS analyses, the same volume of each protein sample was used. Thereby, the volume containing 30 µg proteins was determined for the wild type for each medium.

As a result, 819 proteins were identified from wild type and mutant strain grown in SA medium of which 190 were predicted by locateP to be secreted or membrane-associated. From the wild type and mutant strain grown in TSB medium, 674 proteins were identified of which 155 were predicted to be secreted or membrane-associated. These secreted or membrane-associated proteins were further analysed.

For the analysis of the identified secreted or membrane-associated proteins, the intensities of the proteins in the wild type samples were compared to the intensities of the proteins in the Δ*0364* mutant samples and expressed as fold change. Here, the threshold for a biological

significance was set at a fold change of 2 (resemble log2 fold changes ≥1 for induced proteins or ≤-1 for repressed proteins). Among the secreted or membrane-associated proteins, 75.2% were biologically changed in the Δ*0364* mutant strain compared to wild type when grown in SA medium, and 36.7% were biologically changed when the bacteria were grown in TSB medium (Fig. 11A).

Moreover, many of these biologically changed proteins were identified when bacteria were grown in both media. Here, 44 proteins were biologically changed in the Δ*0364* mutant from both media, while only 8 proteins exclusively changed in the mutant from TSB medium. Interestingly, under SA medium conditions, an additional 91 proteins changed in the Δ*0364* mutant strain (Fig. 11B).

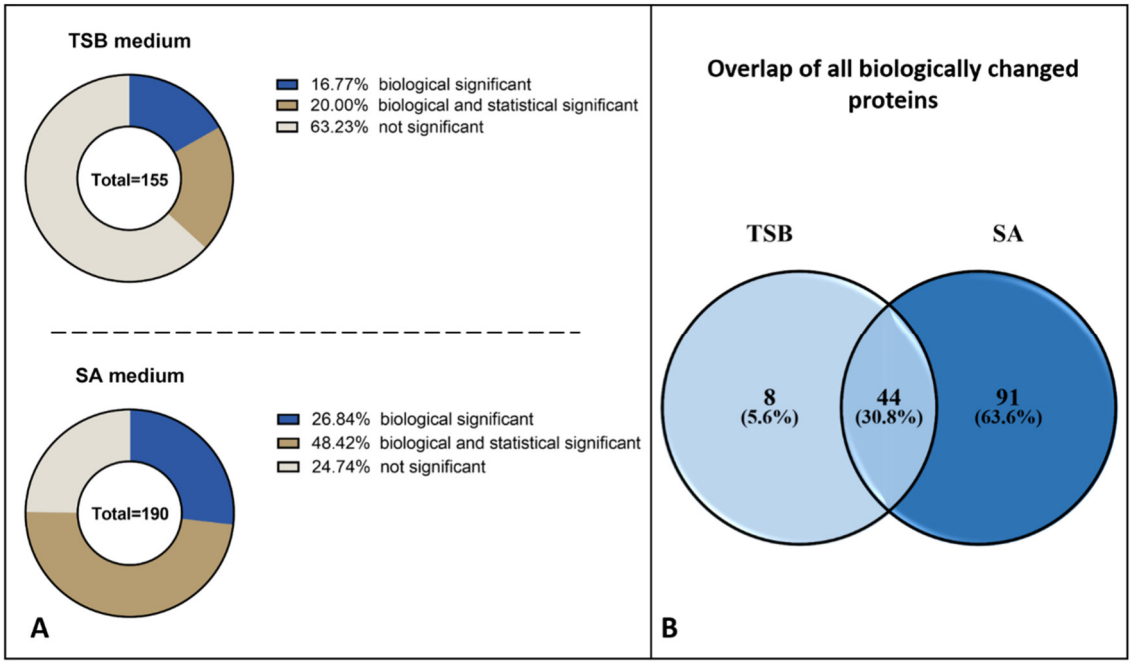

Figure 11 Significantly changed proteins between Newman WT and Newman Δ*0364*
All secreted or membrane-associated proteins that were identified from the extracellular protein extracts of *S. aureus* Newman WT and *S. aureus* Newman Δ*0364* that were grown in TSB or SA medium were compared. Here, they are displayed regarding their change in the Δ*0364* strain compared to the wild type. The threshold for a biological significance was set at 2 (resembles log2 fold changes ≥1 for induced proteins or ≤-1 for repressed proteins).
(A) The depiction shows the percentages of not significantly changed proteins, only biologically significantly changed proteins, and changed proteins with a biological and statistical significance. For a statistical significance, the p-value was below 0.05.
(B) Overlap of all biologically significant proteins that are changed by at least 2 folds in *S. aureus* Newman Δ*0364* compared to *S. aureus* Newman WT grown in TSB and SA medium.

In order to get higher confidence regarding the changed proteins in the *S. aureus Newman Δ*0364 strain, a statistical analysis was performed using t-test analysis. In the course of this, the p-value was generated and a threshold for a statistical significance was set at 0.05. For further analysis, only proteins with statistical and biological significance were considered and further described as significantly changed proteins.

When the bacteria were grown in TSB medium, 31 significantly changed proteins were identified in the mutant strain. Most of these were lower abundant in the Δ*0364* mutant strain (Fig. 12A). Additionally, 92 proteins were significantly changed in the mutant strain, when the bacteria were grown in SA medium. Most of these were also lower-abundant in the Δ*0364* mutant strain (Fig. 12B). Consequently, most significantly changed proteins were lower-abundant in the Δ*0364* mutant strain compared to wild type. Moreover, a significantly higher number of proteins changed in the mutant strain compared to the wild type, when the bacteria were grown in SA medium, indicating a higher importance of NWMN_0364 in this medium compared to TSB medium.

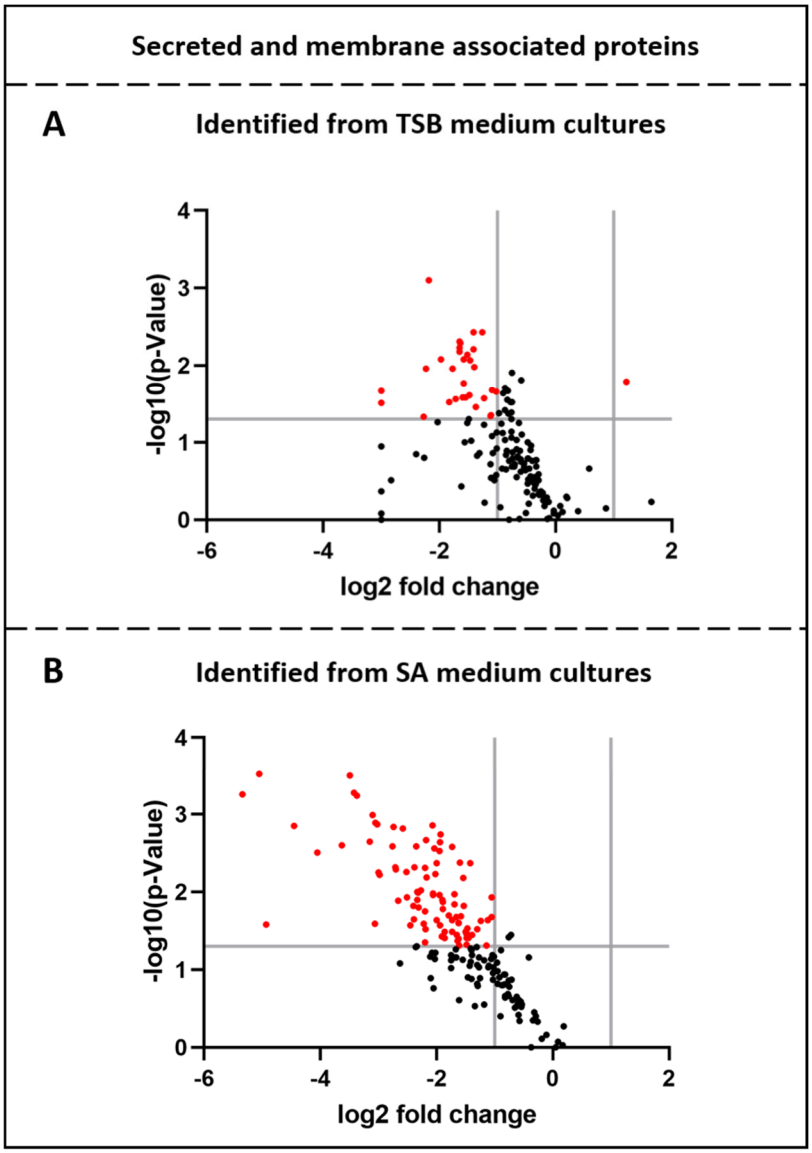

Figure 12 Volcano plot of the secreted and membrane associated proteins
The depiction shows all identified extracellular and membrane-associated proteins regarding their log2 fold change and p-value (shown as –log10) from the *S. aureus* Newman Δ*0364* strain compared to the wild type. Grey lines indicate the thresholds for biological significance, log2 fold change 1 and -1, while negative log2 fold changes indicate a lower abundance of the protein in the mutant strain. For statistical significance, the threshold was set at a -log10 (p-value) of 1.3 (resembles a p-value of 0.05). Depicted in red are proteins with biological and statistical significance.
(A) Extracellular proteins identified from the strains grown in TSB medium.
(B) Extracellular proteins identified from the strains grown in SA medium.

In order to get more information about the proteins, protein functions of the significantly changed proteins were examined. The function of these proteins was predicted using KEGG pathways. From the significantly changed proteins in the mutant strain, either grown in TSB or SA, most were predicted to be involved in virulence or are extracellular enzymes. 071% of the significantly changed proteins from TSB medium and 38% of the significantly changed proteins from SA medium belong to this category (Fig. 13). The next functional category consists of proteins associated with transport processes, with 6% of the

significantly changed proteins from TSB medium and 24% from SA medium. The last functional category that could be detected for the significantly changed proteins is cell wall and membrane-associated functions. Here, 10% of the significantly changed proteins from TSB medium belong to this category as well as 15% from SA medium (Fig. 13).

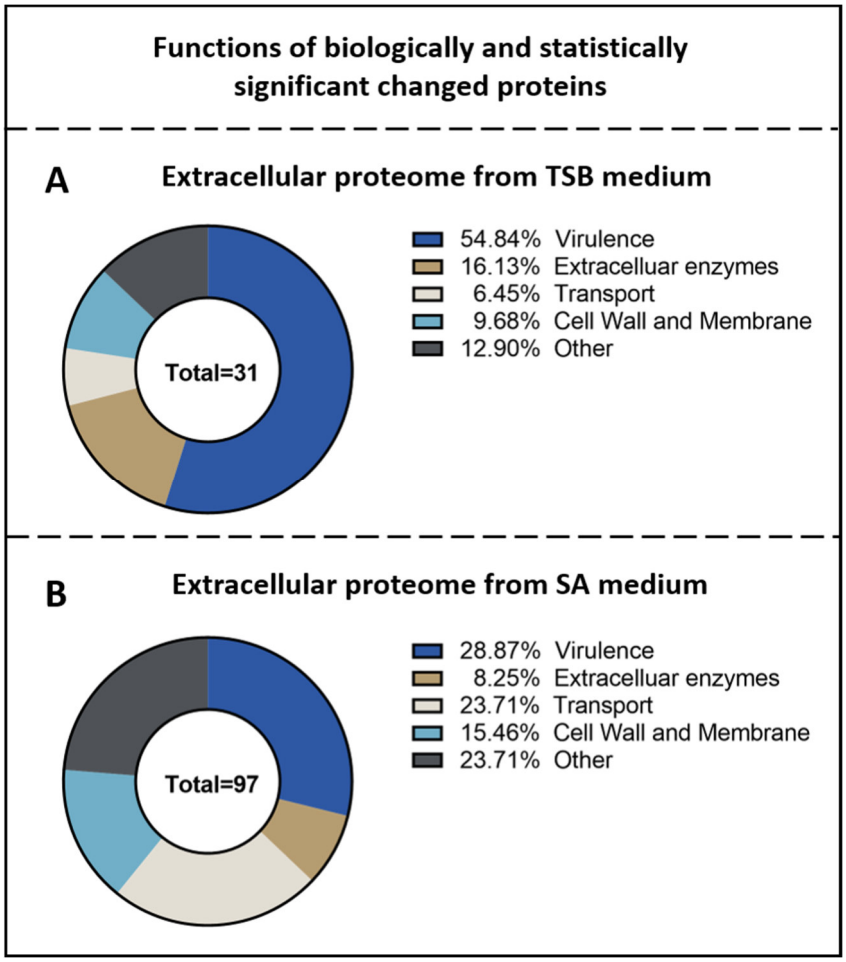

Figure 13 Functions of biologically and statistically significantly changed proteins
The function of the significantly changed proteins in the *S. aureus* Newman Δ*0364* mutant strain compared to wild type grown in TSB or SA medium was predicted using KEGG pathways.
(A) Functions of significantly changed proteins from TSB cultures.
(B) Functions of significantly changed proteins from SA cultures.

Among the significantly changed virulence factors and extracellular enzymes, pore forming toxins (Hla, HlgABC, LukDEFS), immune evasion proteins like the chemotaxis inhibitory protein (CHIPS), coagulase or the staphylococcal immunoglobulin G binding protein (Sbi), or serine proteases (SplABDE) were found (Tab. 14; 15). Additionally, superantigen-like proteins (Ssl 1,2,4-9) were exclusively found among the significantly changed proteins from SA cultures (Tab. 15). SaeP, the repressor protein of the virulence regulatory system SaeRS, was notably reduced in the mutant strain with a log2 fold change of -1.91 in the mutant from

SA medium (Tab. 15) and with a log2 fold change of -1.65 in the mutant from TSB medium (Tab. 14). It is also notable that most significantly changed virulence factors, like the pore forming toxins, Sbi, or CHIPS, are regulated by SaeRS [64] [89] [160] [161] [162]. Altogether, 25 out of 31of the significantly changed proteins in the Δ*0364* mutant strain grown in TSB medium were found to be regulated by the virulence regulatory system SaeRS (Fig. 14). For SA medium, 31 out of 92 proteins are known to be regulated by the SaeRS system (Fig. 15). Consequently, these results indicate a connection between the NWMN_0364 function and virulence as well as the virulence regulatory system SaeRS.

Besides virulence associated proteins, a significant number of proteins involved in transport processes, like the Isd proteins (Isd ABCEH) that are important for iron uptake by using haemoglobin as iron source, are among the proteins with lower abundancies in the Δ*0364* mutant strain [163]. Substrate-binding proteins of ABC transporter which are important for the uptake of amino acids and peptides (MetQ1, MetQ2, Opp-3A, TcyA, OpuCC) or metal ions (ModA, CntA) also belong to this group. Another big group consists of proteins connected to cell wall and membrane. These are proteins like the penicillin-binding proteins (Pbp2, Pbp3), cell wall amidases (LytH, Sle1), or transglycosylases (SceD, IsaA) (Tab. 15). Most of these proteins were significantly changed in the Δ*0364* mutant strain when grown in SA medium. Only a few were significantly changed in the Δ*0364* mutant strain when grown in TSB medium, like the transglycosylase SceD or an iron compound ABC transporter substrate-binding protein (Tab. 14).

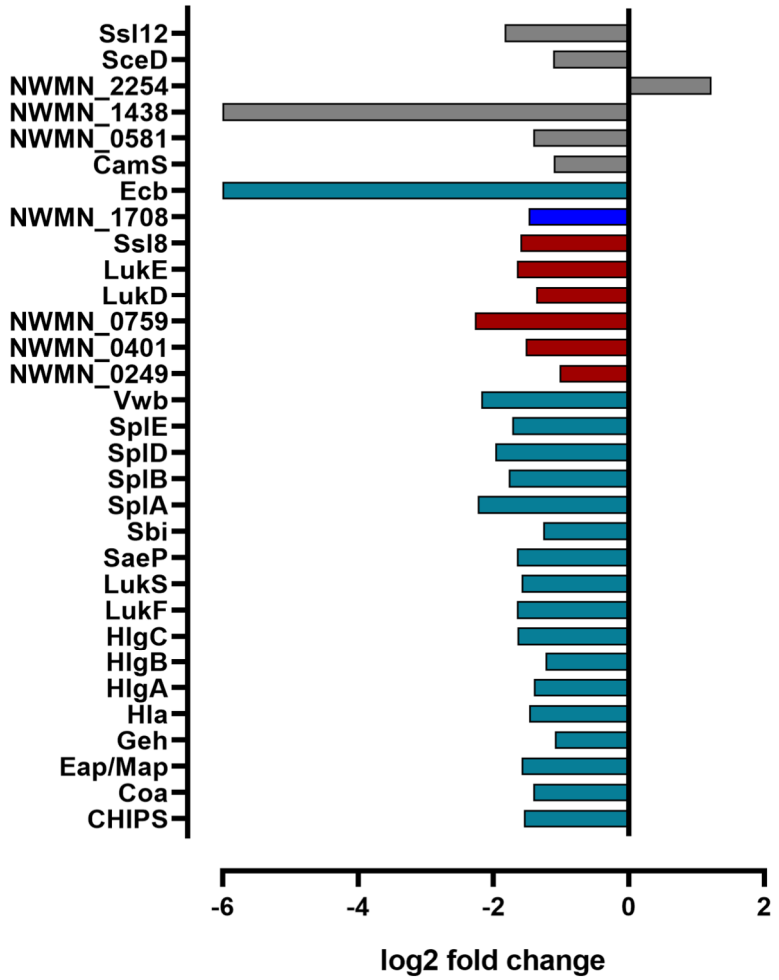

Figure 14 Significantly changed proteins in the Δ*0364* mutant compared to WT grown in TSB medium
The displayed proteins were biologically and statistically changed in the *S. aureus* Newman Δ*0364* strain compared to the wild type when the bacteria were grown in TSB medium. The threshold for a biological significance was set at 2 (resemble log2 fold changes ≥1 for induced proteins or ≤-1 for repressed proteins), and for a statistical significance, the p-value was below 0.05. The depiction shows the log2 fold changes. Blue: the transcription of the encoding gene is regulated by WalKR; red: the transcription of the encoding gene is regulated by SaeRS; cyan: the transcription of the encoding gene is regulated by WalKR and SaeRS.

These significantly changed proteins in the mutant strain that are not related to virulence cannot be explained by a genetic regulation of the SaeRS system. However, they also give hints regarding the function of NWMN_0364. The significantly changed proteins mainly were lower-abundant in the mutant strain and diverse in their functions. Thus, in the Δ*0364* mutant strain, a diminished protein secretion might be a possible option. Interestingly, when *S. aureus* Newman WT and Δ*0364* mutant strains were grown in SA medium, proteins important for the transport of proteins from the cytoplasm to the extracellular environment via the Sec-translocation pathway were identified as lower-abundant in the mutant strain. Here, SecDF had a log2 fold change of - 2.03 but was statistically not significant, and also the

YajC protein was only identified in the wild type strain. In contrast to this, when the *S. aureus* Newman WT and Δ*0364* mutant strains were grown in TSB medium, SecDF had not been identified and YajC was not significant with a log2 fold change of -0.8. Consequently, the proteome data indicates a connection between the NWMN_0364 function and protein secretion when the bacteria are in SA medium conditions.

A diminished protein secretion can have several causes. One possibility is a genetic regulation of the genes encoding the proteins of the Sec-translocation pathway. Here, one regulatory system is the WalKR two-component system. This system is important for cell wall biosynthesis, and it has already been shown that it influences the expression of the *NWMN_0364* gene [86]. Especially the WalKR activating proteins WalH and WalI were reduced in the mutant strain when bacteria were grown in SA medium but not in TSB medium. They were not statistically significant but had a log2 fold change of - 0.96 and - 1.67. This indicates a WalKR effect in the mutant strain, and to support this assumption, the genetic regulations of significantly changed proteins were determined by means of literature regarding an influence by the WalKR system [80] [86]. As a result, 31 out of 92 proteins were found to be genetically regulated by WalKR when bacteria were grown in SA medium (Fig. 15). Furthermore, 19 out of 31 significantly changed proteins were found to be regulated by the WalKR two-component system when the bacteria were grown in TSB medium (Fig. 14). This result indicates an effect on the WalKR system in the Δ*0364* mutant strain when the bacteria are in SA medium conditions.

Summing up, in *S. aureus* Newman Δ*0364*, the extracellular proteins were reduced, especially virulence factors. This strengthens the assumption that NWMN_0364 is important for the virulence of *S. aureus*, and it might be important for the accumulation of virulence factors. Additionally, a connection of the NWMN_0364 function to the SaeRS system and the WalKR system is possible. The function of NWMN_0364 seems to be more important under synthetic medium conditions.

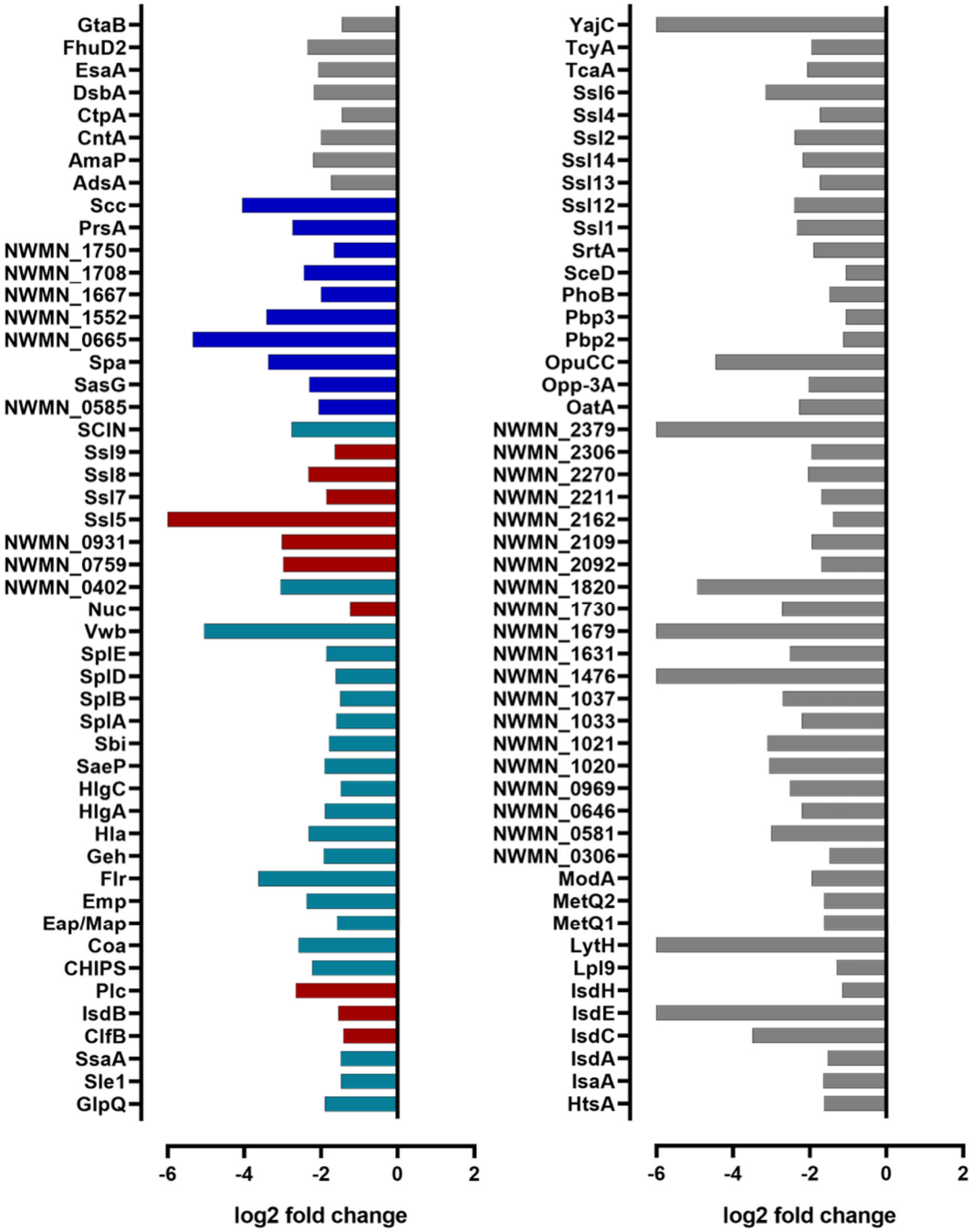

Figure 15 Significantly changed proteins in the Δ*0364* mutant compared to WT grown in SA medium
The displayed proteins were biologically and statistically changed in the *S. aureus* Newman Δ*0364* strain compared to the wild type when the bacteria were grown in SA medium. The threshold for a biological significance was set at 2 (resembles log2 fold changes ≥1 for induced proteins or ≤-1 for repressed proteins), and for a statistical significance, the p-value was below 0.05. The depiction shows the log2 fold changes. Blue: the transcription of the encoding gene is regulated by WalKR; red: the transcription of the encoding gene is regulated by SaeRS; cyan: the transcription of the encoding gene is regulated by WalKR and SaeRS.

3.2.5 NWMN_0364 Is Important for Transcription of Virulence Genes and the *sae* Operon

Referring to the extracellular proteome analyses, there is a strong indication that NWMN_0364 might interfere with the SaeRS-dependent regulation of virulence factors. SaeRS is a two-component system and mainly activates the transcription of genes encoding these virulence factors. In order to investigate whether the observed differences in the amount of these virulence factors in the mutant strain are triggered by changes in the transcriptional activity of their respective genes, relative transcript levels for selected genes were determined. These selected genes were *sbi* and *hlgC* coding for the staphylococcal immunoglobulin binding protein (Sbi) and the γ-haemolysin toxin (HlgC). Both proteins were found to be significantly reduced in the mutant strain during proteome analysis, and both corresponding promoters have a different affinity when it comes to the binding of SaeR, the transcriptional regulator of SaeRS. The promoter of s*bi* possesses one binding site, while the promoter of *hlgC* possesses two binding sites (Fig. 15) [99]. For this reason, two situations are covered in this experiment: an activation with a low amount of active SaeR (*sbi*) as well as an activation with a high amount of active SaeR (*hlgC*).

For the experiment, the complete RNA was isolated from *S. aureus* Newman wild type and *S. aureus* Newman *Δ0364* cells growing in staphylococcal synthetic medium (SA). The sampling was performed similar to the proteomic experiments at OD_{500} 2.5 and in triplicates. As a result, the RNA levels of *sbi* and *hlgC* were much lower in the *Δ0364* mutant compared to the wild type (Fig. 16). Consequently, the lower amounts of Sbi and HlgC observed in the proteome analysis can be due to a lower transcriptional activity of their respective genes.

The genes *sbi* and *hlgC* are regulated by SaeRS. The activity of SaeRS can be viewed by the expression of the *sae* operon, due to its self-regulatory properties [101]. In this experiment, the relative RNA intensities of the *saeP* and *saeS* gene were determined, which displayed the first and the last gene in the operon (Fig. 16). The same RNA samples as before in the experiment for *sbi* and *hlgC* were used.

In this experiment, the RNA levels of *saeS* and *saeP* were much lower in the *Δ0364* mutant, with about 30–35% of the intensities detected in the wild type. According to these results, it could be speculated that the SaeRS system was less active in *S. aureus* Newman *Δ0364*, resulting in lower amounts of SaeRS-dependent virulence factors.

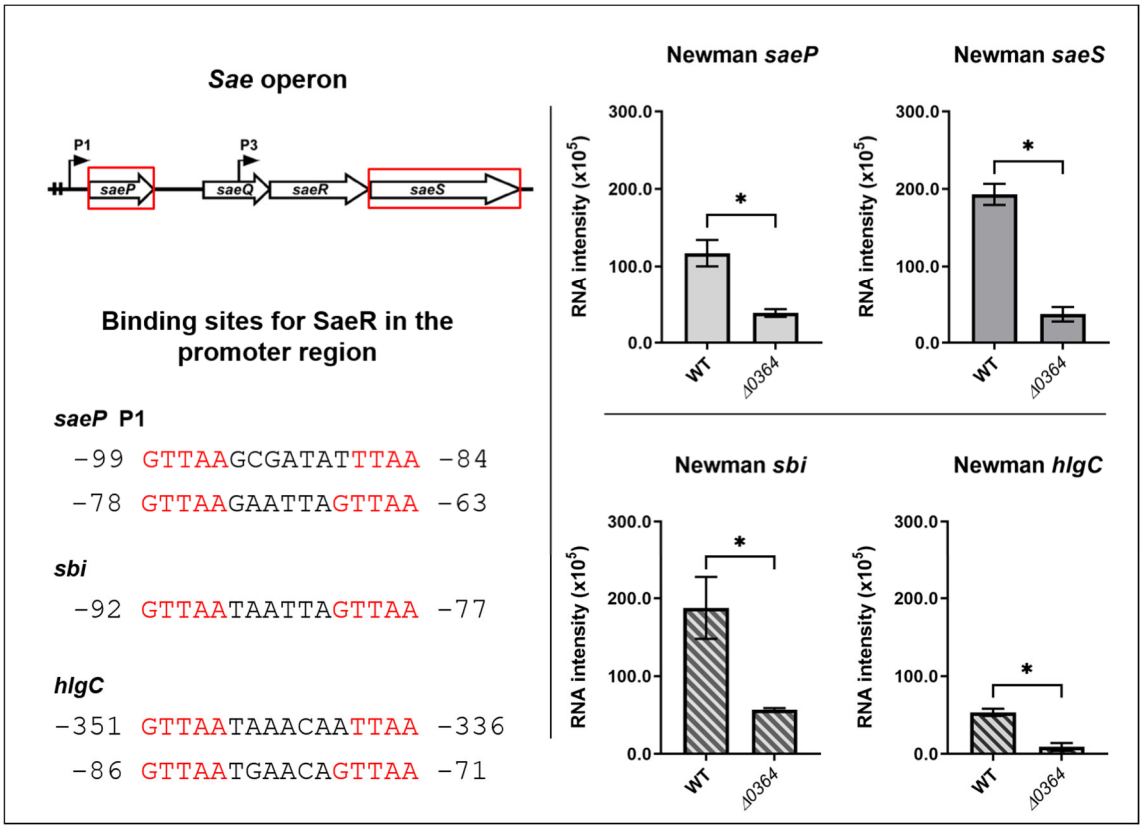

Figure 16 RNA analysis of Newman WT and Δ*0364* grown in SA medium
Left: The depiction shows the organisation of the *sae* operon and the binding sites for SaeR, the transcriptional regulator [95] [99]. Right: The depiction shows the RNA intensities of the genes *saeP, saeS*, *sbi*, and *hlgC* from the strain Newman wild type and Δ*0364* mutant cultivated in staphylococcal synthetic medium (SA). This experiment was performed in triplicates, and the RNA was sampled at stationary growth at an OD_{500} 2.5. Then the transcript levels were analysed. The * indicates a p-value below 0.05.

The strain Newman has a L18P substitution in the first transmembrane helix of the SaeS protein. This leads to a constitutively active kinase domain, which in turn leads to a constant expression of SaeRS-dependent virulence factors [98]. In order to exclude that the here observed effects of NWMN_0364 on SaeRS-dependent virulence gene expression are strain-specific, the strain *S. aureus* COL, which does not possess the L18P substitution, was included in this study. In the COL strain, SACOL0444 is the orthologue to NWMN_0364 with 100% nucleotide sequence similarity. The wild type and a Δ*0444* mutant strain, kindly provided by V. Westermann (University of Greifswald), were cultivated in SA medium to OD_{500} 2.5, under the same conditions as the Newman strain. The RNA was isolated in triplicates and used for the determination of relative RNA levels. As before in Newman, the genes *saeP* and *saeS* of the *sae* operon were chosen; furthermore, *sbi* and *hlgC* were chosen for the SaeR-regulated genes.

The results display a significantly reduced transcript level for *sbi* in the Δ*0444* mutant strain, which only reached about 30% of the wild type transcript level. However, no significant

change in the RNA level was observed for *hlgC* (Fig. 17). For the genes from the *sae* operon, *saeP* and *saeS* also showed a significant reduction in the RNA level in the Δ*0444* mutant strain, which only reached about 10% of the wild type transcript level (Fig. 17). With this, the COL Δ*0444* mutant strain showed an altered genetic regulation due to a less active SaeRS system. For this reason, a Newman strain-specific effect of NWMN_0364 could be excluded.

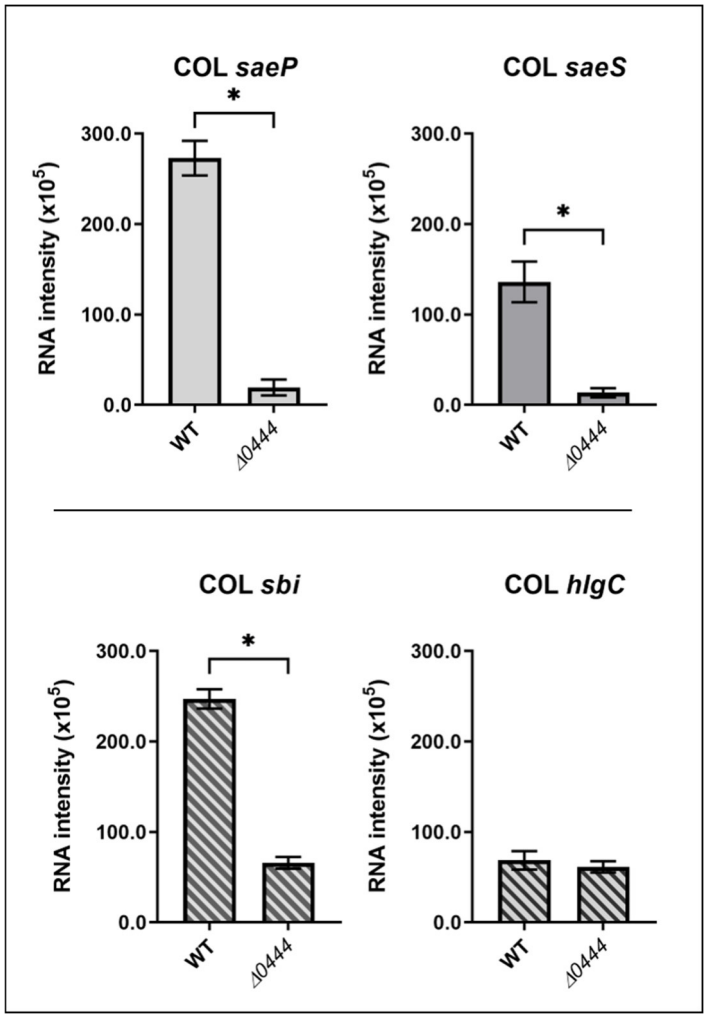

Figure 17 RNA analysis of COL WT and Δ*0444* grown in SA medium
The depiction shows the RNA intensities of the genes saeP, saeS, sbi, and hlgC from the strain COL wild type and Δ*0444* mutant cultivated in staphylococcal synthetic medium (SA). This experiment was performed in triplicates, and the RNA was sampled at stationary growth at an OD_{500} 2.5. Then the transcript levels were analysed. The * indicates a p-value below 0.05.

The proteome analyses had shown that lower amounts of virulence factors were identified in the Δ*0364* mutant strain when the bacteria were grown in SA medium as well as in TSB medium. Thus, a transcriptional analysis was also performed for *S. aureus* Newman/COL WT and Δ*0364/Δ0444* strains grown in TSB medium to confirm a gene expression effect that could cause the lower amounts of proteins in the proteome analysis. Here, the bacteria were

cultivated until post-exponential growth, and RNA sampling was performed similar to the proteomic experiments at OD_{600} 7 in triplicates. Moreover, the same genes of the *sae* operon, *saeS* and *saeP*, were analysed. The results for the *saeS* and *saeP* gene show no significant differences between wild type and mutant RNA levels in Newman or COL strain (Fig. 18).

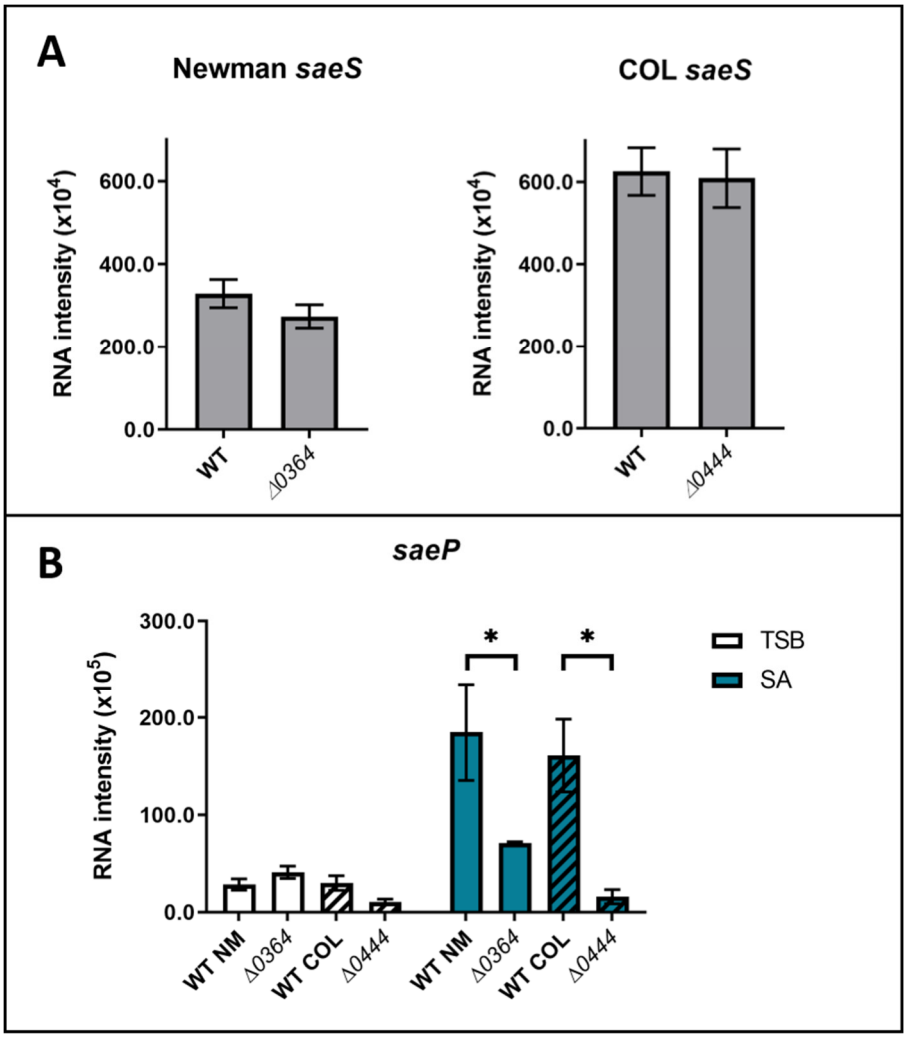

Figure 18 RNA analysis of Newman/COL WT and Δ*0364/Δ0444* grown in TSB/SA
The depiction shows the RNA intensities of the strains COL and Newman wild type and Δ*0364/Δ0444* strains. The * indicates a p-value below 0.05.
(A) RNA levels of *saeS* from strains cultivated in tryptic soy broth (TSB). This experiment was performed in triplicates, and the RNA was sampled at stationary growth at an OD_{600} 7.
(B) RNA levels of *saeP* from strains cultivated in TSB and staphylococcal synthetic medium (SA). This experiment was performed in triplicates, and the RNA was sampled at stationary growth at an OD_{500} 2.5.

In order to directly compare the transcript levels of *saeP* in TSB and SA medium, RNA from *S. aureus* Newman/COL WT and Δ*0364/Δ0444* strains grown in SA and TSB medium was used in the same experiment. The results show severe differences when the strains were grown in TSB or SA medium. In TSB, the wild type *saeP* RNA level was much lower than in SA medium. This is true for both strains. In addition, the *saeP* RNA level of the mutant was also slightly lower in TSB compared to SA but not as severely as in the wild type. Interestingly, the wild type RNA levels in the Newman strain in TSB were in fact below the RNA level of the mutant strain in SA medium (Fig. 18B). These experiments demonstrate that the transcription of the *sae* operon is not altered when WT and mutant strains are grown in TSB medium, leading to the assumption that the effects of NWMN_0364 on the SaeRS activity are medium-dependent.

3.3 Interaction Partner of NWMN_0364

The phenotypic analyses of the Δ*0364* mutant provide first hints regarding the function of NWMN_0364. Accordingly, NWMN_0364 may influence the activity of the SaeRS system and possibly also other systems like WalKR. In order to get more information about the NWMN_0364 function, the goal of the following experiments was to identify proteins directly interacting with NWMN_0364.

3.3.1 Generation of a *S. aureus* Newman *0364-strep* Mutant

For interaction studies, a Newman *0364-strep* mutant was generated. This mutant possesses a NWMN_0364 variant with a C-terminal Strep-tag that can be used to enrich NWMN_0364 and its interaction partners via affinity chromatography. For the construction of the mutant, the strain *S. aureus* Newman Δ*0364* was used to insert the constructed plasmid pMAD-0364-strep containing the gene NWMN_0364 connected to the eight amino acid Strep-tag (amino acids WSHPQFEK) (see 2.5). The bacteria used this plasmid to insert the *0364-strep* gene back into the genomic locus of the originally deleted *NWMN_0364* via homologous recombination (Fig. 19). The resulting mutant was verified by PCR and DNA sequencing.

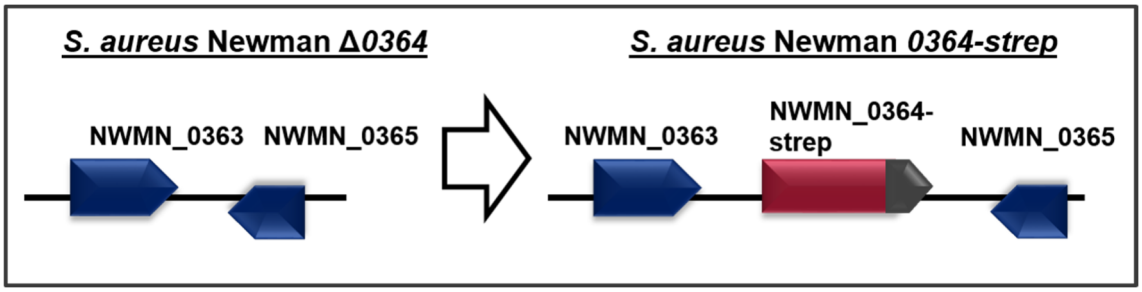

Figure 19 Genomic organisation of *S. aureus* Newman 0364-strep
The depiction shows the genomic organisations of NWMN_0364 and its neighbour genes in *S. aureus* Newman Δ*0364* and the *S. aureus* Newman 0364-strep strain. The insertion of 0364-strep was generated using homologous recombination. Red: gene encoding NWMN_0364; grey: the sequence for the Strep-tag.

3.3.2 Possible Interaction Partners of NWMN_0364 Are SaeP and Substrate-binding Proteins of ABC-transporter

For the following interaction assays, protein extracts were needed, and a Western blot analysis was performed to investigate in which protein extract NWMN_0364 could be found. As a lipoprotein, NWMN_0364 is covalently bound to phospholipids localised on the outside of the cytoplasmic membrane. Thus, by means of the Western blot analysis, NWMN_0364 was detected both in membrane and in extracellular protein extracts (Fig. 20).

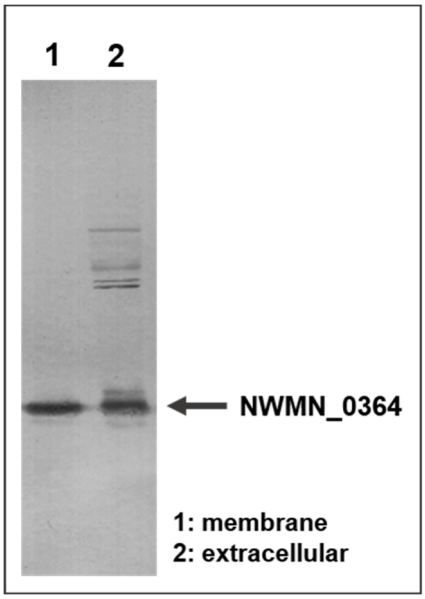

Figure 20 Western blot membrane proteins compared to extracellular proteins
Membrane proteins and extracellular proteins were isolated from *S. aureus* Newman cultivated in TSB medium and grown until optical density 7. Polyclonal antibodies specific for NWMN_0364 were used.

Interaction Partners of NWMN_0364 from Membrane Protein Extract

The first *in vivo* interaction assay was set up for NWMN_0364 to find interaction partners. This assay was a co-immunoprecipitation assay where the strains *S. aureus* Newman wild type and Δ*0364* were cultivated in SA medium until stationary growth phase. Formaldehyde was used to crosslink interacting proteins, and membrane proteins were isolated. Subsequently, NWMN_0364 and its interaction partner were isolated via protein A beads containing antibodies specifically for NWMN_0364, and eluates were analysed on a 12% SDS-gel. Here, the Δ*0364* strain served as a negative control. The results show that the protein A beads containing antibodies specifically for NWMN_0364 bind more proteins from the protein extracts of the Δ*0364* mutant strain than from the wild type strain (Fig. 21). Regarding this result, the samples from the Δ*0364* strain were not used as negative control, and only the three replicates of the wild type samples were analysed with respect to interaction partners.

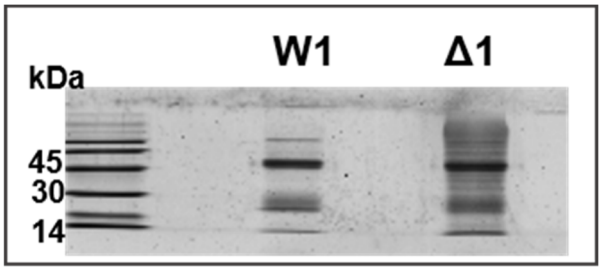

Figure 21 Co-immunoprecipitation eluates from Newman WT and Δ*0364*
The strains *S. aureus* Newman WT and Δ*0364* were cultivated in SA medium to stationary growth phase, proteins were cross-linked via formaldehyde, and membrane proteins were extracted. NWMN_0364 plus the bound interaction partner was isolated via protein A beads containing antibodies specifically for NWMN_0364. The depiction shows elutions from protein A beads from the first replicate. W: eluate of the wild type; Δ: eluate of the Δ*0364* mutant.

After analysing the eluted NWMN_0364 with its bound interaction partners from WT samples via LC/MS/MS, 413 proteins were identified. In order to eliminate false positives and to find real interaction partners, the intensity of NWMN_0364, which resembles the abundance of NWMN_0364, was a reference for the relative intensities of all other identified proteins. Thus, only proteins with a relative intensity of at least 0.02 and a relative standard deviation (RSD) of max 0.35 were included, which showed a robust and reproducible relative intensity among replicates. Only three candidates fulfilled these requirements (Fig. 22, Tab. 16): a 30S ribosomal protein S12 (RpsL), a methionine ABC transporter substrate-binding protein (MetQ1), and SaeP, the negative regulatory protein of the SaeRS

system. The most abundant protein in this assay was SaeP, with a relative intensity of 0.083 and an RSD of 0.29. In sum, this first *in vivo* interaction assay reveals SaeP and MetQ1 as possible interaction partners of NWMN_0364.

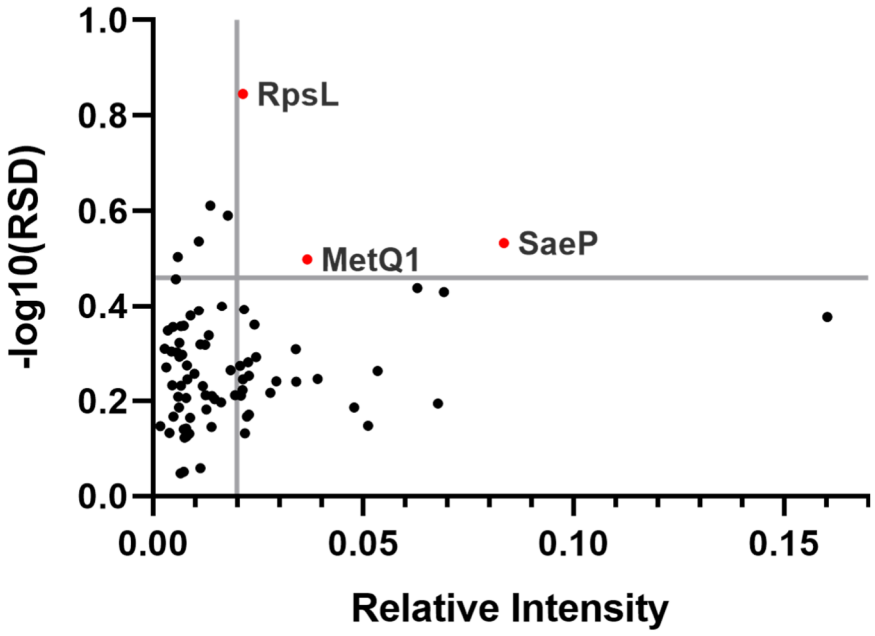

Figure 22 Possible interaction partners of NWMN_0364 from Co-IP
The depiction shows the identified proteins from a co-immunoprecipitation assay performed in triplicates. The strain *S. aureus* Newman WT was cultivated in SA medium to stationary growth phase, proteins were cross-linked via formaldehyde, and membrane proteins were extracted. Using protein A beads containing antibodies specifically for NWMN_0364, NWMN_0364 and possible interaction partners were co-purified. After the elution of NWMN_0364, possible interacting proteins were identified by LC-MS/MS analyses. Only proteins with a relative intensity of at least 0.01 were considered as possible interaction partners. The relative intensity demonstrates the abundance of the identified protein compared to the bait protein NWMN_0364. RSD: The relative standard deviation determines the reproducibility over three replicates. The thresholds for possible interaction partners were set to >0.02 for the relative intensity and to <0.35 for the RSD (equals –log10 (RSD) >0.46). Proteins above these thresholds were identified as possible interaction partners and marked in red. These are SaeP, the regulatory protein of SaeRS with a relative intensity of 0.083 and an RSD of 0.29, MetQ1, a methionine ABC transporter substrate-binding protein with a relative intensity of 0.036 and an RSD of 0.32, and RpsL, a 30S ribosomal protein with a relative intensity of 0.021 and an RSD of 0.14.

Interaction Partners of NWMN_0364 from Extracellular Protein Extract

A strep-tag pull-down assay was used as a second approach to find interaction partners of NWMN_0364. Here, the strains *S. aureus* Newman *0364-strep* and wild type were cultivated in TSB medium until stationary growth. Formaldehyde was added to bind NWMN_0364 to its interaction partner, and extracellular proteins were prepared. This experiment was performed in triplicates, and the Newman WT strain served as a negative control. Using

affinity chromatography, NWMN_0364 was co-purified with its interaction partners. Eluates were analysed on an SDS-gel. As expected, significantly higher protein amounts were present in elutions from the *0364-strep* strain compared to those from the wild type strain (Fig. 23).

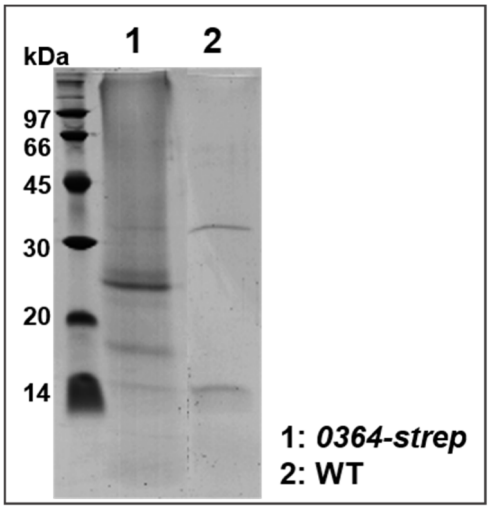

Figure 23 Strep-tag pull-down assay, eluates from Newman WT and 0364-strep
The strains S. aureus Newman WT and 0364-strep were cultivated in TSB medium until stationary growth, proteins were cross-linked via formaldehyde, extracellular proteins were sampled, and NWMN_0364 plus its bound interaction partner was isolated via affinity chromatography. The depiction shows the elutions from affinity chromatography from the first replicate.

After analysing the eluted proteins via LC-MS/MS, a total amount of 439 proteins was identified from both extracts. In order to find specific interaction partners, only proteins with at least 40-fold higher intensity in the *0364-strep* samples compared to wild type samples were considered. Moreover, the intensity of NWMN_0364, which resembles the abundance of NWMN_0364, was used as a reference for relative intensities of all identified proteins. In the end, only proteins with a relative intensity of at least 0.001 and a relative standard deviation (RSD) of max 0.35, which showed a robust and reproducible relative intensity among replicates, were considered as specific interaction partners. Only eight proteins met these requirements. Five of these were substrate-binding proteins of ABC transporters (Fig. 24, Tab. 17). These are two methionine (MetQ1, MetQ2), an amino acid (TcyA), a manganese (MntC), and a molybdate (ModA) transporter. The most abundant and most reproducible protein in this assay was MntC with a relative intensity of 0.032 and an RSD of 0.04. In addition, the hypothetical protein NWMN_0753, the dihydrolipoyl dehydrogenase PdhD, and a 50S ribosomal protein L22 (RplV) were identified as possible interaction partners. Summing up, this *in vivo* interaction assay reveals possible interaction partners of NWMN_0364 among substrate-binding proteins of ABC transporters.

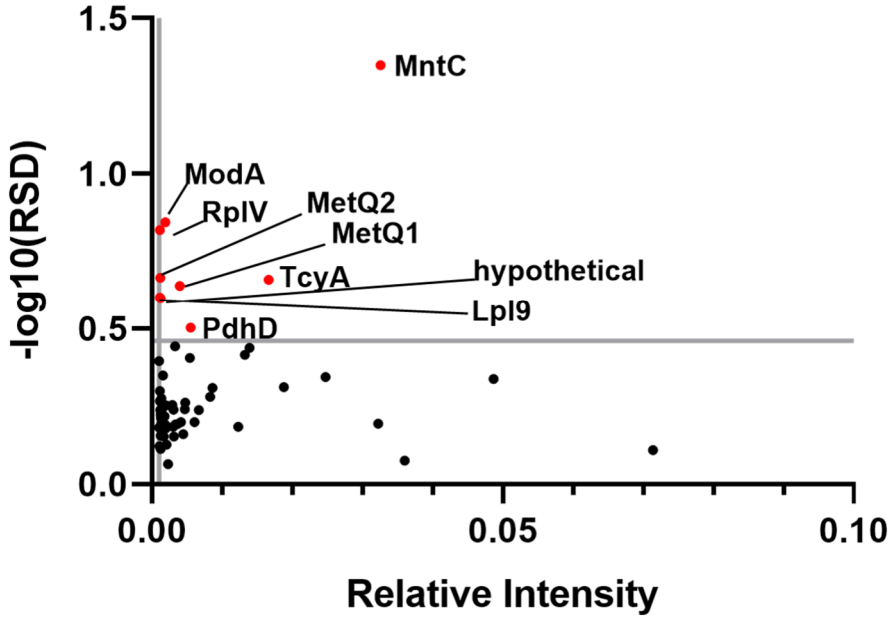

Figure 24 Possible interaction partners of NWMN_0364 in TSB medium
The depiction shows the identified proteins from a strep-tag pull-down assay performed in triplicates. The strains *S. aureus* Newman WT and *0364-strep* were cultivated in TSB medium until stationary growth, proteins were cross-linked via formaldehyde, extracellular proteins were sampled, and NWMN_0364 plus its bound interaction partner was isolated via affinity chromatography. After the elution of NWMN_0364 with its interaction partner and the measurement via LC-MS/MS, only possible interaction partners with a relative intensity of at least 0.01 were considered. The relative intensity demonstrates the abundance of the identified protein compared to the bait protein NWMN_0364. RSD: The relative standard deviation determines the reproducibility over three replicates. The thresholds for possible interaction partners were set to >0.02 for the relative intensity and to <0.35 for the RSD (equals –log10 (RSD) >0.46). Proteins above these thresholds were identified as possible interaction partners and marked in red.

3.3.4 Production of Recombinant Proteins NWMN_0364, SaeP, MetQ1 and TcyA

For further elucidation of the protein interaction of NWMN_0364, NWMN_0364, SaeP, MetQ1, and TcyA were recombinantly produced. SaeP was chosen, as it was the most abundant possible interaction partner in the co-immunoprecipitation assay, and it regulates the virulence regulatory system SaeRS. A connection of NWMN_0364 and SaeRS was indicated before by the proteome and transcriptional analysis. MetQ1 was the protein of choice as it appeared in both *in vivo* interaction assays, and TcyA was a representative of the strep-tag pull-down assay with the second highest relative intensity among the possible interaction partners (Fig. 24). The proteins were expressed in *E. coli* with a Strep-tag allowing purification via affinity chromatography. Due to the low yield of TcyA and MetQ1, these proteins were not further purified after affinity chromatography. Furthermore, the analysis of these proteins on an SDS-gel showed that they run on the gel corresponding to their calculated molecular weight (TcyA 27.3 kDa, MetQ1 28.5 kDa; Fig. 24). Even without

size exclusion chromatography, the proteins were pure, as only one prominent protein band was visible on a 12% SDS-gel.

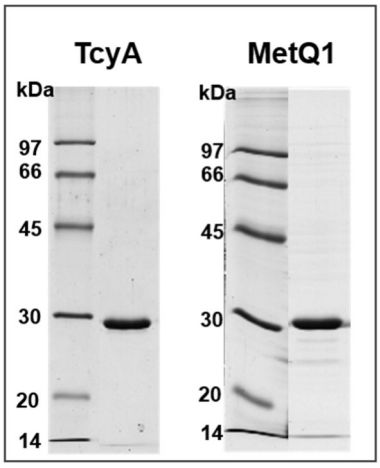

Figure 25 Recombinant proteins MetQ1 and TcyA
After expression in *E. coli* and affinity chromatography, the proteins MetQ1 and TcyA were analysed on a 12% denaturing SDS-gel using a colloidal Coomassie staining solution and the low molecular weight standard from GE healthcare.

After affinity chromatography, the recombinant proteins NWMN_0364 and SaeP were further purified using a size exclusion chromatography. The resulting elutions showed only one prominent protein band on an SDS gel (Fig. 26). The observed bands of these two recombinant proteins run a bit higher than it was predicted by their calculated molecular weights (NWMN_0364 20.4 kDa, SaeP 15 kDa). Moreover, UV absorption during size exclusion chromatography demonstrated two distinct protein peaks for NWMN_0364 as well as for SaeP (Fig. 26). Analysing these peaks on an SDS-gel shows for NWMN_0364 that the higher peak corresponds to the molecular weight of NWMN_0364, while the smaller peak corresponds to a much smaller protein. In fact, the analysis of the peaks from the SaeP sample shows that both peaks correspond to the same protein band on the SDS-gel, indicating that both peaks belong to the recombinant SaeP. The two peaks for SaeP indicate different oligomerisation states for SaeP. Consequently, NWMN_0364, SaeP, MetQ1, and TcyA were successfully recombinantly generated and purified.

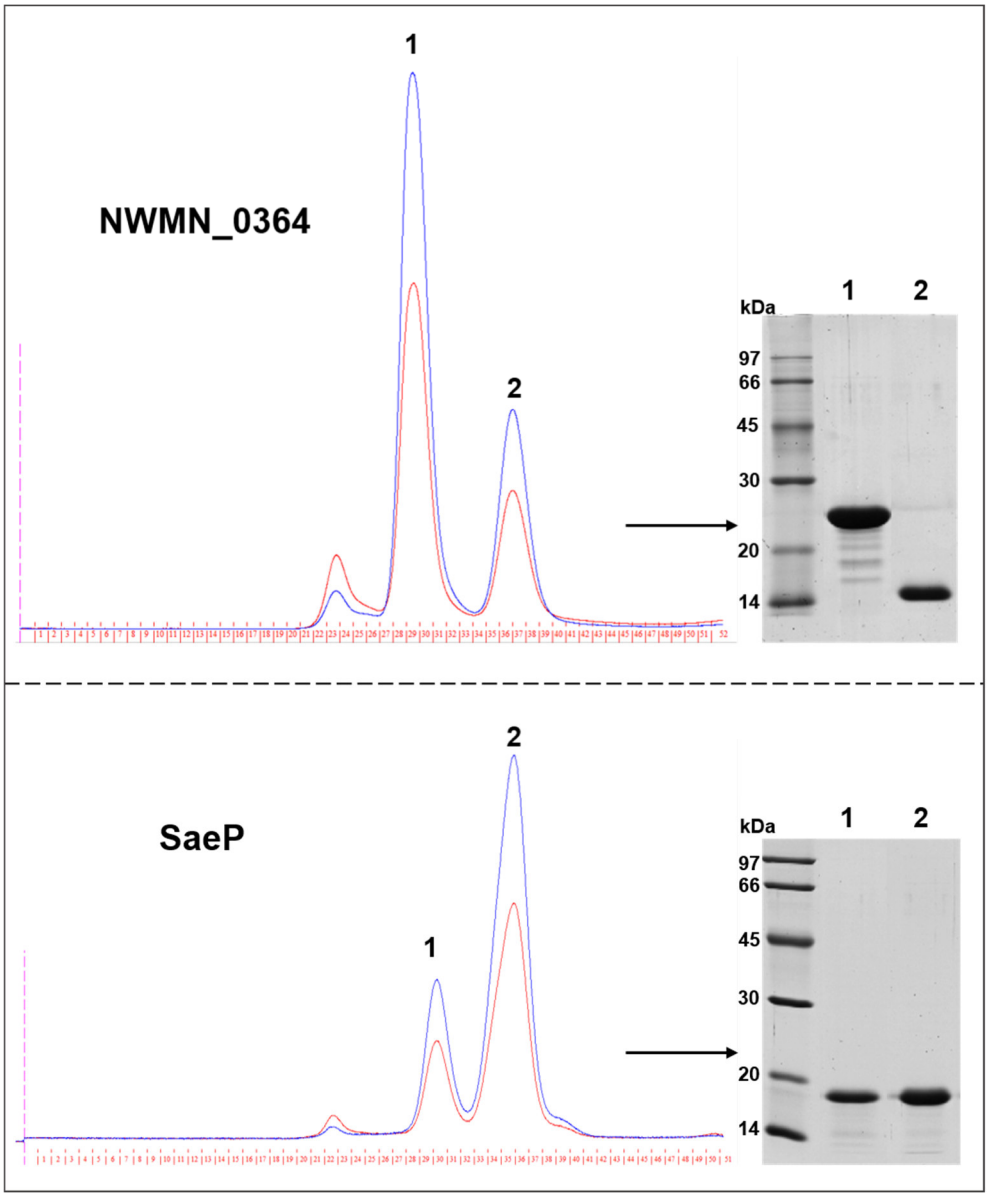

Figure 26 Recombinant proteins NWMN_0364 and SaeP
The curve resembles the UV absorption of the proteins during size exclusion chromatography; 280nm (blue) and 260nm (red). The x-axis shows the elution fraction. The peaks were analysed on 12% denaturing SDS-gel using a colloidal Coomassie staining solution and the low molecular weight standard from GE healthcare (right-hand side).

3.3.5 Protein Stability of NWMN_0364, SaeP, TcyA and MetQ1

An important fact for *in vitro* interaction assays is the correct folding and the stability of the proteins. In order to analyse this, melting curves were performed with the recombinant proteins NWMN_0364, SaeP, MetQ1, and TcyA. Here, the proteins were heated up to 95°C. In the process, changes in UV absorption indicate an unfolding of the protein, and melting points can be determined.

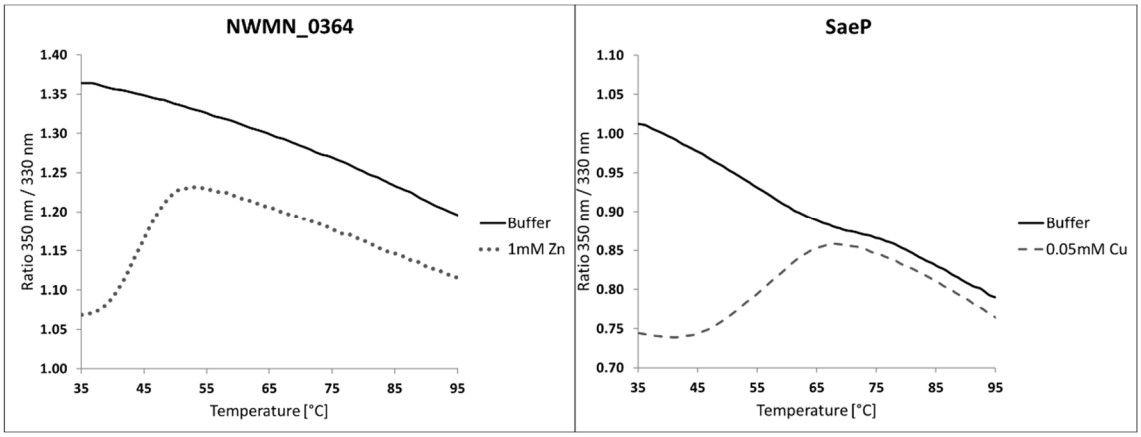

Figure 27 Melting curves of SaeP and NWMN_0364
Temperature is plotted against the UV absorption. The depiction shows the proteins in the buffer: 20mM HEPES, 50mM NaCl, pH7.5.; NWMN_0364 with the addition of 1mM $ZnCl_2$ and SaeP with the addition of 0.05mM $CuCl_2$. Melting curves were performed using 0.5 – 1 mg/mL protein and the Tycho NT6 (NanoTemper Technologies GmbH, München DE).

Without any additives in their buffer, NWMN_0364 and SaeP showed no melting points (Fig. 27). In order to determine if NWMN_0364 and SaeP need co-factors for a proper melting curve, the recombinant proteins were mixed with different metal ions that are known to be co-factors in other proteins. These are $MgCl_2$, $CaCl_2$, $FeSO_4$, $FeCl_3$, $MnCl_2$, Na_2MoO_4, $NiCl_2$, $CoCl_2$, $ZnCl_2$, and $CuCl_2$. Interestingly, Zn^{2+} was able do drive NWMN_0364 into a nice melting curve with a melting point at 44°C, and Cu^{2+} drove SaeP into a nice melting curve with a melting point at 53°C (Fig. 27). All other tested metals did not influence the melting behaviour of NWMN_0364 or SaeP (Fig. 39). This experiment shows that NWMN_0364 needs Zn^{2+} and SaeP needs Cu^{2+} to obtain a proper melting curve.

The recombinant proteins TcyA and MetQ1 were also tested for their melting behaviour. In the course of this, TcyA already displayed a nice melting curve with a melting point at 53.8°C in a buffer solution without additives (Fig. 28). On the contrary, the melting curve of MetQ1 only had a little absorption change at 79.3°C. Moreover, for both proteins, the influence of Zn^{2+} and Cu^{2+} was tested, as these metal ions are important for NWMN_0364 and SaeP. The result indicates no effect of these metal ions on the melting behaviour of TcyA and MetQ1. Nevertheless, other co-factors were added to MetQ1 to investigate whether a change in the melting behaviour of MetQ1 could be obtained. These were $MgCl_2$, $CaCl_2$, $MnCl_2$, Na_2MoO_4, $NiCl_2$, $CoCl_2$, $ZnCl_2$, and $CuCl_2$, but they showed no effect on the melting curve of MetQ1 (Fig. 28). These experiments show that TcyA and maybe MetQ1 already had a protein fold in the buffer solution, that could be denatured during heating, and no co-factor was identified to change their melting behaviour.

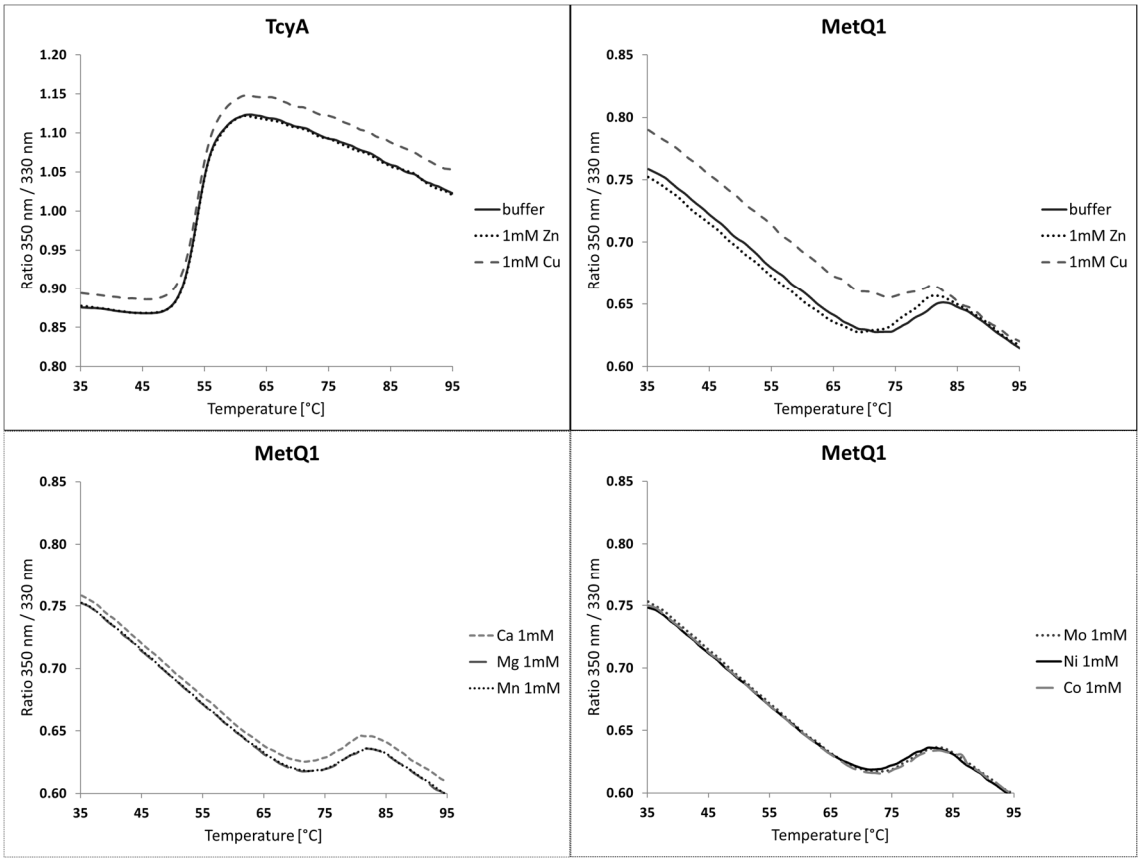

Figure 28 Melting curves TcyA and MetQ1 with metal ions
Temperature is plotted against the UV absorption. The depiction shows the proteins MetQ1 and TcyA with the addition of 1 mM $ZnCl_2$ and $CuCl_2$. MetQ1 was shown with the following metal salts: $MgCl_2$, $CaCl_2$, $MnCl_2$, Na_2MoO_4, $NiCl_2$, $CoCl_2$, $ZnCl_2$, and $CuCl_2$. Buffer: 20mM HEPES, 50mM NaCl, pH7.5. Melting curves were performed using 0.5 – 1 mg/mL protein and the Tycho NT6 (NanoTemper Technologies GmbH, München DE).

3.3.6 NWMN_0364 Dimerises and Interacts with SaeP

The *in vivo* interaction assays indicate an interaction between NWMN_0364 and SaeP as well as between NWMN_0364 and substrate binding proteins of the ABC transporter. In order to confirm these interactions, gel shift assays were performed using the recombinant proteins NWMN_0364, SaeP, TcyA, and MetQ1. Gel shift assays allow the analysis of oligomerisation states and protein interaction as the proteins are fixed in their states with formaldehyde and visualised on an SDS-PAGE.

NWMN_0364 and SaeP were tested regarding their oligomerisation states in the buffer and with the addition of $ZnCl_2$ and $CuCl_2$, which had previously shown an effect on the melting behaviour of these proteins. As a result, SaeP showed higher oligomerisation states with the addition of Cu^{2+}, and NWMN_0364 also displayed higher oligomerisation states with the addition of Zn^{2+}. Moreover, when both proteins were mixed together and $ZnCl_2$ and $CuCl_2$ were added, an additional band appeared on the SDS-gel with a size corresponding to an NWMN_0364-SaeP complex. By means of further analysis of this band via LC-MS/MS,

NWMN_0364 as well as SaeP were identified in this interaction band (Fig. 29). Furthermore, an additional overload of $ZnCl_2$ or $CuCl_2$ did not influence the amount of interacting proteins but influenced the amount of protein oligomerisation. Nevertheless, the addition of EDTA led to the dissociation of the complex (Fig. 29). These results show an interaction between the recombinant proteins NWMN_0364 and SaeP.

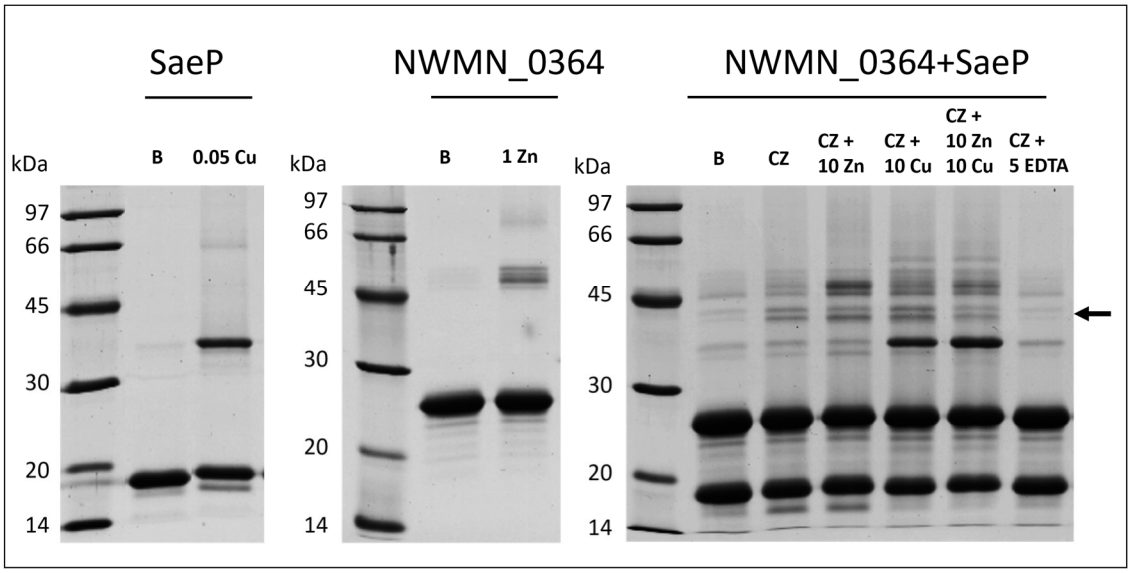

Figure 29 Interaction assays of NWMN_0364 and SaeP
In order to visualise oligomerisation states and interaction under different conditions, gel shift assays were used, fixing the proteins in their oligomerisation states with the help of formaldehyde. Here, 20 µM NWMN_0364 and SaeP were used alone and together, in combination with $CuCl_2$, $ZnCl_2$ and EDTA. The numbers connected to Zn, Cu, and EDTA correspond to mM concentrations. B: buffer solution: 20mM HEPES, 50mM NaCl, pH7.5. CZ: a buffer solution containing 1 mM $ZnCl_2$ and 0.05mM $CuCl_2$. The arrow shows the height of the NWMN_0364-SaeP interacting band.

The recombinant proteins NWMN_0364 and TcyA were examined regarding their interacting ability. As the melting curves only suggested the co-factor Zn^{2+} for NWMN_0364 and no co-factor for TcyA, only Zn^{2+} was added to the NWMN_0364-TcyA sample. The analysis of the oligomerisation state reveals that TcyA does not show a significantly higher oligomerisation (Fig.29). When both proteins were mixed, an interaction of NWMN_0364 and TcyA could not be observed (Fig. 30).

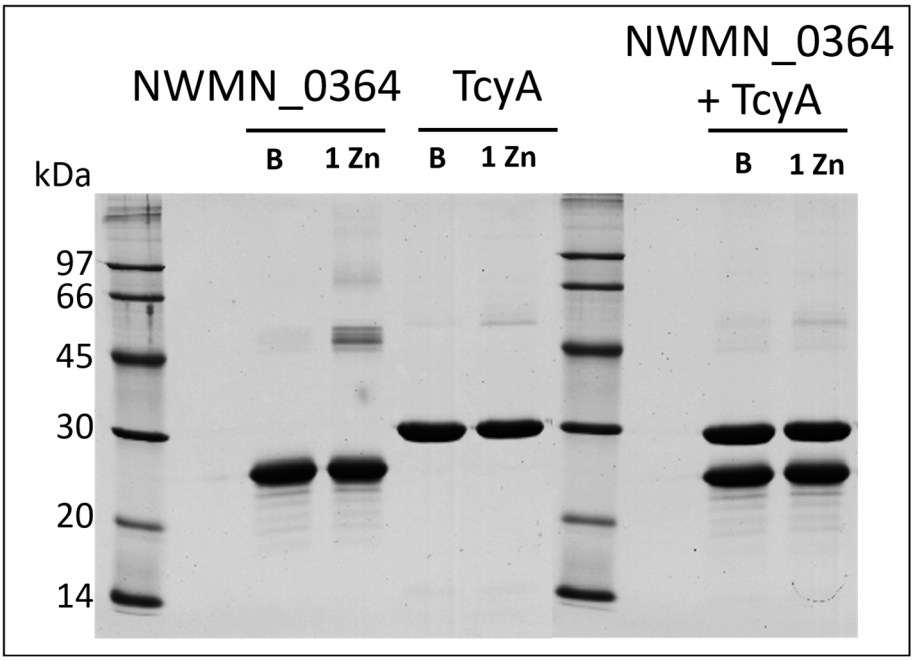

Figure 30 Interaction assays of NWMN_0364 and TcyA
To visualize oligomerization states and interaction under different conditions, gel shift assays were used, fixing the proteins in their oligomerization states by formaldehyde. Here, 20 µM NWMN_0364 and TcyA were used alone and together, in combination with $ZnCl_2$. The numbers connected to Zn and Cu correspond to mM concentrations. B: Buffer: 20mM Hepes, 50mM NaCl, pH7.5.

The recombinant proteins NWMN_0364 and MetQ1 were examined regarding their interacting ability. As the melting curves only suggested Zn^{2+} as a co-factor for NWMN_0364 and no co-factor for MetQ1, only Zn^{2+} was added to the NWMN_0364-MetQ1 sample. The analysis of the oligomerisation state reveals that MetQ1 does not show a significantly higher oligomerisation (Fig. 31). When both proteins were mixed, an interaction of NWMN_0364 and MetQ1 could not be observed (Fig. 31).

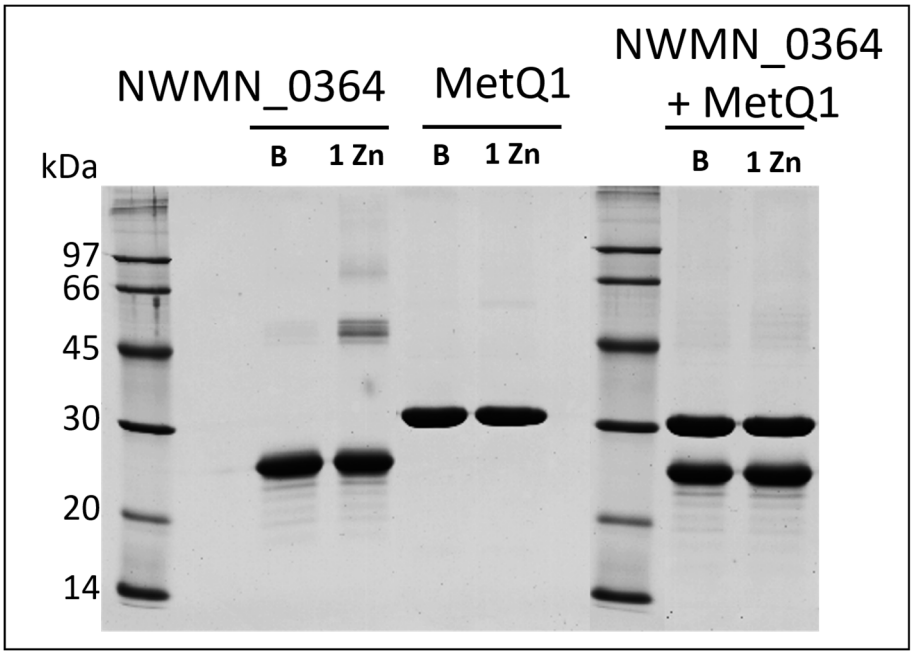

Figure 31 Interaction assays of NWMN_0364 and MetQ1
In order to visualise oligomerisation states and interaction under different conditions, gel shift assays were used, fixing the proteins in their oligomerisation states with the help of formaldehyde. Here, 20 µM NWMN_0364 and MetQ1 were used alone and together, in combination with $ZnCl_2$. The numbers connected to Zn and Cu correspond to mM concentrations. B: buffer: 20mM HEPES, 50mM NaCl, pH7.5.

3.3.7 NWMN_0364 Binds to SaeP with the C-terminal PepSY Domain

NWMN_0364 and SaeP are the only recombinant proteins that showed an interaction in the gel shift assay. The next goal was to determine the direct interacting parts of the two proteins. Therefore, the NWMN_0364-SaeP complex was further characterised regarding the interaction sites of both proteins by chemical cross-linking with amine-reactive MS-cleavable cross-linkers. The cross-linkers used were DSBU for long range distances, with a linker of 12.5 Å, and CDI for short range distances, with a linker of 2.6 Å. These cross-linkers mainly connect lysine residues within proteins and on the protein-protein interface. Due to its cleavability in the MS2 scans during LC-MS/MS analysis, the determination of cross-linked amino acids is possible [150] [149]. For this experiment, NWMN_0364 and SaeP were mixed in different buffer conditions because it had been shown before that Zn^{2+} and Cu^{2+} are important for the binding of NWMN_0364 to SaeP. These metal ions were used alone or in combination in the protein interaction samples. After cross-linking, the proteins were analysed on an SDS-PAGE regarding their cross-linking efficiency and complex formation. The result shows that both proteins were very efficiently cross-linked, represented by the blurred protein bands, by 0.2 mM DSBU and 1 mM CDI (Fig. 32A, B). Interestingly, the cross-linked NWMN_0364 showed a band shift on the SDS-gel whenever Zn^{2+} was present in the

buffer (Fig. 32A). Moreover, the cross-linked SaeP showed slightly less blurred proteins bands whenever Cu^{2+} was present in the buffer (Fig. 32A). This shows an influence of Zn^{2+} on the protein fold of NWMN_0364 and an influence of Cu^{2+} on the protein fold of SaeP. However, this behaviour was not observed when the proteins were cross-linked with CDI (Fig. 32B). Especially the NWMN_0364-SaeP 1:1 complex was only cross-linked with DSBU in the presence of Zn^{2+} and Cu^{2+} (Fig. 32A).

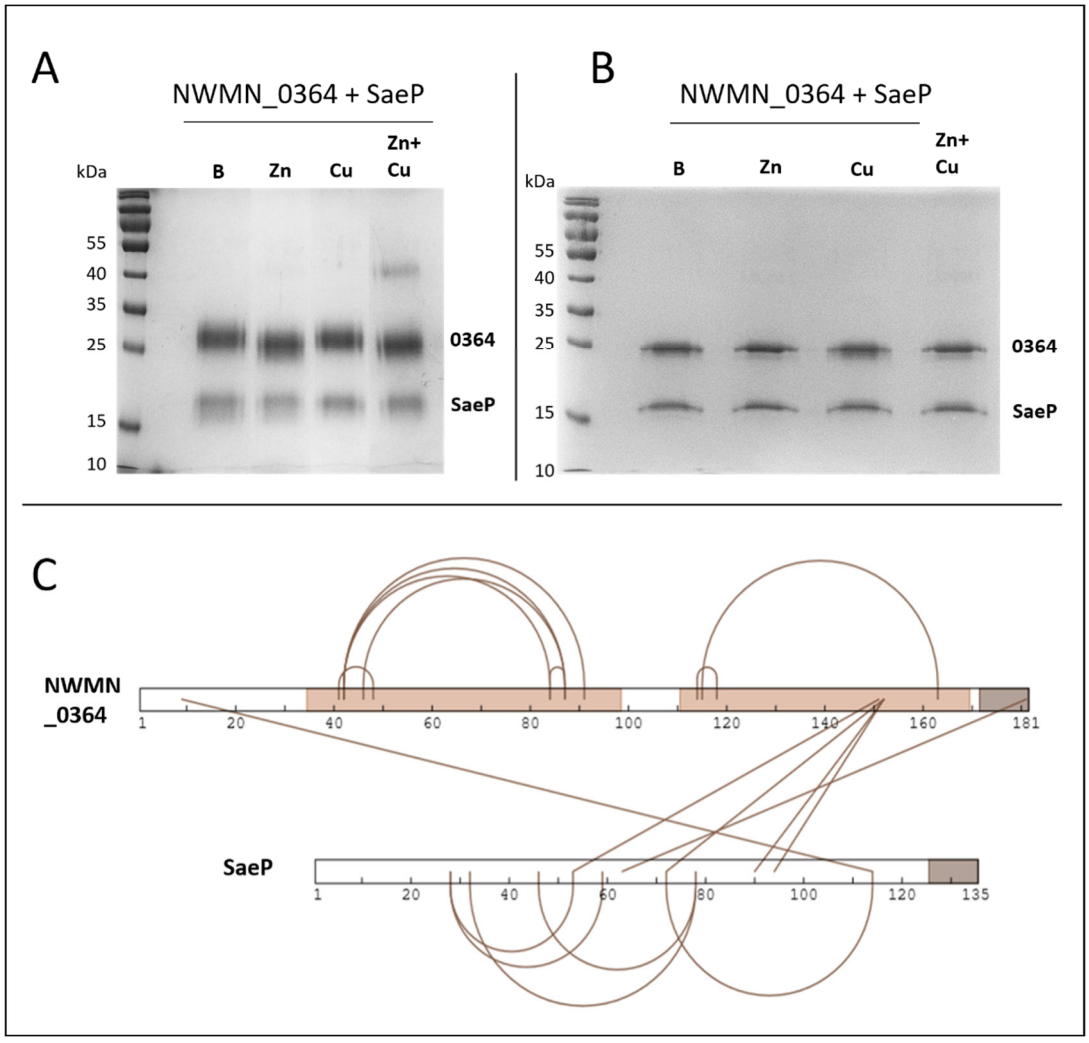

Figure 32 Chemical crosslinking of NWMN_0364 and SaeP
A) SDS-PAGE with NWMN_0364 and SaeP cross-linked with 0.2 mM DSBU showing a 1:1 complex. B: buffer solution. Zn: $ZnCl_2$ 1mM. Cu: $CuCl_2$ 0.05mM.
(B) SDS-PAGE with NWMN_0364 and SaeP cross-linked with 1 mM CDI. B: buffer solution. Zn: $ZnCl_2$ 1mM. Cu: $CuCl_2$ 0.05mM.
(C) Overview of the cross-links from the NWMN_0364-SaeP complex. The numbers display the amino acids in the recombinant proteins. The PepSY domains of NWMN_0364 are displayed in light brown, and the Strep-tag sequences are displayed in dark brown.

Intramolecular cross-links give insights into the conformation of NWMN_0364 and SaeP, while the intermolecular cross-links allow the definition of the interaction sites between the two proteins in the 1:1 complex. Therefore, both the cross-linked complex and the cross-linked monomers of NWMN_0364 and SaeP were analysed.

After analysing the cross-linked complex of NWMN_0364 and SaeP, several unique intramolecular cross-links were identified, nine within NWMN_0364 and five within SaeP. Furthermore, the experiment revealed six intermolecular unique cross-link sites between both proteins. Most of the intermolecular cross-links were found between the C-terminal PepSY domain of NWMN_0364, around position 150, and SaeP. For SaeP, the intermolecular cross-links were mainly located in the region comprising amino acids 50 to 118 (Fig. 32C).

The monomers of NWMN_0364 and SaeP were analysed for all buffer conditions (buffer, Zn^{2+}, Cu^{2+}, Zn^{2+} + Cu^{2+}). For NWMN_0364, 39 unique intramolecular cross-link sites were found (37 DSBU, 2 CDI) in the buffer control, 26 (20 DSBU, 6 CDI) with the addition of Zn^{2+}, 38 (36 DSBU, 2 CDI) with the addition of Cu^{2+}, and 36 (33 DSBU, 3 CDI) with the addition of Zn^{2+} and Cu^{2+}. Interestingly, under buffer conditions without additives, the cross-links were most diversely distributed over the protein and cross-links, connecting the N-terminus to the C-terminal PepSY-domain This was the case under all buffer conditions, except for the sample with the addition of Cu^{2+} (Fig. 33). Moreover, with the addition of Zn^{2+}, the cross-links connecting the two PepSY domains diminished, while at the same time, cross-links connecting the N-terminus to the C-terminal PepSY domain accumulated (Fig. 33).

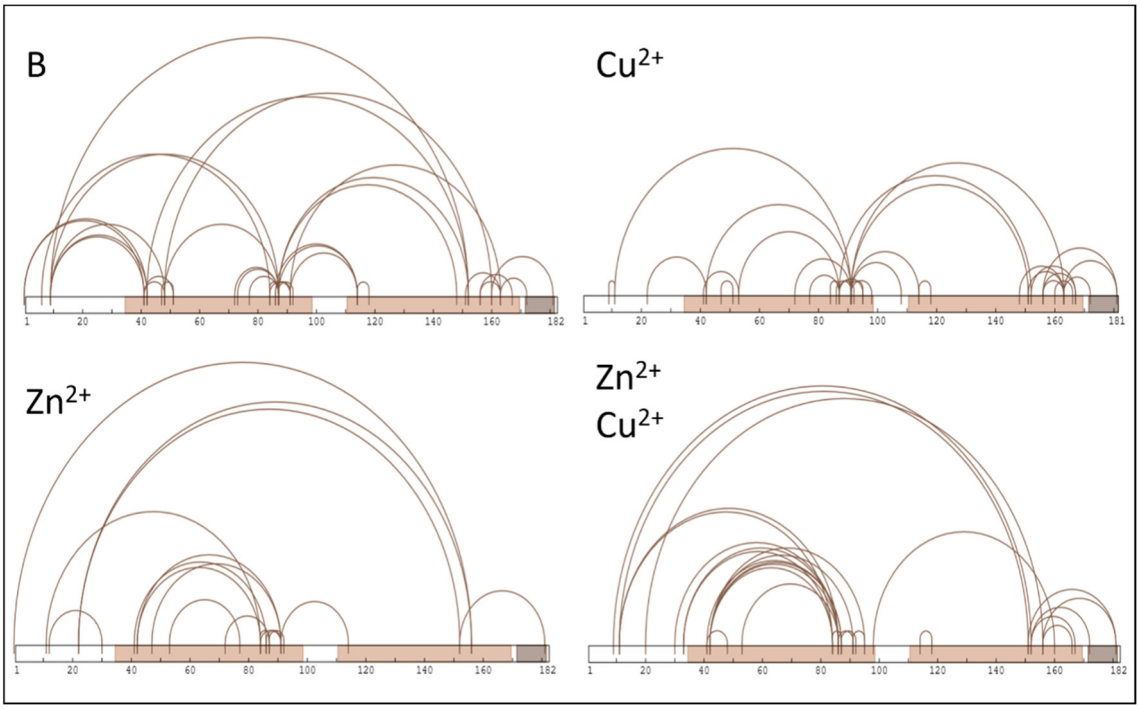

Figure 33 Intramolecular cross-links of NWMN_0364
Cross-links derived from 0.2 mM DSBU cross-linking under different buffer conditions: with the addition of 1mM $ZnCl_2$ and/or 0.05 mM $CuCl_2$. B: buffer solution. The numbers display the amino acids in the recombinant proteins. The PepSY domains of NWMN_0364 are displayed in light brown, and the strep-tag sequences are displayed in dark brown.

The results of the SaeP monomers show 24 unique intramolecular cross-link sites (22 DSBU, 2 CDI) in the buffer control, 5 (3 DSBU, 2 CDI) with the addition of Zn^{2+}, 10 (10 DSBU, 0 CDI) with the addition of Cu^{2+}, and 16 (16 DSBU, 0 CDI) with the addition of Zn^{2+} and Cu^{2+}. Again, the result of the buffer control shows the highest variety of cross-links. Interestingly, with the addition of Cu^{2+}, the cross-links connecting the N- and the C-terminus diminish (Fig. 34).

In sum, the XL-MS experiments reveal that the C-terminal PepSY domain of NWMN_0364 interacts with SaeP, and Zn^{2+} as well as Cu^{2+} influence the conformation of NWMN_0364 and SaeP.

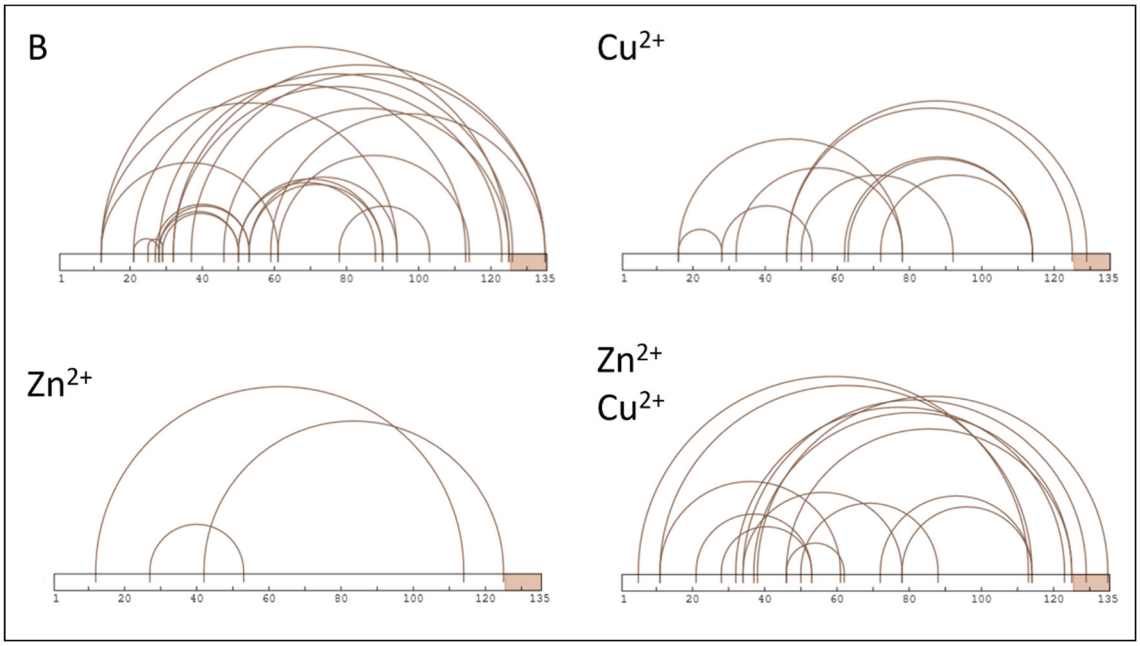

Figure 34 Intramolecular cross-links of SaeP
Cross-links derived from 0.2 mM DSBU cross-linking under different buffer conditions: with the addition of 1mM $ZnCl_2$ and/or 0.05 mM $CuCl_2$. B: buffer solution. The numbers display the amino acids in the recombinant proteins. The Strep-tag sequences are displayed in dark brown.

3.4 Structural Model of NWMN_0364

The protein structure of NWMN_0364 has not been solved yet. The intramolecular cross-links that were obtained from the chemical cross-linking experiments provide information about the structure of NWMN_0364. These were used to calculate an atomic model of NWMN_0364.

This structural modelling was done by Dr. Christian Tüting (Kastritis Laboratory for Biomolecular Research, University of Halle-Wittenberg).

The I-TASSER web server was used to generate a structure of NWMN_0364 based on a structural homologue, a putative lipoprotein from *C. difficile* (PDB-ID: 4EXR). This protein has a 28% sequence identity and a 75% sequence similarity to NWMN_0364. The bound sodium ion in the template structure was not considered by I-TASSER, but as NWMN_0364 probably binds a Zn^{2+} ion, the bound ion from the template structure was superimposed to the model, and the structure was refined using MODELLER. Moreover, using MODELLER, the N-terminal Gly19 was added de novo.

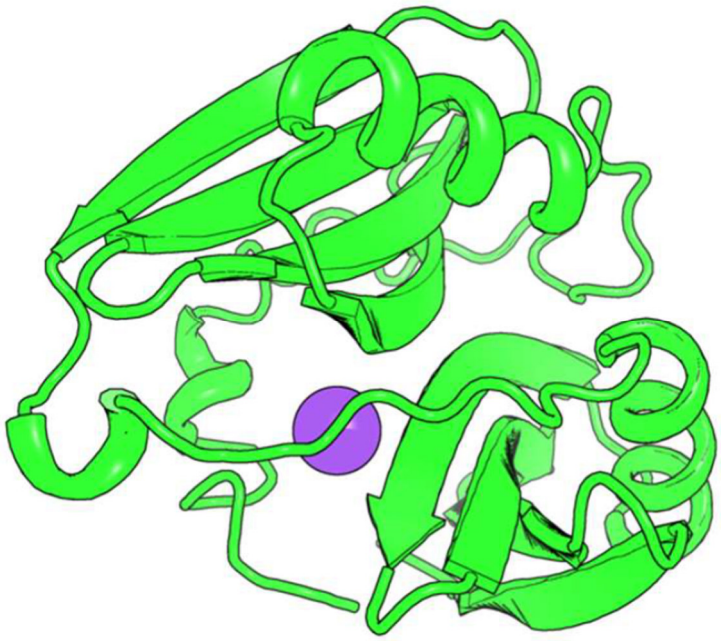

Figure 35 Monomeric model of NWMN_0364.
The structure was modelled by Dr. Christian Tüting (Kastritis Laboratory for Biomolecular Research, University of Halle-Wittenberg), using the programmes I-TASSER and MODELLER, based on a structural homologue from *C. difficile* (PDB-ID: 4EXR). The bound ion is shown as a purple sphere.

The two PepSY domains of NWMN_0364 dominate its structure with each consisting of one α-helix in combination with a β-sheet fold (Fig. 35). A bound metal ion resides in the interface of the PepSY domains. Moreover, the N-terminal region is folded backwards to the metal ion in a helical manner.

In order to verify the structural model, the obtained intramolecular cross-links of NWMN_0364 from all buffer conditions (buffer, Zn^{2+}, Cu^{2+}, Zn^{2+} + Cu^{2+}) were mapped on the monomeric model. For the cross-links with DSBU, a Euclidian distance cut-off was set at 30Å, and for the cross-links with CDI, it was set at 25Å. The cross-links deriving from the Strep-tag were not considered. When the cross-links from the buffer control were mapped on the model, many violating cross-links were spanning through the molecule that did not match the allowed Euclidian distance (Fig. 36). Many of these violating cross-links were linked to the N-terminal region. In contrast to this, the cross-links from buffer conditions containing Zn^{2+} or Cu^{2+} showed a higher satisfaction with the monomeric model of NWMN_0364, especially whenever Zn^{2+} was present (Fig. 36, Tab. 18). These results indicate that without Zn^{2+}, NWMN_0364 is a highly flexible protein, especially the N-terminal region, and upon the binding of Zn^{2+}, the protein takes on a more stable conformation, which is shown here with the help of the monomeric model of NWMN_0364.

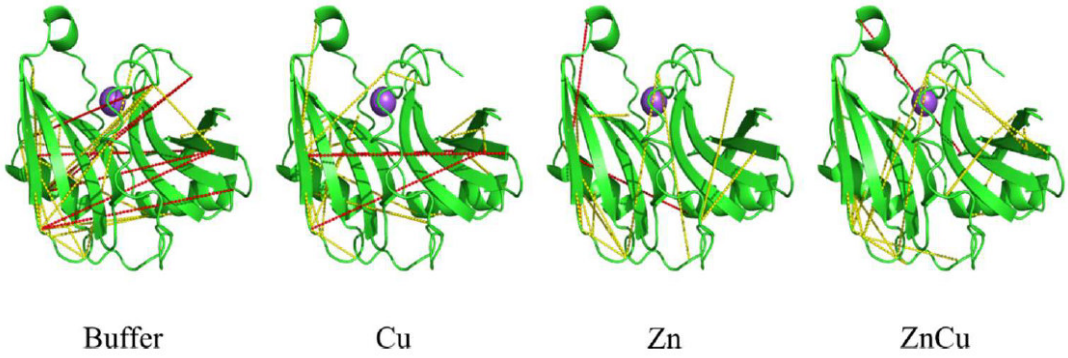

Figure 36 Cross-link mapping on the NWMN_0364 structure
The mapping was done by Dr. Christian Tüting (Kastritis Laboratory for Biomolecular Research, University of Halle-Wittenberg) using cross-links with DSBU with a Euclidian distance cut-off at 30Å and cross-links with CDI with a Euclidian distance cut-off at 25Å. The obtained cross-links came from NWMN_0364 in different buffer conditions (buffer, Zn^{2+}, Cu^{2+}, Zn^{2+} + Cu^{2+}). Violating cross-links that do not confirm the model are shown in red; satisfying cross-links that support the model are shown in yellow.

4 Discussion

4.1 Hypothesis of the NWMN_0364 (Pvr) Function

The aim of this study was the functional analysis of the so far hypothetical protein NWMN_0364. Concluding from all results of this study, a hypothesis was generated. This hypothesis is based on the major findings that in a *Δ0364* mutant strain, the virulence as well as the amount of virulence factors were reduced due to a reduced transcription of virulence genes and the *sae* operon encoding the SaeRS virulence regulatory system. Additionally, an interaction between NWMN_0364 and SaeP could be shown in this study. Together, these findings indicate that NWMN_0364 is able to activate the major virulence regulatory system SaeRS. This activation is mediated by the binding of NWMN_0364 to SaeP, whereby the inhibitory properties of SaeP on the sensor kinase SaeS can be blocked. This leads to a free SaeS, and the signal transduction can proceed. Thereby, a full activation of SaeRS and the expression of virulence factors is possible (Fig. 37). Based on the observed function of NWMN_0364, this protein was renamed as "PepSY containing, virulence regulating protein" (Pvr).

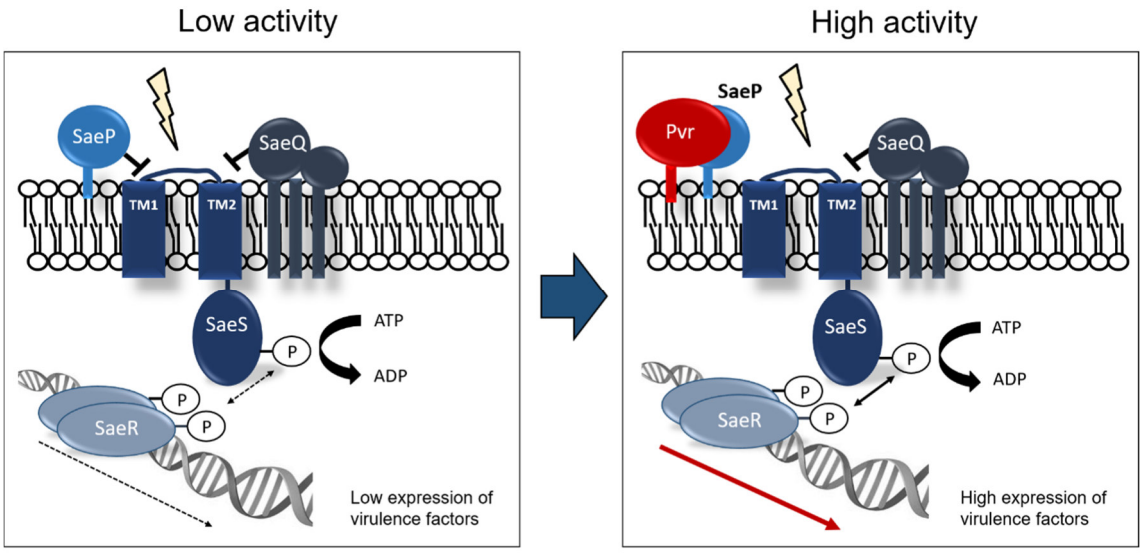

Figure 37 Overview of the SaeRS system switching from low activity to high activity with influence of Pvr on the four proteins SaeP, SaeQ, SaeR and SaeS.
SaeR – response regulators, SaeS- sensor histidine kinase, SaeP and SaeQ negative regulatory proteins of SaeS activity. The yellow arrow indicates an activation signal upon which the histidine kinase SaeS is autophosphorylated (P) under ATP hydrolysis and which transfers the phosphoryl group to SaeR, which can then bind to DNA and activate the transcription of many virulence factors. This signal transduction can be blocked by SaeP and SaeQ. In order to prevent this blocking, Pvr binds to SaeP and thereby possibly blocks the inhibition of SaeP on the histidine kinase. Thus, the signal transduction can proceed, and virulence factors can be expressed.

The hypothesis that Pvr activates the virulence regulatory system SaeRS is likely, as Pvr is a lipoprotein like SaeP, and thereby, they are in close proximity. Moreover, regulatory proteins of two-component systems often lie within one operon, as SaeP and SaeQ from the SaeRS system or WalH and WalI from the WalKR system. However, Pvr does not lie in the *sae* operon, but there are examples where a regulator of a two-component system is located apart from the operon of the two-component system. In *Salmonella enterica,* SlyB negatively regulates the two-component system PhoP/PhoQ, which is important for Mg^{2+} sensing. Here, *slyB* does not lie within an operon with *phoPQ* [164].

4.2 Pvr Is Important for Virulence and Regulates SaeRS

Initially, hints regarding a virulence-related function of Pvr came from literature. First, Pvr is a lipoprotein, and a connection of lipoproteins to virulence was indicated in several studies. On the one hand, due to their lipid moiety, they are targets of the TLR2-activated immune response, but on the other hand, the loss of all lipoproteins in *S. aureus* shows an effect on bacterial virulence itself [22] [165]. Second, a study demonstrated that patients with high IgG titres against Pvr less frequently develop sepsis symptoms than those with low IgG titres against Pvr [128].

The importance of Pvr for the virulence of *S. aureus* is clearly displayed by the experiments of this study. The infection assay shows that the Δ*0364 (*Δ*pvr)* mutant is not able to kill the human macrophages as efficiently as the wild type strain. Normally, upon the killing of macrophages, *S. aureus* cells are released into the extracellular environment [166]. The release of bacteria from macrophages was not investigated during the infection assay of this study, as only the living macrophages were counted and released bacteria were directly lysed by the presence of lysostaphin in the culture medium. However, it is very likely that this process occurred here. This process of macrophage killing and escape of the bacteria is dependent on the SaeRS system. In a study of Münzenmayer *et al*., they demonstrated that especially the pore forming toxins LukSF and Pvl are important for the escape from human macrophages [92]. According to the data from the extracellular proteome from Newman WT and Δ*0364* (Δ*pvr*) grown in SA medium from this study, the pore forming toxins LukSF, corresponding to LukSF in the study of Münzenmayer *et al.,* were identified in lower amounts, with a log2 fold change of -1.10 and -1.31, in the Δ*0364* (Δ*pvr*) mutant, but without statistical significance. This indicates that a release of the bacteria also occurred in the infection assay from this study. However, the extracellular proteome displayed the accumulation of virulence factors in culture medium, and the expression of virulence factors

might differ inside the macrophages. Another issue is that the strain Newman does not possess Pvl, which was discovered to be important for the escape from human macrophages, so there might be strain differences existing in accomplishing macrophage escape. Furthermore, the infection assay only shows a lower ability of macrophage killing due to the loss of Pvr, and the question still remains, whether the mutant strain is replicating, persistent, or even killed by the macrophages. This needs to be further elucidated. Nevertheless, a connection of Pvr to the SaeRS system is indicated by these findings.

After observing a reduced virulence in the Δ*0364* (Δ*pvr*) mutant strain *in vivo*, the proteome analysis supports the assumption that the Pvr function is connected to virulence. Here, many virulence factors regulated by SaeRS were significantly lower in the Δ*0364* (Δ*pvr*) mutant. These findings indicate that the reduced virulence of the mutant might be the result of lower amounts of virulence factors. The proteome analysis only displays protein accumulation. Thus, the lower accumulation of virulence factors can be due to various reasons. One possibility is a defect in protein secretion due to which the virulence factors can no longer be transported to the extracellular environment. Another reason can be a proteolytic effect leading to a degradation of virulence factors. The last possibility is a downregulation at the transcriptional level. This downregulation at the transcriptional level was shown to be a cause for the lower accumulation of virulence factors in the Δ*0364* (Δ*pvr*) using RNA analysis of the genes *sbi* and *hlgC* encoding the corresponding virulence factors Sbi and HlgC. Hence, the question of how the genetic regulation is altered in the Δ*0364* (Δ*pvr*) strain arises. Here, the extracellular proteome indicated a connection to the SaeRS system. Thus, a possible altered transcriptional regulation via SaeRS was then examined via RNA analysis. Due to its self-regulatory properties, a different SaeRS activity can be displayed by the transcription: the *sae* operon [101]. The results of a transcriptional analysis of the *sae* operon indicate a less active SaeRS system in the Δ*0364* (Δ*pvr*) mutant, leading to the assumption that Pvr activates SaeRS.

The effect of Pvr on SaeRS is severe, as the RNA levels of the *sae* operon in the Δ*pvr* mutants only reached 10–35% of the RNA intensities of the wild type strain (Fig.15). This is quite astonishing, as in the Newman strain, a constantly active SaeRS system is described due to the constantly active sensor kinase SaeS [98]. Thus, it seems that Pvr is not directly involved in the activation of the sensor kinase SaeS but performs a function that is necessary for an active SaeRS system beyond the active kinase.

The importance of Pvr for the activation of the SaeRS system could also be detected in the strain *S. aureus* COL. Here, RNA levels of the *sae* operon and *sbi* were lower in the *Δpvr*

mutant strain (Fig. 15, 16). Thus, it can be assumed that this function of Pvr on virulence is not restricted to the strain Newman. However, in the strain COL, only RNA levels were examined, and an in vivo effect on virulence in the COL strain has not been checked yet.

The tested genes showed lower RNA level in both strains, except for the *hlgC* gene. In COL, the differences on the transcript level could not be observed as it was the case in Newman. The gene *hlgC* encodes the γ-haemolysin component C.

The different effects of Pvr on the RNA levels of *hlgC* in Newman and COL might have several reasons. First, it can be an effect of the SaeRS system. In this context, it must be assumed that the general activity of SaeRS in the COL strain is lower compared to Newman, and the different effects on *sbi* and *hlgC* on RNA level might be due to a SaeR dose-dependent effect. Here, *sbi* possesses one binding site for SaeR in its promoter region, while *hlgC* possesses two (Fig. 15) [99]. Concluding, *sbi* can be transcribed with a much lower phosphorylated SaeR present. Nevertheless, *saeP* also has two binding sites and shows a significantly lower RNA level in the Δ*pvr* mutant. Consequently, it is unlikely that the differences of the *hlgC* transcription in the mutant in Newman and COL result from a SaeRS effect.

A second explanation for this difference might be a different interplay between different virulence regulators in Newman and COL, as *hlgC* is not solely regulated by SaeRS but also by *agr* and particularly Rot [76] [63]. If the strain COL has a differentially regulated Rot, it consequently has different expression of toxins, which has not been examined so far but should be tested further.

4.3 Conditions Affecting the Virulence Function of Pvr

From the experiments of this study, the hypothesis was drawn that Pvr activates SaeRS via SaeP. However, the question still remains if it is a constant activation or if it is restricted to specific conditions. The infection assay of this study shows that the Pvr function is essential under infective conditions in macrophages. Moreover, during this study, it could be observed that the importance of the Pvr function differs when the bacteria are grown in different media. Already the proteome analyses as well as the transcriptional analyses showed differences when the bacteria were grown in a complex TSB medium compared to a chemically defined medium SA.

The lower activity of the SaeRS system in the Δ*0364* (Δ*pvr*) mutant grown in SA medium could not be observed when *S. aureus* Newman WT and Δ*0364* (Δ*pvr*) mutant were grown in TSB medium. Indeed, no significant difference between WT and Δ*0364* (Δ*pvr*) mutant

could be detected when observing the transcription of the *sae* operon. In contrast to this, in the proteome from TSB, proteins regulated by the SaeRS system were observed in lower amounts in the Δ*0364* (Δ*pvr*) mutant strain. Even though no significant difference was detected on the RNA level, even a slight difference might result in a significant difference concerning protein accumulation over time. Comparing the extracellular proteins of Newman WT and Δ*0364* (Δ*pvr*) mutant, grown in either TSB or SA medium, a much greater effect on the proteins from the Δ*0364* (Δ*pvr*) mutant grown in SA medium was observed. These results indicate that the activity or function of Pvr is more important when the bacteria grow in SA medium.

One cause of a higher Pvr activity in SA medium could be the probably higher amounts of Pvr in this medium. Its expression is regulated by SigB, and SigB was shown to be highly active in SA medium [142]. Another explanation could be signals in SA medium that trigger the activity of Pvr. Moreover, a higher SaeRS activity in SA medium can be due to the different nutrient composition in the stationary growth phase at which these phenotypes were observed. It is possible that the nutrient composition during stationary growth in SA medium triggers the activity of the transcriptional regulator CodY, which can influence SaeRS activity. Under high nutrient supply, the transcription of the *sae* operon is suppressed by CodY, which releases the promoter under low nutrient supply [111]. Nevertheless, the Δ*0364* (Δ*pvr*) mutant failed to activate the SaeRS system under nutrient composition in SA stationary growth phase, which can be due to the fact that Pvr is involved in nutrient sensing connected to CodY, or it can add a new layer of regulation and respond to other signals in SA medium. One possibility could be the amount of Cu^{2+} and Zn^{2+} which is important for the binding of Pvr to SaeP.

Additionally, the RNA analysis revealed that the SaeRS system is strongly induced in SA medium (Fig. 17), and the Δ*0364* (Δ*pvr*) mutant failed to activate the SaeRS system here. A strong activation of the SaeRS system in minimal medium was demonstrated by Cho *et al*. (2015) [110]. However, in this study, they observed that the strain Newman already had an activated SaeRS system in complex medium that could not be further induced in minimal medium. The Newman strain used for the experiments in the present study did not show this behaviour, instead, SaeRS could be further activated in SA medium, similar to the strain COL. Possible explanations for this are differences in the media used in the study by Cho *et al.* and this study. In the study by Cho *et al*., they used RPMI (Corning) medium as minimal medium. This medium consists of different concentrations of amino acids (from 0.02mM to 2mM), with most concentrations below 1mM. In contrast to this, the concentrations of all amino acids in the synthetic medium used in this study are 1mM. Furthermore, a big

difference between both media is that the RPMI medium is not supplemented with trace elements like Fe, Mn, Zn, Cu, Ni, or Mo, but SA medium is (see 2.3.4). Moreover, there still is the possibility that one of the strains could have obtained mutations that alter the behaviour of the strain.

4.4 Pvr, a Connection Between two Virulence Regulators

S. aureus possesses many different virulence regulatory proteins. One of these is the alternative sigma factor B (SigB) which is known to activate the transcription of several genes upon stress situations as well as to regulate virulence. The transcription of *pvr* is under the control of SigB. Thus, a connection between SigB and SaeRS could be mediated over Pvr. A connection of these two regulators might be possible as both are upregulated at stationary growth phase. So far, this is the only known signal to overlap with both regulators. However, there was no signal identified that had opposite effects on both regulators [48] [49] [50] [110] [167]. In this regard, two possible situations appear for the binding of Pvr to SaeP. First, Pvr can always bind to SaeP, and the activation of the SaeRS system is regulated by the amount of Pvr present on the surface, which is mediated by SigB. Second, the binding of Pvr and SaeP might not be possible without a signal, like changes in environmental conditions or the presence of co-factors. In this case, SigB would not directly regulate SaeRS over Pvr amounts, but an additional trigger would be needed, leading to a more specific regulation. A proteome study of Hempel *et al*. [168] deals with a Δ*sigB* mutant in which Pvr was not detected anymore, indicating a strong regulatory influence of SigB on the expression of Pvr. Nevertheless, in the same study, they identified SaeP in the Δ*sigB* mutant as not changed in exponential growth and slightly upregulated in stationary growth. As the expression of SaeP is activated by the SaeRS system, this leads to the assumption that under the conditions of the study by Hempel *et al*., the mere presence of Pvr is not enough to activate SaeRS.

4.5 Zn^{2+} and Cu^{2+} Ions Are Important for Pvr Function

The experiments of this study with recombinant proteins show a clear influence of Zn^{2+} on Pvr. In this context, the cross-linking reveals a conformational change of the monomeric Pvr upon the addition of Zn^{2+} (Fig. 31, 32). Here, already on the SDS-gel, a protein shift of Pvr was observed in the presence of Zn^{2+}, which indicates a conformational change. Moreover, in the buffer control, a high number of unique cross-link sites was identified, which had a

great variety. The number and variety decrease upon the addition of Zn^{2+}, which leads to the conclusion that the structure of Pvr is highly flexible in the buffer and stabilises in the presence of Zn^{2+}. This is supported by the structural model as many cross-links from buffer control do not agree with the monomeric model of Pvr, but with the addition of Zn^{2+}, the cross-links satisfy within the distances in model. Especially the N-terminal region (residues 20-47) is connected with a great number of violating cross-links in the buffer control that have not been observed in Zn-buffer. Thus, it seems that especially the N-terminal region is highly flexible and can be stabilised upon Zn^{2+} binding to the monomer. Additionally, Cu^{2+} seems to influence the conformation of Pvr, too. It did not strongly reduce the number of cross-links, but it reduced the variety of cross-links in a way that cross-links from N- to C-terminus are completely abolished. This is also represented in the structural model where more cross-links are in the correct distance when Cu^{2+} is present in the buffer compared to the buffer control.

Furthermore, the gel shift assays indicate that, in the presence of Zn ions, Pvr oligomerises. A dimeric state and a possible tetramer were observed. It still remains unclear how Zn^{2+} can bind to Pvr, whether it binds in one monomer, or additionally also in the dimeric interface. A typical Zn^{2+} binding site could not be observed in the sequence of Pvr. It possesses no cysteine and only one histidine, which are the typical Zn^{2+} binding sites. However, it has a lot of negatively charged amino acids (D, E) that might be able to coordinate Zn^{2+} [169]

The experiments of this study show a clear influence of Cu^{2+} on SaeP. The cross-linking reveals a conformational change of the monomeric SaeP upon the addition of Cu^{2+} (Fig. 31, 33). Here, already on the SDS-gel, the monomeric bands narrowed in the presence of Cu^{2+}, which indicates a conformational change. Moreover, in the buffer control, a great number of unique crosslink sites was identified, which had a great variety. Also for SaeP, the number and variety decrease upon the addition of Cu^{2+}, indicating that a highly flexible SaeP in the buffer is stabilised upon the addition of Cu^{2+}. Zn^{2+} extremely decreases the cross-link number, showing an effect of Zn^{2+} on SaeP. Furthermore, the gel shift assays indicate that, in the presence of Cu^{2+}, SaeP oligomerises. A dimeric state and a possible tetramer were observed.

Interestingly, the oligomerisation of Pvr and SaeP could not be displayed by DSBU cross-linking. Maybe the dimeric interface is not covered with enough lysine residues in the correct distances, which are needed by DSBU for cross-linking.

The Pvr/SaeP complex could be cross-linked with DSBU only in the presence of Zn^{2+} and Cu^{2+}, indicating an importance of these metal ions. Here, the metal ions could be needed as

co-factors, where Zn^{2+} binds Pvr and Cu^{2+} binds SaeP. This may result in conformational changes and functionally active proteins that are able to bind. On the other hand, Cu^{2+} and Zn^{2+} could also be important for the complex formation itself and bind at the interface of both proteins. This needs to be further elucidated. Whether the dimerization plays a role for the function of these proteins is still unclear, as the complex is only a 1:1 complex, and overloads of Cu^{2+} and Zn^{2+} only promoted the dimerization of the proteins and did not interfere with the complex formation. The fact that the complex has not been observed with CDI cross-linking could be due to the smaller spacer size of CDI. Its distance is only 2.6 Å, while DSBU has 12.5 Å. It seems that the lysine residues at the interaction site are too far apart for CDI.

So far, the results indicate that Cu^{2+} and Zn^{2+} are co-factors for the proteins SaeP and Pvr. Nevertheless, the binding of Cu^{2+} and Zn^{2+} to the proteins does not seem very strong because strong binding co-factors would be bound to recombinant proteins upon expression in *E. coli*, which was not true for SaeP and Pvr. Accordingly, the concept of a Cu^{2+}- and Zn^{2+}-sensing mechanism is brought up because both metal ions are key players during infections. These two ions are essential protein co-factors that are needed for bacterial growth. Thus, at the site of infection, calprotectin, a human protein, is present, which captures Mn^{2+} and Zn^{2+} ions to limit these for the bacteria and thereby inhibit bacterial growth [110]. Furthermore, when the bacteria are taken up by macrophages into the phagosome, divalent metal ions like Fe^{2+}, Mn^{2+}, or Zn^{2+} can be removed to withdraw essential nutrients. Macrophages are also able to use Cu^{2+} and Zn^{2+} in high concentrations to intoxicate the pathogens present in the phagosome [38] [39]. From *S. aureus*' point of view, it might be reasonable to sense extracellular Cu^{2+} and Zn^{2+} contents and react to it with virulence activation via the SaeRS system. SaeRS is a two-component system, and in literature, there are many examples saying that two-component systems are able to sense metal ions, like the PhoP/PhoQ from *Salmonella enterica* that is sensitive to Mg^{2+} concentrations, or the PmrA/PmrB system that is able to detect external Fe^{3+} concentrations [170] [171]. Moreover, it is described for SaeRS that metal ions influence its activity. Fe, Cu, and Zn are known to suppress the SaeRS system, and Cu and Zn are able to inhibit the autokinase activity of the SaeS protein [109] [110]. The exact mechanism via which these metal ions interfere with the signal transduction is still unclear. It is assumed that they compete with the Mg^{2+} co-factor of SaeS, resulting in an inactive kinase. So far, no connection to SaeP has been considered.

4.6 PepSY Domain Function

Pvr consists of two PepSY domains that make up most of the protein. The precise function of PepSY domains has not been clarified so far. Initially, a protease inhibitory function was dedicated to the PepSY domain, as it was found in the propeptide of peptidases that are only active when the propeptide is cleaved off [172]. Functions of proteins harbouring two PepSY domains are mostly unknown. There are only a few proteins with known functions, like YpeB from *Bacillus subtilis.* YpeB is important for sporulation and its mechanistic function is the inhibition of the activity of the peptidoglycan amidase SleB [157] [158]. Accordingly, a protein inhibitory function of the PepSY domains has been postulated. This is also supported by the results of this study. Here, Pvr is important for the activation of SaeRS and binds SaeP. If it had an activity promoting function on SaeP, it would not result in a SaeRS activation but rather in a repression. Therefore, it is likely that Pvr has an inhibitory effect on SaeP. An inhibitory effect alone would not explain why most proteins with two PepSY domains localise in a membrane-associated or extracellular manner in Gram-positive bacteria and periplasmically in Gram-negative bacteria (Fig. 6). This localisation seems favourable for a protein with only two PepSY domains. A variety of functions is possible in these localisations; here, many proteins reside that are involved in transport of nutrients, signal sensing, defence, energy metabolism, or cell wall and membrane metabolism. The functions of these two PepSY domains need to be further elucidated. Nevertheless, this study reveals a few hints regarding their functions. The cross-linking assay of the Pvr/SaeP complex shows intermolecular cross-links from the C-terminal PepSY domain to SaeP and none from the N-terminal PepSY domain. This leads to the assumption that only the C-terminal domain interacts with SaeP. This is unexpected, as both domains are predicted as PepSY domains. However, the sequence identity of both PepSY domains is about 28%. Therefore, it might be that both PepSY domains display different functions in the Pvr protein. There are different possibilities in this context. On the one hand, the N-terminal PepSY domain could also have inhibitory functions in a self-inhibition of the protein, whereby it could block the C-terminal PepSY domain. This could be a similar function like the PepSY domains in the propeptide of M4 peptidases. In M4 peptidases, the propeptide is cleaved to activate the peptidase. This has not been observed for Pvr so far, but the smaller protein observed after recombinant expression Pvr in *E. coli* could be a cleavage product of the protein (Fig. 25). However, the experiments of this study show that the full length Pvr is able to bind SaeP in the presence of Cu^{2+} and Zn^{2+}. Thus, there might be a possibility to activate the C-terminal PepSY domain other than cleavage. This is supported by the cross-link experiments where cross-links between both PepSY domains were identified in buffer

conditions that could not be detected anymore when Zn^{2+} was present in the buffer. Here, the Zn^{2+} binding may result in the release of the C-terminal PepSY domain, and thereby, the domain could be activated.

On the other hand, these cross-links might also be abolished due to the conformational change of the protein upon Zn^{2+} binding, and the proximity of the PepSY domains before could be a coincidence without any inhibitory effects. Thus, it can be speculated that the function of the N-terminal PepSY domain is different from that at the C-terminus.

4.7 Pvr Displays More Functional Possibilities

Considering the results from the proteome analyses and the interaction assays, the function of Pvr to activate the virulence regulatory system might not be the only possibility. In the study by Graf *et al*. (2018), they predict a function for Pvr that is connected to cell wall and membrane [114]. Moreover, there are other studies in which Pvr appears to be influenced by cell wall stress situations [129] [86]. The results of the extracellular proteome from the strains grown in TSB medium could be nicely explained by the effect of Pvr on the SaeRS system. However, when considering the extracellular proteome from the strains grown in SA medium besides SaeRS regulated proteins, many other proteins were affected by a loss of Pvr. The previously reported connection to cell wall stress and the influence of the WalKR system on the expression of *pvr* lead to the assumption that the WalKR system might also be affected in the Δ*0364* (Δ*pvr*) mutant strain [86]. In the extracellular proteome, it was obvious that many significantly changed proteins were regulated by WalKR, but this was also the case for many without known WalKR regulation. However, the proteins WalI and WalH, which lie within the *wal* operon and positively influence the WalKR system, were found in lower amounts but not statistically significant in the Δ*0364* (Δ*pvr*) mutant strain [80]. Moreover, WalKR is known to upregulate the Sec-translocation pathway which is important for protein export. Proteins involved in this pathway were identified in the extracellular proteome from Newman WT and Δ*0364* (Δ*pvr*) grown in SA medium; these are SecD, SecF, and YajC. These proteins were reduced in the Δ*0364* (Δ*pvr*) mutant strain. These results lead to the assumption that Pvr might influence the WalKR system in a positive way. This might explain why most extracellular proteins were reduced in the Δ*0364* (Δ*pvr*) mutant strain.

Concluding from the results of this study, Pvr positively influences SaeRS and WalKR, while WalKR also positively influences SaeRS but negatively influences Pvr (Fig. 38) [86]. This controversial interplay might be a negative feedback control to adjust WalKR and SaeRS

activity. Feedback controls are well-known mechanisms that are used by two-component systems to regulate their own activity to prevent hyperactivity [173]. A similar feedback control has been described for WalKR with the membrane protein SpdC (Fig. 38) [174]. In contrast to Pvr, SpdC is positively influenced by WalKR but has negative effects on the WalKR regulon itself. Additionally, both activate SaeRS. A feedback control by Pvr might be an additional level of regulation, as the interplay between WalKR and Pvr is reverse when compared to WalKR and SpdC.

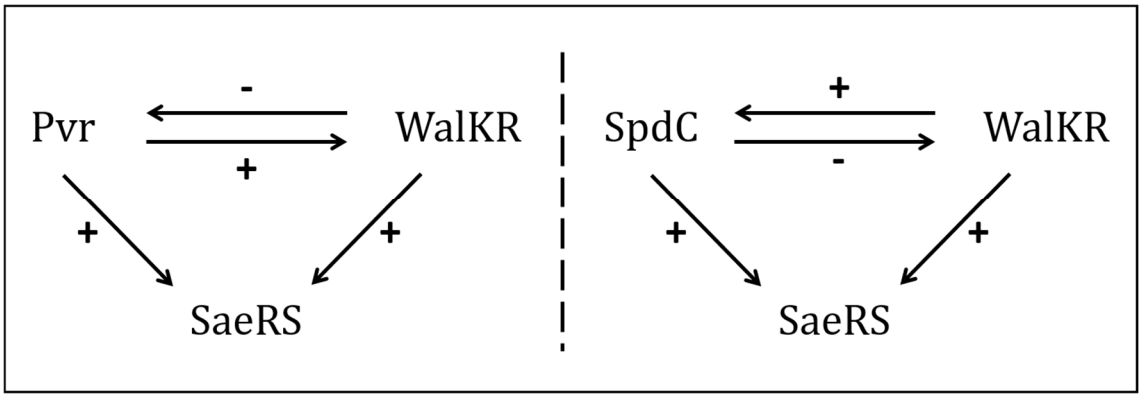

Figure 38 Regulation between Pvr, WalKR, and SaeRS
The arrows indicate the direction of regulation. + indicates a positive effect, - indicates a negative effect.

A different function of Pvr, besides SaeRS activation, is also suggested by the co-immunoprecipitation assay, where additional interaction partners beside SaeP are identified (Fig. 23). The 30S ribosomal protein S12 might be a contaminant as it is a cytoplasmic protein, but MetQ1 could be an interaction partner. This protein is a substrate-binding protein of a methionine ABC transporter and thus a lipoprotein with the same localisation as Pvr. So far, there is no evidence that MetQ1 is in SaeRS- or WalKR-dependent regulation.

The strep-tag pull-down assay reveals substrate-binding proteins of ABC transporter like MetQ1 as possible interaction partners.

It might be possible that, in complex medium, the function of Pvr is not as important as in SA medium, as is also indicated by the proteome and the RNA analyses. Thus, the interaction partners that were pulled down from Newman WT grown in TSB medium might be false positives due to a lack of a real interaction partner and the close proximity of the substrate-binding proteins of the ABC transporter to Pvr, as they are also lipoproteins. Another possibility is that the real interaction partner could not be pulled down in this assay because the Pvr protein in the *S. aureus* strain used for this assay possesses a Strep-tag on the C-

terminal end. This might interfere with protein function. The assumption that the substrate-binding proteins of the ABC transporter might be false positives is supported by the gel shift assays of the recombinant proteins because a complex of Pvr and MetQ1 or TcyA could not be cross-linked with formaldehyde.

Nevertheless, the substrate-binding proteins of ABC transporter might be the real interaction partners that are important for the Pvr function. The fact that a complex could not be cross-linked with the recombinant proteins might be due to missing additives that might be important for binding, just like Cu^{2+} and Zn^{2+} were important for the Pvr-SaeP binding. So far, any important additives have not been identified. On the other hand, there is the possibility that the recombinant proteins TcyA and MetQ1 are not active. In their recombinant form, the anchor to the membrane and a Strep-tag added to their C-terminus are missing. This tag might alter the protein function of the recombinant protein.

All the *in vivo* experiments that were done with the Δ*0364* (Δ*pvr*) mutant that showed that Pvr is involved in virulence and might activate the SaeRS system were not complemented with the Pvr protein. This was due to experimental issues, meaning that a complementation did not function. Here, a re-integration of the NWMN_0364 gene into the original locus resulted in a totally different phenotype compared to WT and mutant, indicating that the re-integration interfered with other genetic material. A second strategy to express *NWMN_0364* from an overexpression plasmid resulted in the complementation of the phenotype in the mutant strain. However, already the empty plasmid that was used as the negative control could complement the phenotype of Δ*0364* (Δ*pvr*) mutant. Thus, it cannot be excluded that the effects observed in this study were due to a secondary effect in the mutant strain. However, the fact that two independent mutants, in the COL and the Newman strain, showed the same phenotype in the RNA assays supports the hypothesis that Pvr activates the SaeRS system. Moreover, this is also supported by the interaction experiments *in vivo*, where SaeP was pulled down as a possible interaction partner, and the interaction experiments with recombinant proteins, especially the cross-linking experiments, which show that the recombinant protein Pvr interacts with SaeP.

5 Outlook

This study gives first insights into the function of the previously unknown protein NWMN_0364, that was renamed here as “PepSY containing, virulence regulating protein” (Pvr), based on its virulence activating function. This function includes the activation of the virulence regulatory system SaeRS by binding to SaeP.

At the beginning, many experiments were done using a deletion mutant of Pvr. So far, complementation could not be obtained but should be done in the future to exclude secondary effects.

Moreover, the direct effect of Pvr on SaeRS could be determined in more detail to answer questions which remain open, as for example, if SaeP still binds SaeS upon the binding of Pvr or if Pvr binds other members of the SaeRS system, maybe even SaeQ or SaeS itself. In order to answer these questions, there is a great variety of protein interaction assays which could be used, like pull-down assays with Strep-tagged protein variants, recombinant proteins with cross-linking experiments, bacterial two-hybrid or split GFP systems. Additionally, the exact role of the metal ions Zn^{2+} and Cu^{2+} should be determined in order to examine whether these metal ions are co-factors for the activity of Pvr, or if this metal binding might be a signal for SaeRS activation sensed by Pvr and SaeP. In order to answer this question, transcriptional analyses of the *sae* operon and SaeRS-regulated genes could be performed using a wild type and a Δ*0364* (Δ*pvr*) mutant to clarify whether these bacteria differentially regulate the SaeRS system upon the addition of Zn and Cu ions in high or low concentrations. However, investigation of the signals that trigger the Pvr-based activation of SaeRS is an important point to find the conditions under which Pvr is active and possibly also how it is activated. The already known signals that influence the SaeRS system, such as H_2O_2, pH, NaCl, or fatty acids, are good starting points to check their influence on the SaeRS activation in wild type and Δ*0364* (Δ*pvr*) mutant. Furthermore, in order to evaluate how Pvr might be activated, the role of the oligomerisation behaviour and the precise function of the two PepSY domains should be studied in more detail. The investigation of the role of the PepSY domains, in particular, is of special interest. Here, the C- and the N-terminal PepSY domains can be deleted separately, and the mutants having only one of the PepSY domains can be used for a functional analysis regarding the here discovered effects of NWMN_0364 on the SaeRS system or for testing for new functions. Additionally, amino acids essential for the PepSY domain function should be identified by mutating single amino acids in a recombinant protein followed by a functional analysis, like binding assays to SaeP.

The results of this study indicate that Pvr possibly has an additional function besides its inhibitory activity regarding the SaeRS system. There is evidence concerning effects of Pvr on the WalKR system, which should be analysed in more detail. Here, the Δ*0364* (Δ*pvr*) mutant can be used to analyse phenotypes that might occur from a differentially active WalKR system. For instance, in a WalKR depletion mutant, the cell wall thickens, and thereby, the resistance against lysostaphin increases. Thus, electron microscopy and lysostaphin lysis assays might give hints regarding a WalKR effect in the mutant. Additionally, the transcriptional regulation of the WalKR operon and WalKR-regulated genes could be determined in comparison to the wild type and the Δ*0364* (Δ*pvr*) mutant.

In conclusion, this study reveals a lot about the Pvr function, but there are still many open questions that are worth investigating.

6 References

[1] A. Ogston, "Über Abscesse," *Archive für Klinische Chirurgie,* vol. 25, pp. 588-600, 1880.

[2] A. Ogston, "Micrococcus poisoning," *J.Anat.Physiol.,* vol. 171054, pp. 24-58, 1882.

[3] S. Cowan, "Classification of staphylococci by slide agglutination," *The Journal of Pathology and Bacteriology,* vol. 48, pp. 169-173, 1939.

[4] S. Cowan, C. Shaw and R. Williams, "Type strain for Staphylococcus aureus Rosenbach," *J. Gen. Microbiol.,* vol. 10, pp. 174-176, 1954.

[5] G. A. Somerville and R. A. Proctor, "The Biology of Staphylococci," in *Staphylococci in Human Disease, 2nd edition*, Blackwell Publishing, 2009, pp. 3-18.

[6] S. R. Gill, D. E. Fouts, G. L. Archer, E. F. Mongodin, R. T. DeBoy, J. Ravel, I. T. Paulsen, J. F. Kolonay, L. Brinkac, M. Beanan, R. J. Dodson, S. C. Daugherty, R. Madupu, S. V. Angiuoli, A. S. Durkin, D. H. Haft, J. Vamathevan, H. Khouri, T. Utterback, C. Lee, G. Dimitrov, L. Jiang, H. Qin, J. Weidman, K. Tran, K. Kang, I. R. Hance, K. E. Nelson and C. M. Fraser, "Insights on Evolution of Virulence and Resistance from the Complete Genome Analysis of an Early Methicillin-Resistant Staphylococcus aureus Strain and a Biofilm-Producing Methicillin-Resistant Staphylococcus epidermidis Strain," *Journal of Bacteriology,* vol. Vol.187, no. No. 7, pp. 2426-2438, 2005.

[7] R. E. O. Williams, "Healthy carriage of Staphylococcus aureus: Its prevalence and importance," *Bacteriol.Rev.,* vol. Vol. 27, pp. 56-71, 1963.

[8] N. H. R. Eriksen, F. Espersen, V. T. Rosdahl and K. Jensen, "Carriage of Staphylococcus aureus among 104 healthy persons during a 19-month period," *Epidemiol. Infect.,* vol. 115, pp. 51-60, 1995.

[9] T. J. Foster, "Colonization and infection of the human host by staphylococci: adhesion, survival and immune evasion," *Veterinary Dermatology,* vol. 20, pp. 456-470, 2009.

[10] S. S. Huang and R. Platt, "Risk of Methicillin-Resistant Staphylococcus aureus Infection after Previous Infection or Colonization," *CID,* vol. 36, pp. 281-285, 2003.

[11] H. F. Wertheim, M. C. Vos, A. Ott, A. v. Belkum, A. Voss, J. A. Kluytmans, P. H. v. Keulen, C. M. Vandenbroucke-Grauls, M. H. Meester and H. A. Verbrugh, "Risk and outcome of nosocomial Staphylococcus aureusbacteraemia in nasal carriers versus non-carriers," *Lancet,* vol. 364, pp. 703-705, 2004.

[12] M. Herrmann and M. S. Smeltzer, "Clinical Significance in Humans," in *Staphylococcus-Genetics and Physiology*, Caister Academic Press, 2016, pp. 23-43.

[13] D. Grumann, U. Nübel and B. M. Bröker, "Staphylococcus aureus toxins – Their functions and genetics," *Infection, Genetics and Evolution,* vol. 21, p. 583–592, 2014.

[14] W. M. M. Kirby, "EXTRACTION OF A HIGHLY POTENT PENICILLIN INACTIVATOR FROM PENICILLIN RESISTANT STAPHYLOCOCCI," *Science,* vol. Vol. 99, no. Issue 2579, pp. 452-453, 1944.

[15] R. Knox, "A New Penicillin (BRL 1241) Active Against Penicillin-resistant Staphylococci," *Br Med J.,* vol. 2, no. 5200, p. 690–693, 1960.

[16] M. P. Jevons, "“Celbenin” - resistant Staphylococci," *Br Med J.,* vol. 1, no. 5219, p. 124–125, 1961.

[17] F. Layer, B. Strommenger, C. Cuny, I. Noll, A. Klingeberg and G. Werner, "Eigenschaften, Häufigkeit und Verbreitung von MRSA in Deutschland – Update 2017/2018," *Epid Bull,* vol. 42, pp. 437-442, 2019.

[18] F. Layer, C. Cuny, B. Strommenger, G. Werner and W. Witte, "Aktuelle Daten und Trends zu Methicillin-resistenten Staphylococcus aureus (MRSA)," *Bundesgesundheitsbl.,* vol. 55, p. 1377–1386, 2012.

[19] T. Ganz, "Defensins: antimicrobial peptides of innate immunity," *Nature Reviews Immunology,* vol. Vol. 3, pp. 710-720, 2003.

[20] T. J. Foster, J. A. Geoghegan, V. K. Ganesh and M. Höök, "Adhesion, invasion and evasion: the many functions of the surface proteins of Staphylococcus aureus," *Nature Reviews,* vol. Vol. 12, pp. 49-62, 2014.

[21] S. J. Galli, N. Borregaard and T. A. Wynn, "Phenotypic and functional plasticity of cells of innate immunity: macrophages, mast cells and neutrophils," *Nature Immunology,* vol. Vol. 12, no. No. 11, pp. 1035-1044, 2011.

[22] A. O. Aliprantis, R.-B. Yang, M. R. Mark, S. Suggett, B. Devaux, J. D. Radolf, G. R. Klimpel, P. Godowski and A. Zychlinsky, "Cell Activation and Apoptosis by Bacterial Lipoproteins Through Toll-like Receptor-2," *Science,* vol. Vol. 285, no. 5428, pp. 736-739, 1999.

[23] M. V. Norgard, L. L. Arndt, D. R. Akins, L. L. Curetty, D. A. Harrich and J. D. Radolf, "Activation of Human Monocytic Cells by Treponema pallidum an Borrelia burgdorferi Lipoproteins and Synthetic Lipopeptides Proceeds via a Pathway Distinct from That of Lipopolysaccharide but Involves the Transcriptional Activator NF-kB," *Infection and Immunity,* vol. Vol. 64, no. No. 9, pp. 3845-3852, 1996.

[24] G. Rawadi, J. Garcia, B. Lemercier and S. Roman-Roman, "Signal Transduction Pathways Involved in the Activation of NF-kB, AP-1, and c-fos by Mycoplasma fermentans

Membrane Lipoproteins in Macrophages," *Journal of Immunology,* vol. 162, no. 1, pp. 2193-2203, 1999.

[25] J. R. Dunkelberger and W.-C. Song, "Complement and its role in innate and adaptive immune responses," *Cell Research,* vol. Vol. 20, no. No. 1, pp. 34-50, 2010.

[26] A. N. Spaan, B. G. Surewaard, R. Nijland and J. A. v. Strijp, "Neutrophils Versus Staphylococcus aureus: A Biological Tug ofWar," *Annu. Rev. Microbiol.,* vol. Vol. 67, pp. 629-650, 2013.

[27] C. J. de Haas, K. E. Veldkamp, A. Peschel, F. Weerkamp, W. J. Van Wamel, E. C. Heezius, M. J. Poppelier, K. P. Van Kessel and J. A. van Strijp, "Chemotaxis Inhibitory Protein of Staphylococcus aureus, a Bacterial Antiinflammatory Agent," *J. Exp. Med,* vol. Vol. 199, no. No. 5, pp. 687-695, 2004.

[28] S. H. M. Rooijakkers, M. Ruyken, A. Roos, M. R. Daha, J. S. Presanis, R. B. Sim, v. W. J. B. Wamel, K. P. M. van Kessel and J. A. G. van Strijp, "Immune evasion by a staphylococcal complement inhibitor that acts on C3 convertases," *Nature Immunology,* vol. Vol. 6, no. No. 9, pp. 920-927, 2005.

[29] T. Chavakis, M. Hussain, S. M. Kanse, G. Peters, R. G. Bretzel, J.-I. Flock, M. Herrmann and K. T. Preissner, "Staphylococcus aureus extracellular adherence protein serves as anti-inflammatory factor by inhibiting the recruitment of host leukocytes," *Nature Medicine,* vol. Vol. 8, no. No. 7, pp. 687-693, 2002.

[30] J. Bestebroer, M. J. J. G. Poppelier, L. H. Ulfman, P. J. Lenting, C. V. Denis, K. P. M. van Kessel, J. A. G. van Strijp and C. J. C. de Haas, "Staphylococcal superantigen-like 5 binds PSGL-1 and inhibitsP-selectin–mediated neutrophil rolling," *Blood,* vol. Vol. 109, no. No. 7, pp. 2936-2943, 2007.

[31] D. Oliveira, A. Borges and M. Simões, "Staphylococcus aureus Toxins and Their Molecular Activity in Infectious Diseases," *Toxins,* vol. 10, no. 252, 2018.

[32] I. Inoshima, N. Inoshima, G. A. Wilke, M. E. Powers, K. M. Frank, Y. Wang and J. B. Wardenburg, "A Staphylococcus aureus pore-forming toxin subverts the activity of ADAM10 to cause lethal infection in mice," *nature medicine,* vol. Vol. 17, no. No. 10, pp. 1310-1315, 2011.

[33] A. Valeva, I. Walev, M. Pinkernell, B. Walker, H. Bayley, M. Palmer and S. Bhakdi, "Transmembrane β-barrel of staphylococcal α-toxin forms in sensitive but not in resistant cells," *Proc. Natl. Acad. Sci.,* vol. Vol. 94, pp. 11607-11611, 1997.

[34] R. S. Flannagan, V. Jaumouillé and S. Grinstein, "The Cell Biologyof Phagocytosis," *Annu. Rev. Pathol. Mech. Dis.,* vol. Vol. 7, pp. 61-98, 2012.

[35] G. L. Lukacs, O. D. Rotstein and S. Grinstein, "Determinants of the phagosomal pH in macrophages. In situ assessment of vacuolar H(+)-ATPase activity, counterion conductance, and H+ "leak"," *Journal of Biological Chemistry,* vol. Vol. 266, no. No. 36, pp. 24540-24548, 1991.

[36] J. P. Gaut, G. C. Yeh, H. D. Tran, J. Byun, J. P. Henderson, G. M. Richter, M.-L. Brennan, A. J. Lusis, A. Belaaouaj, R. S. Hotchkiss and J. W. Heinecke, "Neutrophils employ the myeloperoxidase system to generate antimicrobial brominating and chlorinating oxidants during sepsis," *PNAS,* vol. Vol. 98, no. No. 21, pp. 11961-11966, 2001.

[37] A. Molloy and C. Winterbourn, "Release of iron from phagocytosed Escherichia coli and uptake by neutrophil lactoferrin," *Blood,* vol. Vol. 75, pp. 984-989, 1990.

[38] N. Jabado, A. Jankowski, S. Dougaparsad, V. Picard, S. Grinstein and P. Gros, "Natural Resistance to Intracellular Infections: Natural Resistance–Associated Macrophage Protein 1 (Nramp1) Functions as a Ph-Dependent Manganese Transporter at the Phagosomal Membrane," *Journal of Experimental Medicine,* vol. Vol. 192, no. No. 9, pp. 1237-1248, 2000.

[39] D. Wagner, J. Maser, B. Lai, Z. Cai, C. E. B. III, K. H. z. Bentrup, D. G. Russell and L. E. Bermudez, "Elemental Analysis of Mycobacterium avium-, Mycobacterium tuberculosis-, and Mycobacterium smegmatis-Containing Phagosomes Indicates Pathogen-Induced Microenvironments within the Host Cell's Endosomal System," *Journal of Immunology,* vol. Vol. 174, no. No. 3, pp. 1491-1500, 2005.

[40] A. Forsgren and K. Nordström, "PROTEIN A FROM STAPHYLOCOCCUS AUREUS: THE BIOLOGICAL SIGNIFICANCE OF ITS REACTION WITH IgG," *Annals of the New York Academy of Sciences,* vol. Vol. 236, no. No. 1, 1974.

[41] S. Itoh, E. Hamada, G. Kamoshida, R. Yokoyama, T. Takii, K. Onozaki and T. Tsuji, "Staphylococcal superantigen-like protein 10 (SSL10) binds to human immunoglobulin G (IgG) and inhibits complement activation via the classical pathway," *Molecular Immunology,* vol. Vol. 47, no. No. 4, pp. 932-938, 2010.

[42] E. J. Smith, L. Visai, S. W. Kerrigan, P. Speziale and T. J. Foster, "The Sbi Protein Is a Multifunctional Immune Evasion Factor of Staphylococcus aureus," *Infection and Immunity,* vol. Vol. 79, no. No. 9, pp. 3801-3809, 2011.

[43] G. L. Mandell, "Catalase, superoxide dismutase, and virulenceof Staphylococcus aureus. In vitro and in vivostudies with emphasis on staphylococcal--leukocyte interaction," *Journal of Clinical Investigation,* vol. Vol. 55, no. No. 3, pp. 561-566, 1975.

[44] G. Y. Liu, A. Essex, J. T. Buchanan, V. Datta, H. M. Hoffman, J. F. Bastian, J. Fierer and V. Nizet, "Staphylococcus aureus golden pigment impairs neutrophil killing and promotes

virulence through its antioxidant activity," *Journal of Experimental Medicine,* vol. Vol. 202, no. No. 2, pp. 209-215, 2005.

[45] M. Sieprawska-Lupa, P. Mydel, K. Krawczyk, K. Wójcik, M. Puklo, B. Lupa, P. Suder, J. Silberring, M. Reed, J. Pohl, W. Shafer, F. McAleese, T. Foster, J. Travis and J. Potempa, "Degradation of Human Antimicrobial Peptide LL-37 by Staphylococcus aureus-Derived Proteinases," *Antimicrobial Agents and Chemotherapy,* vol. Vol. 48, no. No. 12, pp. 4673-4679, 2004.

[46] A. L. DuMont, P. Yoong, B. G. J. Surewaard, M. A. Benson, R. Nijland, J. A. G. v. Strijp and V. J. Torres, "Staphylococcus aureus Elaborates Leukocidin AB To Mediate Escape from within Human Neutrophils," *Infection and Immunity,* vol. Vol. 81, no. No. 5, pp. 1830-1841, 2013.

[47] C. Jenul and A. R. Horswill, "Regulation of Staphylococcus aureus virulence," *Microbiol Spectr.,* vol. 6, no. 1, 2019.

[48] I. Kullik and P. Giachino, "The alternative sigma factor sigB in Staphylococcus aureus: regulation of the sigB operon in response to growth phase and heat shock," *Arch Microbiol,* vol. 167, pp. 151-159, 1997.

[49] J. Pane´-Farre´, B. Jonas, K. Förstner, S. Engelmann and M. Hecker, "The sigB regulon in Staphylococcus aureus and its regulation," *International Journal of Medical Microbiology,* vol. 296, pp. 237-258, 2006.

[50] J.´Pane-Farre, B. Jonas, S. W. Hardwick, K. Gronau, R. J. Lewis, M. Hecker and S. Engelmann, "Role of RsbU in Controlling SigB Activity in Staphylococcus aureus following Alkaline Stress," *Journal of Bacteriology,* vol. Vol. 191, no. No. 8, pp. 2561-2573, 2009.

[51] M. Bischoff, P. Dunman, J. Kormanec, D. Macapagal, E. Murphy, W. Mounts, B. Berger-Bächi and S. Projan, "Microarray-Based Analysis of the Staphylococcus aureus sig B Regulon," *Journal of Bacteriology,* vol. Vol. 186, no. No. 13, pp. 4085-4099, 2004.

[52] H. Pförtner, M. S. Buriana, S. Michalik, M. Depke, P. Hildebrandt, V. M. Dhoplea, J. Pané-Farré, M. Hecker, F. Schmidt and U. Völker, "Activation of the alternative sigma factor SigB of Staphylococcus aureus following internalization by epithelial cells – An in vivo proteomics perspective," *International Journal of Medical Microbiology,* vol. Vol. 304, no. No. 2, pp. 177-187, 2014.

[53] L. Tuchscherr, M. Bischoff, S. M. Lattar, M. N. Llana, H. Pförtner, S. Niemann, J. Geraci, H. V. d. Vyver, M. J. Fraunholz, A. L. Cheung, M. Herrmann, U. Völker, D. O. Sordelli, G. Peters and B. Löffler, "Sigma Factor SigB Is Crucial to Mediate Staphylococcusaureus Adaptation duringChronic Infections," *PLoS Pathog,* vol. 11(4): e1004870, 2015.

[54] A. Karlsson, P. Saravia-Otten, K. Tegmark, E. Morfeldt and S. Arvidson, "Decreased Amounts of Cell Wall-Associated Protein A and Fibronectin-Binding Proteins in Staphylococcus aureus sarA Mutants due to Up-Regulation of Extracellular Proteases," *Infection and Immunity,* vol. Vol. 69, no. No. 8, pp. 4742-4748, 2001.

[55] A. L. Cheung, J. M. Koomey, C. A. Butler, S. J. Projan and V. A. Fischetti, "Regulation of exoprotein expression in Staphylococcus aureus by a locus (sar) distinct from agr," *Proc. Nati. Acad. Sci.,* vol. Vol. 89, pp. 6462-6466, 1992.

[56] Y. Liu, A. C. Manna, C.-H. Pan, I. A. Kriksunov, D. J. Thiel, A. L. Cheung and G. Zhang, "Structural and function analyses of the global regulatory protein SarA from Staphylococcus aureus," *PNAS,* vol. Vol. 103, no. No. 7, pp. 2392-2397, 2006.

[57] A. L. Cheung and S. J. Projan, "Cloning and sequencing of sarA of Staphylococcus aureus, a gene required for the expression of agr," *Journal of Bacteriology,* vol. Vol. 176, no. No. 13, pp. 4168-4172, 1994.

[58] J. M. Morrison, K. L. Anderson, K. E. Beenken, M. S. Smeltzer and P. M. Dunman, "The staphylococcal accessory regulator, SarA, is an RNA-binding protein that modulates the mRNA turnover properties of late-exponential and stationary phase Staphylococcus aureus cells," *Front. Cell. Inf. Microbio.,* vol. 2:26, 2012.

[59] A. Manna and A. L. Cheung, "Characterization of sarR, a Modulator ofsar Expression in Staphylococcus aureus," *Infection and Immunity,* vol. Vol. 69, no. No. 2, pp. 885-896, 2001.

[60] T. T. Luong, S. W. Newell and C. Y. Lee, "mgr, a Novel Global Regulator in Staphylococcus aureus," *Journal of Bacteriology,* vol. Vol. 185, no. No. 13, pp. 3703-3710, 2003.

[61] T. T. Luong, P. M. Dunman, E. Murphy, S. J. Projan and C. Y. Lee, "Transcription Profiling of the mgrA Regulon in Staphylococcus aureus," *Journal of Bacteriology,* vol. Vol. 188, no. No. 5, pp. 1899-1910, 2006.

[62] P. R. Chen, T. Bae, W. A. Williams, E. M. Duguid, P. A. Rice, O. Schneewind and C. He, "An oxidation-sensing mechanism is used by the globalregulator MgrA inStaphylococcus aureus," *nature chemical biology,* vol. Vol. 2, no. No. 11, pp. 591-595, 2006.

[63] B. Said-Salim, P. M. Dunman, F. M. McAleese, D. Macapagal, E. Murphy, P. J. McNamara, S. Arvidson, T. J. Foster, S. J. Projan and B. N. Kreiswirth, "Global Regulation of Staphylococcus aureus Genes by Rot," *Journal of Bacteriology,* vol. Vol. 185, no. No. 2, pp. 610-619, 2003.

[64] M. A. Benson, S. Lilo, T. Nygaard, J. M. Voyich and V. J. Torres, "Rot and SaeRS Cooperate To Activate Expression of the Staphylococcal Superantigen-Like Exoproteins," *Journal of Bacteriology,* vol. Vol. 194, no. No. 16, pp. 4355-4365, 2012.

[65] A. C. Manna and B. Ray, "Regulation and characterization of rot transcription in Staphylococcus aureus," *Microbiology,* vol. Vol. 153, no. No. 5, pp. 1538-1545, 2007.

[66] E. Geisinger, R. P. Adhikari, R. Jin, H. F. Ross and R. P. Novick, "Inhibition of rot translation by RNAIII, a key feature of agr function," *Mol. Microbiology,* vol. Vol. 61, no. No. 4, pp. 1038-1048, 2006.

[67] R. Gao, T. R. Mack and A. M. Stock, "Bacterial response regulators:versatile regulatory strategies fromcommon domains," *TRENDS in Biochemical Sciences,* vol. Vol.32, no. No.5, pp. 225-234, 2007.

[68] J. A. Hoch, "Two-component and phosphorelay signal transduction," *Current opinion in Microbiology,* vol. Vol.3, no. No.2, pp. 165-170, 2000.

[69] M. Y. Galperin, "Structural Classification of Bacterial Response Regulators: Diversity of Output Domains and Domain Combinations," *Journal of Bacteriology,* vol. Vol. 188, no. No. 12, p. 4169–4182, 2006.

[70] F. Mika and R. Hengge, "A two-component phosphotransfer network involving ArcB, ArcA, and RssB coordinates synthesis and proteolysis of sigS (RpoS) in E. coli," *Genes Dev.,* no. 19, pp. 2770-2781, 2005.

[71] J. Xu, H. C. Chiang, M. K. Bjursell and J. I.Gordon, "Message from a human gut symbiont: sensitivity is a prerequisite for sharing," *Trends in Microbiology,* vol. Vol. 12, no. 1, pp. 21-28, 2004.

[72] N. Majdalani, M. Heck, V. Stout and S. Gottesman, "Role of RcsF in Signaling to the Rcs Phosphorelay Pathway in Escherichia coli," *Journal of Bacteriology,* vol. Vol. 187, no. No. 19, pp. 6770-6778, 2005.

[73] R. R. Novick, S. J. Projan, J. Kornblum, H. F. Ross, G. Ji, B. Kreiswirth, F. Vandenesch and S. Moghazeh, "The agr P2 operon: an autocatalytic sensory transduction system in Staphylococcus aureus," *Mol. Gen. Genet.,* vol. 248, pp. 446-458, 1995.

[74] S. Y. Queck, M. Jameson-Lee, A. E. Villaruz, T.-H. L. Bach, B. A. Khan, D. E. Sturdevant, S. M. Ricklefs, M. Li and M. Otto, "RNAIII-Independent Target Gene Control by the agr Quorum-Sensing System: Insight into the Evolution of Virulence Regulation in Staphylococcus aureus," *Molecular cell,* vol. 32, no. 1, pp. 150-158, 2008.

[75] R. Novick, H. Ross, S. Projan, J. Kornblum, B. Kreiswirth and S. Moghazeh, "Synthesis of staphylococcal virulence factors is controlled by a regulatory RNA molecule," *Embo J.,* vol. 12, pp. 3967-3975, 1993.

[76] M. Thoendel, J. S. Kavanaugh, C. E. Flack and A. R. Horswill, "Peptide Signaling in the Staphylococci," *Chem. Rev.,* vol. 111, no. 1, pp. 117-151, 2011.

[77] G. Ji, R. C. Beavis and R. P. Novick, "Cell density control of staphylococcal virulence mediated by an octapeptide pheromone," *Proc. Natl. Acad. Sci.,* vol. 92, no. 26, pp. 12055-12059, 1995.

[78] G. Ji, R. Beavis and R. P. Novick, "Bacterial Interference Caused by Autoinducing Peptide Variants," *Science,* vol. 276:5321, pp. 2027-2030, 1997.

[79] P. K. Martin, T. Li, D. Sun, D. P. Biek and M. B. Schmid, "Role in Cell Permeability of an Essential Two-Component System in Staphylococcus aureus," *Journal of Bacteriology,* vol. Vol. 181, no. No. 12, p. 3666–3673, 1999.

[80] D. R. Cameron, J.-H. Jiang, X. Kostoulias, D. J. Foxwell and A. Y. Peleg, "Vancomycin susceptibility in methicillin-resistant Staphylococcus aureus is mediated by YycHI activation of the WalRK essential two-component regulatory system," *Sci. Rep.,* vol. 6:30823, 2016.

[81] I. R. Monk, N. Shaikh, S. L. Begg, M. Gajdiss, L. K. Sharkey, J. Y. Lee, S. J. Pidot, T. Seemann, M. Kuiper, B. Winnen, R. Hvorup, B. M. Collins, G. Bierbaum, S. R. Udagedara, J. R. Morey, N. Pulyani, B. P. Howden, M. J. Maher, C. A. McDevitt, G. F. King and T. P. Stinear, "Zinc-binding to the cytoplasmic PAS domain regulates the essential WalK histidine kinase of Staphylococcus aureus," *nature communications,* vol. 10:3067, 2019.

[82] M. Villanueva, B. García, J. Valle, B. Rapún, I. R. d. l. Mozos, C. Solano, M. Martí, J. R. Penadés, A. Toledo-Arana and ñ. Lasa, "Sensory deprivation in Staphylococcus aureus," *Nature communications,* vol. 9, no. 523, 2018.

[83] S. Dubrac and T. Msadek, "Identification of Genes Controlled by the Essential YycG/YycF Two-Component System of Staphylococcus aureus," *Journal of Bacteriology,* vol. Vol. 186, no. No. 4, p. 1175–1181, 2004.

[84] S. Dubrac, I. G. Boneca, O. Poupel and T. Msadek, "New Insights into the WalK/WalR (YycG/YycF) Essential Signal Transduction Pathway Reveal a Major Role in Controlling Cell Wall Metabolism and Biofilm Formation in Staphylococcus aureus," *Journal of Bacteriology,* vol. Vol. 189, no. No. 22, p. 8257–8269, 2007.

[85] A. Delaune, O. Poupel, A. Mallet, Y.-M. Coic, T. Msadek and S. Dubrac, "Peptidoglycan Crosslinking Relaxation Plays an Important Role in Staphylococcus aureus WalKR Dependent Cell Viability," *PLoS ONE,* vol. 6(2), no. e17054, 2011.

[86] A. Delauné, S. Dubrac, C. Blanchet, O. Poupel, U. Mäder, A. Hiron, A. Leduc, C. Fitting, P. Nicolas, J.-M. Cavaillon, M. Adib-Conquy and T. Msadek, "The WalKR System Controls Major Staphylococcal Virulence Genes and Is Involved in Triggering the Host Inflammatory Response," *Infection and Immunity,* vol. Vol. 80, no. No.10, p. 3438–3453, 2012.

[87] A. T. Giraudo, C. G. Raspanti, A. Calzolari and R. Nagel, "Characterization of a Tn551-mutant of Staphylococcus aureus defective in the production of several exoproteins," *Canadian Journal of Microbiology,* vol. Vol. 40, no. No. 8, pp. 677-681, 1994.

[88] K. Rogasch, V. Rühmling, J. Pane´-Farre´, D. Höper, C. Weinberg, S. Fuchs, M. Schmudde, B. M. Bröker, C. Wolz, M. Hecker and S. Engelmann, "Influence of the Two-Component System SaeRS on Global Gene Expression in Two Different Staphylococcus aureus Strains," *Journal of Bacteriology,* vol. Vol. 188, no. No. 22, p. 7742–7758, 2006.

[89] J. E. Cassat, N. D. Hammer, J. P. Campbell, M. A. Benson, D. S. Perrien, L. N. Mrak, M. S. Smeltzer, V. J. Torres and E. P. Skaar, "A Secreted Bacterial Protease Tailors the Staphylococcus aureus Virulence Repertoire to Modulate Bone Remodeling during Osteomyelitis," *Cell Host & Microbe,* vol. 13, pp. 759-772, 2013.

[90] C. P. Montgomery, S. Boyle-Vavra and R. S. Daum, "Importance of the Global Regulators Agr and SaeRS in the Pathogenesis of CA-MRSA USA300 Infection," *PLoS ONE,* vol. 5(12): e15177, 2010.

[91] K. E. Beenken, L. N. Mrak, A. K. Zielinska, D. N. Atwood, A. J. Loughran, L. M. Griffin, K. A. Matthews, A. M. Anthony, H. J. Spencer, R. A. Skinner, G. R. Post, C. Y. Lee and M. S. Smeltzer, "Impact of the functional status of saeRS on in vivo phenotypes of Staphylococcus aureus sarA mutants," *Molecular Microbiology,* vol. 92, no. 6, p. 1299–1312, 2014.

[92] L. Münzenmayer, T. Geiger, E. Daiber, B. Schulte, S. E. Autenrieth, M. Fraunholz and C. Wolz, "Influence of Sae-regulated and Agr-regulated factors on the escape of Staphylococcus aureus from human macrophages," *Cellular Microbiology,* vol. 18, no. 8, p. 1172–1183, 2016.

[93] H. Cho, D.-W. Jeong, C. Li and T. Bae, "Organizational Requirements of the SaeR Binding Sites for a sae Operon in Staphylococcus aureus," *Journal of Bacteriology,* vol. Vol. 194, no. No. 11, p. 865–2876, 2012.

[94] Q. Liu, H. Cho, W.-S. Yeo and T. Bae, "The Extracytoplasmic Linker Peptide of the Sensor Protein SaeS Tunes the Kinase Activity Required for Staphylococcal Virulence in Response to Host Signals," *Plos Pathogen,* vol. 11(4): e1004799, 2015.

[95] Q. Liu, W.-S. Yeo and T. Bae, "The SaeRS Two-Component System of Staphylococcus aureus," *Genes,* vol. 7, no. 81, pp. 1-20, 2016.

[96] M. E. Olson, T. K. Nygaard, L. Ackermann, R. L. Watkins, O. W. Zurek, K. B. Pallister, S. Griffith, M. R. Kiedrowski, C. E. Flack, J. S. Kavanaugh, B. N. Kreiswirth, A. R. Horswill and J. M. Voyich, "Staphylococcus aureus Nuclease Is an SaeRS-Dependent Virulence Factor," *Infection and Immunity,* vol. Vol. 81, no. No.4, p. 1316–1324, 2013.

[97] M. S. Ramundoa, C. O. Beltramea, A. M. N. Botelhoa, L. R. Coelhoa, M. C. Silva-Carvalhoa, B. T. Ferreira-Carvalhoa, M. F. Nicolásb, I. A. Guedesb, L. E. Dardenneb, J. O'Gara und A. M. Sá Figueiredo, „A unique SaeS allele overrides cell-density dependent expression of saeR and lukSF-PV in the ST30-SCCmecIV lineage of CA-MRSA," *International Journal of Medical Microbiology,* Bd. 306, pp. 367-380, 2016.

[98] R. P. Adhikari and R. P. Novick, "Regulatory organization of the staphylococcal sae locus," *Microbiology,* vol. 154, p. 949–959, 2008.

[99] F. Sun, C. Li, D. Jeong, C. Sohn, C. He and T. Bae, "In the Staphylococcus aureus Two-Component System sae, the Response Regulator SaeR Binds to a Direct Repeat Sequence and DNA Binding Requires Phosphorylation by the Sensor Kinase SaeS," *Journal of Bacteriology,* vol. Vol. 192, no. No. 8, p. 2111–2127, 2010.

[100] T.-P. Kod, C.-Y. Huangb, c, T.-J. Hsiehd, S.-C. Chena, Y.-R. Chena, C.-S. Yanga, H.-C. Kuoe, W.-L. Wange, T.-H. Hsiaoe, C.-H. Line and Y. Chen, "Crystal structures of Staphylococcal SaeR reveal possible DNA-binding modes," *Biochemical and Biophysical Research Communications,* vol. 474, pp. 686-690, 2016.

[101] R. P. Novick and D. Jiang, "The staphylococcal saeRS system coordinates environmental signals with agr quorum sensing," *Microbiology,* vol. 149, p. 2709–2717, 2003.

[102] D.-W. Jeong, H. Cho, M. B. Jones, K. Shatzkes, F. Sun, Q. Ji, Q. Liu, S. N. Peterson, C. He and T. Bae, "The auxiliary protein complex SaePQ activates thephosphatase activity of sensor kinase SaeS in the SaeRStwo-component system of Staphylococcus aureus," *Molecular Microbiology,* vol. 86 (2), pp. 331-348, 2012.

[103] M. M. Collins, R. K. Behera, K. B. Pallister, T. J. Evans, O. Burroughs, C. Flack, F. E. Guerra, W. Pullman, B. Cone, J. G. Dankoff, T. K. Nygaard, S. R. Brinsmade and J. M. Voyich, "The Accessory Gene saeP of the SaeR/S Two-Component Gene Regulatory System Impacts Staphylococcus aureus Virulence During Neutrophil Interaction," *Front. Microbiol.,* vol. 11:561, 2020.

[104] T. Geiger, C. Goerke, M. Mainiero, D. Kraus and C. Wolz, "The Virulence Regulator Sae of Staphylococcus aureus: Promoter Activities and Response to Phagocytosis-Related Signals," *Journal of Bacteriology,* vol. Vol. 190, no. No. 10, p. 3419–3428, 2008.

[105] M. E. Ericson, C. Subramanian, M. W. Frank and C. O. Rock, "Role of Fatty Acid Kinase in Cellular Lipid Homeostasis and SaeRS-Dependent Virulence Factor Expression in Staphylococcus aureus," *mBio,* Vols. 8:e00988-17, 2017.

[106] Y. Neumann, K. Ohlsen, S. Donat, S. Engelmann, H. Kusch, D. Albrecht, M. Cartron, A. Hurd and S. J. Foster, "The effect of skin fatty acids on Staphylococcus aureus," *Arch Microbiol,* vol. 197, p. 245–267, 2015.

[107] J. Qiu, D. Wang, H. Xiang, H. Feng, Y. Jiang, L. Xia, J. Dong, J. Lu, L. Yu and X. Deng, "Subinhibitory Concentrations of Thymol Reduce Enterotoxins A and B and α-Hemolysin Production in Staphylococcus aureus Isolates," *PLoS One,* vol. 5(3): e9736, 2010.

[108] J.-H. Lee, J.-H. Park, M. H. Cho and J. Lee, "Flavone Reduces the Production of Virulence Factors, Staphyloxanthin and α-Hemolysin, in Staphylococcus aureus," *Curr Microbiol,* vol. 65, p. 726–732, 2012.

[109] J. Baker, S. Sitthisak, M. Sengupta, M. Johnson, R. K. Jayaswal and J. A. Morrissey, "Copper Stress Induces a Global Stress Response in Staphylococcus aureus and Represses sae and agr Expression and Biofilm Formation," *Applied and Environmental Microbiology,* vol. Vol. 76, no. No.1, p. 150–160, 2010.

[110] H. Cho, D.-W. Jeong, Q. Liu, W.-S. Yeo, T. Vogl, E. P. Skaar, W. J. Chazin and T. Bae, "Calprotectin Increases the Activity of the SaeRS Two Component System and Murine Mortality during Staphylococcus aureus Infections," *PLOS Pathogens,* vol. 11(7): e1005026, 2015.

[111] K. D. Mlynek, W. E. Sause, D. E. Moormeier, M. R. Sadykov, K. R. Hill, V. J. Torres, K. W. Bayles and S. R. Brinsmade, "Nutritional Regulation of the Sae Two-Component System by CodY in Staphylococcus aureus," vol. 200, no. 8, pp. 1-16, 2018.

[112] H. Kusch and S. Engelmann, "Secrets of the secretome in Staphylococcus aureus," *International Journal of Medical Microbiology,* vol. 304, no. 2, pp. 133-141, 2014.

[113] K. Rogasch, V. Rühmling, J. Pane´-Farre´, D. Höper, C. Weinberg, S. Fuchs, M. Schmudde, B. M. Bröker, C. Wolz, M. Hecker and S. Engelmann, "Influence of the Two-Component System SaeRS on Global Gene Expression in Two Different Staphylococcus aureus Strains," *Journal of Bacteriology,* vol. 188, no. 22, pp. 7742-7758, 2006.

[114] A. Graf, R. J. Lewis, S. Fuchs, M. Pagels, S. Engelmann, K. Riedel and J. Pané-Farré, "The hidden lipoproteome of Staphylococcus aureus," *International Journal of Medical Microbiology,* vol. Vol. 38, no. No. 6, pp. 569-581, 2018.

[115] S. Hayashi and H. C. Wu, "Lipoproteins in Bacteria," *Journal of Bioenergetics and Biomembranes,* vol. 22, no. 3, pp. 451-471, 1990.

[116] M. Tokunaga, H. Tokunaga and H. C. Wu, "Post-translational modification and processing of Escherichia coli prolipoprotein in vitro," *Proc. Natl. Acad. Sci. USA,* vol. 79, no. 1, pp. 2255-2259, 1982.

[117] K. Sankaran and H. C. Wu, "Lipid Modification of Bacterial Prolipoprotein," *The Journal of Biological Chemistry,* vol. 269, no. 31, pp. 19701-19706, 1994.

[118] M. Regue, J. Remenick, M. Tokunaga, G. A. Mackie and H. C. Wu, "Mapping of the Lipoprotein Signal Peptidase Gene (lsp)," *Journal of Bacteriology,* vol. 158, no. 2, pp. 632-635, 1984.

[119] M. Hussain, S. Ichihara and S. Mizushima, "Mechanism of Signal Peptide Cleavage in the Biosynthesis of the Major Lipoprotein of Escherichia coli Outer Membrane," *The Journal of Biological Chemistry,* vol. 257, no. 9, pp. 5177-5182, 1982.

[120] S. D. Gupta and H. C. Wu, "Identification and subcellular localization of apolipoprotein N-acyltransferase in Escherichia coli," *FEMS Microbiology Letters,* vol. 78, pp. 37-42, 1991.

[121] C. Robichon, D. Vidal-Ingigliardi and A. P. Pugsley, "Depletion of Apolipoprotein N-Acyltransferase Causes Mislocalization of Outer Membrane Lipoproteins in Escherichia coli," *Ther Journal of Biological Chemistry,* vol. 280, no. 2, pp. 974-983, 2005.

[122] J. B. K. Nielsen and J. 0. Lampen, "Glyceride-Cysteine Lipoproteins and Secretion by Gram-Positive Bacteria," *Journal of Bacteriology,* vol. Vol. 152, no. No.1, pp. 315-322, 1982.

[123] K. Kurokawa, H. Lee, K.-B. Roh, M. Asanuma, Y. S. Kim, H. Nakayama, A. Shiratsuchi, Y. Choi, O. Takeuchi, H. J. Kang, N. Dohmae, Y. Nakanishi, S. Akira, K. Sekimizu and B. L. Lee, "The Triacylated ATP Binding Cluster Transporter Substrate-binding Lipoprotein of Staphylococcus aureusFunctions as a Native Ligand for Toll-like Receptor 2," *THE JOURNAL OF BIOLOGICAL CHEMISTRY,* vol. Vol. 284, no. No. 13, p. 8406–8411, 2009.

[124] K. Kurokawa, M.-S. Kim, R. Ichikawa, K.-H. Ryu, N. Dohmae, H. Nakayama and B. L. Lee, "Environment-Mediated Accumulation of Diacyl Lipoproteins over Their Triacyl Counterparts in Staphylococcus aureu," *Journal of Bacteriology,* vol. Vol. 194, no. No.13, p. 3299–3306, 2012.

[125] A. Gründling, "Cell Wall Assembly and Physiology," in *Staphylococcus- Genetics and Physiology*, UK, Caister Academic Press, 2016, pp. 133-170.

[126] S. V. Shahmirzadi, M.-T. Nguyen and F. Götz, "Evaluation of Staphylococcus aureus Lipoproteins: Role in Nutritional Acquisition and Pathogenicity," *Frontiers in Microbiology,* vol. Vol. 7, no. 1404, 2016.

[127] K. Takeda, O. Takeuchi and S. Akira, "Recognition of lipopeptides by Toll-like receptors," *Journal of Endotoxin Research,* vol. Vol. 8, no. No. 6, pp. 459-463, 2002.

[128] S. Stentzel, N. Sundaramoorthy, S. Michalik, M. Nordengrün, S. Schulz, J. Kolata, P. Kloppot, S. Engelmann, L. Steil, M. Hecker, F. Schmidt, UweVölker, M.-C. Roghmanng

and B. M. Bröker, "Specific serum IgG at diagnosis ofStaphylococcus aureusbloodstreaminvasion is correlated with disease progression," *Journal of Proteomics,* vol. 128, pp. 1-7, 2015.

[129] C. J. Balibar, X. Shen, D. McGuire, D. Yu, D. McKenney and J. Tao, "cwrA, a gene that specifically responds to cell walldamage in Staphylococcus aureus," *Microbiology,* vol. 156, pp. 1372-1383, 2010.

[130] M. Zhou, J. Boekhorst, C. Francke and R. J. Siezen, "LocateP: Genome-scale subcellular-location predictor for bacterial proteins," *BMC Bioinformatics,* vol. 9, no. 173, 2008.

[131] R. Edgar, "MUSCLE: multiple sequence alignment with high accuracy and high throughput," *Nucleic Acids Research,* vol. 32, no. 5, pp. 1792-1797, 2004.

[132] S. El-Gebali, J. Mistry, A. Bateman, S. Eddy, A. Luciani, S. Potter, M. Qureshi, L. Richardson, G. Salazar, A. Smart, E. Sonnhammer, L. Hirsh, L. Paladin, D. Piovesan, S. Tosatto and R. Finn, "The Pfam protein families database in 2019," *Nucleic Acids Research,* vol. Vol. 47, no. D1, p. D427–D432, 2019.

[133] TheUniProtConsortium, "UniProt: a worldwide hub of protein knowledge," *Nucleic Acids Research,* vol. 47, no. D1, pp. D506-D515, 2018.

[134] M. Arnaud, A. Chastanet and M. De´barbouille, "New Vector for Efficient Allelic Replacement in Naturally Nontransformable, Low-GC-Content, Gram-Positive Bacteria," *APPL. ENVIRON. MICROBIOL.,* vol. Vol. 70, no. No. 11, p. 6887–6891, 2004.

[135] S. G. N. Grant, J. Jessee, F. R. Bloom and D. Hanahan, "Differential plasmid rescue from transgenic mouse DNAs into Escherichia coli methylation-restriction mutants," *Proc. Natl. Acad. Sci.,* vol. Vol 87, no. 1, pp. 4645-4649, 1990.

[136] W. F. Studier and B. A. Moffatt, "Use of bacteriophage T7 RNA polymerase to direct selective highlevel expression of cloned genes," *Journal of Molecular Biology,* vol. 189, no. 1, pp. 113-130, 1986.

[137] W. M. Shafer and J. J. Iandolo, "Genetics of staphylococcal enterotoxin B in methicillin-resistant isolates of Staphylococcus aureus," *Infect Immun,* vol. 25, pp. 902-911, 1979.

[138] E. Duthie and L. Lorenz, "Staphylococcal coagulase: mode of action and antigenicity," *J Gen Microbiol,* vol. 6, pp. 95-107, 1952.

[139] B. N. Kreiswirth, S. Lofdahl, M. J. Betley, M. O'Reilly, P. M. Schlievert, M. S. Bergdoll and R. P. Novick, "The toxic shock syndrome exotoxin structural gene is not detectably transmitted by a prophage," *Nature,* vol. 305, no. 1, pp. 709-712, 1983.

[140] E. D. Rosenblum und S. Tyrone, „SEROLOGY, DENSITY, AND MORPHOLOGY OF STAPHYLOCOCCAL PHAGES," *J Bacteriol,* Bd. Vol. 88, pp. 1737-1742, 1964.

[141] S. TSUCHIYA, M. YAMABE, Y. YAMAGUCHI, Y. KOBAYASHI, T. KONNO and K. TADA, "ESTABLISHMENT AND CHARACTERIZATION OF A HUMAN ACUTE MONOCYTIC LEUKEMIA CELL LINE (THP-1)," *Int. J . Cancer,* vol. 26, pp. 171-176, 1980.

[142] S. Gertz, S. Engelmann, R.Schmid, K.Ohlsen, J. Hacker and M. Hecker, "Regulation of sigB-dependent transcription of sigB and asp23 in two different S. aureus strains," *Molecular Genetics and Genomics,* vol. Vol. 261, no. 1, pp. 558-566, 1999.

[143] M. D, A. YJ und W. JH, „Simultaneous and rapid isolation of bacterial and eukaryotic DNA and RNA: a new approach for isolating DNA," *Biotechniques,* Bd. 11, Nr. 1, pp. 94-101, 1991.

[144] F. S, P.-F. J, K. C, H. M und E. S., „Anaerobic Gene Expression in Staphylococcus aureus," *Journal of Bacteriology,* Bd. 189, Nr. 11, pp. 4275-4289, 2007.

[145] U. Laemmli, "Cleavage of Structural Proteins during the Assembly of the Head of Bacteriophage T4," *Nature,* vol. 227, no. 5259, pp. 680-685, 1970.

[146] T. M., R. B., R. K. and E. L., "Identification of Proteins Associated with the Pseudomonas aeruginosa Biofilm Extracellular Matrix," *Journal of Proteome Research,* vol. 11, no. 10, pp. 4906-4915, 2012.

[147] C. Lassek, M. Burghartz, D. Chaves-Moreno, A. Otto, C. Hentschker, S. Fuchs, J. Bernhardt, R. Jauregui, R. Neubauer, D. Becher, D. H. Pieper, M. Jahn, D. Jahn and K. Riedel, "A Metaproteomics Approach to Elucidate Host and Pathogen Protein Expression during Catheter-Associated Urinary Tract Infections (CAUTIs)," *Molecular and cellular Proteomics,* vol. 14, no. 4, pp. 989-1008, 2015.

[148] C. Iacobucci, M. Götze, C. H. Ihling, C. Piotrowski, C. Arlt, M. Schäfer, C. Hage, R. Schmidt and A. Sinz, "A cross-linking/mass spectrometry workflow based on MS-cleavable cross-linkers and the MeroX software for studying protein structures and protein–protein interactions," *nature protocols,* vol. 13, p. 2864–2889, 2018.

[149] M. Q. Müller, F. Dreiocker, C. H. Ihling, M. Schäfer and A. Sinz, "Cleavable Cross-Linker for Protein Structure Analysis: Reliable Identification of Cross-Linking Products by Tandem MS," *Anal. Chem.,* vol. 82, no. 16, pp. 6958-6968, 2010.

[150] C. Hage, C. Iacobucci, A. Rehkamp, C. Arlt and A. Sinz, "The First Zero-Length Mass Spectrometry-Cleavable Cross-Linker for Protein Structure Analysis," *Angew. Chem. Int. Ed.,* vol. 56, no. 46, pp. 14551-14555, 2017.

[151] M. Götze, J. Pettelkau, R. Fritzsche, C. H. Ihling, M. Schäfer and A. Sinz, "Automated Assignment of MS/MS Cleavable Cross-Links in Protein 3D-Structure Analysis," *J. Am. Soc. Mass Spectrom.,* vol. 26, no. 1, pp. 83-97, 2015.

[152] J. Yang and Y. Zhang, "I-TASSER server: new development for protein structure and function predictions," *Nucleic Acid Research,* vol. 43, no. W1, pp. W174-W181, 2015.

[153] B. Webb and A. Sali, "Protein Structure Modeling with MODELLER," in *Functional Genomics: Methods and Protocols*, M. Kaufmann, C. Kinger and A. Savelsbergh, Eds., New York, Springer, 2017, pp. 39-54.

[154] A. Kahraman, L. Malmström and R. Aebersold, "Xwalk: computing and visualizing distances in cross-linking experiments," *Bioinformatics,* vol. 27, no. 15, pp. 2163-2164, 2011.

[155] C. Yeats, N. D. Rawlings and A. Bateman, "The PepSY domain: a regulator of peptidase activity in the microbial environment?," *TRENDS in Biochemical Sciences,* vol. Vol.29, no. No.4, pp. 169-172, 2004.

[156] A. Tzanis, K. A. Dalton, A. Hesketh, C. D. d. Henst, M. J. Buttner, A. Thibessard und G. H. Kelemen, „A sporulation-specific, sigF dependent protein, SspA, affects septum positioning in Streptomyces coelicolor," *Molecular Microbiology,* Bd. 91, Nr. 2, pp. 363-380, 2014.

[157] F. M. Boland, A. Atrih, H. Chirakkal, S. J. Foster and A. Moir, "Complete spore-cortex hydrolysis duringgermination ofBacillus subtilis168 requiresSleB and YpeB," *Microbiology,* vol. 146, pp. 57-64, 2000.

[158] Y. Li, X. Y. Butzin, A. Davis, B. Setlow, G. Korza, F. I. Üstock, G. Christie, P. Setlow and B. Hao, "Activity and Regulation of Various Forms of CwlJ, SleB, and YpeB Proteins in Degrading Cortex Peptidoglycan of Spores of BacillusSpecies In Vitroand during Spore Germination," *Journal of Bacteriology,* vol. 195, no. 11, pp. 2530-2540, 2013.

[159] P. K. Lawrence, B. Rokbi, N. Arnaud-Barbe, E. L. Sutten, J. Norimine, K. K. Lahmers and W. C. Brown, "CD4 T Cell Antigens from Staphylococcus aureus Newman Strain Identified following Immunization with Heat-Killed Bacteria," *Clin. Vaccine Immunol.,* vol. 19, no. 4, pp. 477-489, 2012.

[160] X. Liang, C. Yu, J. Sun, H. Liu, C. Landwehr, D. Holmes and Y. Ji, "Inactivation of a Two-Component Signal Transduction System, SaeRS, Eliminates Adherence and Attenuates Virulence of Staphylococcus aureus," *Infection and Immunity,* vol. 74, no. 8, pp. 4655-4665, 2006.

[161] T. K. Nygaard, K. B. Pallister, P. Ruzevich, S. Griffith, C. Vuong and J. M. Voyich, "SaeR Binds a Consensus Sequence within Virulence Gene Promoters to Advance USA300 Pathogenesis," *The Journal of Infectious Diseases,* vol. 201, pp. 241-254, 2010.

[162] M. Pantrangi, V. K. Singh, C. Wolz and S. K. Shukla, "Staphylococcal superantigen-like genes, ssl5 and ssl8, are positively regulated by Sae and negatively by Agr in theNewman strain," *FEMS Microbiol. Lett.,* vol. 308, pp. 175-184, 2010.

[163] N. D. Hammer and E. P. Skaar, "Molecular mechanisms of Staphylococcus aureus iron acquisition," *Annu. Rev. Microbiol.,* vol. 65, pp. 129-147, 2011.

[164] J. C. Perez, D. Shin, I. Zwir, T. Latifi, T. J. Hadley and E. A. Groisman, "Evolution of a Bacterial Regulon Controlling Virulence and Mg2+ Homeostasis," *PLoS Genet,* vol. 5(3): e1000428, 2009.

[165] M. T. Nguyen und F. Götz, „Lipoproteins of Gram-Positive Bacteria: Key Players in the Immune Response and Virulence," *Microbiol Mol Biol Rev,* Bd. 80, Nr. 3, pp. 891-903, 2016.

[166] R. S. Flannagan, B. Heit and D. E. Heinrichs, "Intracellular replication of Staphylococcus aureus in mature phagolysosomes in macrophages precedes host cell death, and bacterial escape and dissemination," *Cellular Microbiology,* vol. 18, no. 4, p. 514–535, 2016.

[167] T. Geiger, C. Goerke, M. Mainiero, D. Kraus and C. Wolz, "The Virulence Regulator Sae of Staphylococcus aureus: Promoter Activities and Response to Phagocytosis-Related Signals," *Journal of Bacteriology,* vol. 190, no. 10, p. 3419–3428, 2008.

[168] K. Hempel, J. Pané-Farré, A. Otto, S. Sievers, M. Hecker and D. Becher, "Quantitative Cell Surface Proteome Profiling for SigB-Dependent Protein Expression in the Human Pathogen Staphylococcus aureus via Biotinylation Approach," *Journal of Proteome Research,* vol. 9, no. 3, pp. 1579-1590, 2010.

[169] I. L. Alberts, K. Nadassy and S. J. Wodak, "Analysis of zinc binding sites in protein crystal structures," *Protein Science,* vol. 7, pp. 1700-1716, 1998.

[170] S. Park and E. A. Groisman, "Signal-specific temporal response by the S almonella PhoP /PhoQ regulatory system," *Molecular Microbiology,* vol. 91, no. 1, p. 135–144, 2014.

[171] M. M. S. M. Wösten, L. F. F. Kox, S. Chamnongpol, F. C. Soncini and E. A. Groisman, "A Signal Transduction System that Responds to Extracellular Iron," *Cell,* vol. 103, no. 1, pp. 113-125, 2000.

[172] C. Yeats, N. D. Rawlings and A. Bateman, "The PepSY domain: a regulator of peptidase activity in the microbial environment?," *TRENDS in Biochemical Sciences,* vol. 29, no. 4, pp. 169-172, 2004.

[173] E. A. Groisman, "Feedback Control of Two-Component Regulatory Systems," *Annu. Rev. Microbiol.,* vol. 70, pp. 103-124, 2016.

[174] O. Poupel, C. Proux, B. Jagla, T. Msadek and S. Dubrac, "SpdC, a novel virulence factor, controls histidine kinase activity in Staphylococcus aureus," *PLoS Pathog,* vol. 14(3): e1006917, 2018.

7 Acknowledgement

Here, I would like to acknowledge all the people that contributed to my work in one or the other way that I was finally able to complete my dissertation.

First, I like to thank Prof. Dr. Susanne Engelmann who gave me the possibility to work on my PhD in her research group on a very interesting topic. It has been a great supervision as she had always supported me and we had great discussions about my work, experiments and ideas. Furthermore, I thank Prof. Dr. Wulf Blankenfeldt for his scientific support, his ideas regarding this work and being the second examiner. Additionally, I thank Prof. Dr. Michael Hust for being the chairman of the examination commission.

Furthermore, I am grateful for the support of Prof. Dr. Andrea Sinz from the Martin-Luther University Halle-Wittenberg, who gave help and ideas for the cross-linking experiments. Further, many thanks go to the research group of Prof. Dr. Andrea Sinz as they had created a pleasant atmosphere when I was working there for several weeks and especially Dirk Tänzler and Christian Ihling who helped me a lot with the experimental procedures of the cross-linking experiments.

I thank Dr. Martin Kucklick for his support regarding mass spectrometry and his help with setting up experimental designs for the proteomic experiments and also the other members of the microbial proteomics research group Birgit Jung, Martin Weinert, Nicole Beier, Erik Lehmann, Alexander Beckmann and all students that contributed to this work throughout my time. We had a great working atmosphere and always helped each other with our projects discussing results, problems and ideas.

Special thanks go to Christina Nitzsche and Gunhild Voß who always helped warmly with any administrative issue.

In the end I am really grateful for the support of my family who motivated and encouraged me. Especially my husband Georg was really patient with me and supported me, particularly whenever experiments needed unusual working hours he took care of our child.

8 Appendix

Table 14 Differential protein amounts in the Δpvr mutant compared to the parental wild type strain in TSB medium

Locus tag[a]	Protein	Function	Fold change[b]	SaeRS regulated[c]
Virulence				
NWMN_0166	Coa	Coagulase precursor	-1.41	+
NWMN_0395	Ssl8	superantigen-like protein 8	-1.60	+
NWMN_0757	Vwb	secreted von Willebrand factor-binding protein precursor	-2.18	+
NWMN_1066	Ecb	fibrinogen-binding protein	DOWN	+
NWMN_1073	Hla	alpha-hemolysin precursor	-1.47	+
NWMN_1075	Ssl12	superantigen-like protein 12	-1.83	
NWMN_1718	LukD	leukocidin LukD precursor	-1.37	+
NWMN_1719	LukE	leukocidin LukE precursor	-1.65	+
NWMN_1872	Eap/Map	MAP domain-containing protein	-1.58	+
NWMN_1877	CHIPS	chemotaxis-inhibiting protein CHIPS	-1.55	+
NWMN_1927	LukF	leukocidin/hemolysin toxin subunit F	-1.65	+
NWMN_1928	LukS	leukocidin/hemolysin toxin subunit S	-1.58	+
NWMN_2317	Sbi	immunoglobulin-binding protein	-1.26	+
NWMN_2318	HlgA	gamma-hemolysin component A	-1.40	+
NWMN_2319	HlgC	gamma-hemolysin component C	-1.64	+
NWMN_2320	HlgB	gamma-hemolysin component B	-1.23	+
Extracellular enzymes				
NWMN_0262	Geh	lipase	-1.09	+
NWMN_1702	SplE	serine protease SplE	-1.72	+
NWMN_1703	SplD	serine protease SplD	-1.97	+
NWMN_1705	SplB	serine protease SplB	-1.77	+
NWMN_1706	SplA	serine protease SplA	-2.23	+
Regulaory Proteins				
NWMN_0677	SaeP	Regulatory protein of the SaeRS system	-1.65	+
Membranes and Transport				
NWMN_0249	NWMN_0249	5'-nucleotidase, lipoprotein e(P4) family protein	-1.02	+
NWMN_0581	NWMN_0581	iron compound ABC transporter iron compound-binding protein	-1.41	

NWMN_1841	CamS	CamS sex pheromone cAM373 precursor	-1.11	
NWMN_1999	SceD	transglycosylase SceD	-1.12	
NWMN_2254	NWMN_2254	multidrug efflux protein	+1.22	
Hypothetical proteins				
NWMN_0401	NWMN_0401	hypothetical protein	-1.52	+
NWMN_0759	NWMN_0759	hypothetical protein	-2.27	+
NWMN_1438	NWMN_1438	Rhodanese domain-containing protein	DOWN	
NWMN_1708	NWMN_1708	hypothetical protein	-1.48	

(a) Locus Tag referring to the *S. aureus* Newman genome sequence annotation

(b) Fold change was determined as the log2 value of the intensity ratio between Δ*pvr* and wild type, negative values indicate a lower amount in the Δ*pvr* mutant strain and positive values indicate a higher amount; DOWN means only identified in the wild type strain. Only fold changes above 1 or below -1 having a p-Value <0.05 were considered

(c) Known SaeRS regulation of the proteins is marked with a + [113] [89] [162] [160] [161] [64]

Table 15 **Differential protein amounts in the Δ*pvr* mutant compared to the parental wild type strain in SA medium**

Locus tag[a]	Protein	Function	Fold change [b]	SaeRS reg [c]	WalKR reg [c]
Virulence					
NWMN_0055	Spa	immunoglobulin G binding protein A precursor (protein A)	-3.37		+
NWMN_0166	Coa	coagulase	-2.58	+	+
NWMN_0388	Ssl1	superantigen-like protein 1	-2.33		
NWMN_0389	Ssl2	superantigen-like protein 2	-2.39		
NWMN_0391	Ssl4	superantigen-like protein 4	-1.73		
NWMN_0392	Ssl5	superantigen-like protein 5	DOWN	+	
NWMN_0393	Ssl6	superantigen-like protein 6	-3.15		
NWMN_0394	Ssl7	superantigen-like protein 7	-1.86	+	
NWMN_0395	Ssl8	superantigen-like protein 8	-2.33	+	
NWMN_0396	Ssl9	superantigen-like protein 9	-1.64	+	
NWMN_0757	Vwb	secreted von Willebrand factor-binding protein precursor	-5.05	+	+
NWMN_0758	Emp	hypothetical protein	-2.38	+	+
NWMN_0760	Nuc	thermonuclease	-1.24	+	
NWMN_1067	Flr	FPRL1 inhibitory protein	-3.63	+	+
NWMN_1070	Scc	fibrinogen-binding protein	-4.05	+	+
NWMN_1073	Hla	alpha-hemolysin	-2.32	+	+
NWMN_1075	Ssl12	superantigen-like protein 12	-2.40		
NWMN_1076	Ssl13	superantigen-like protein 13	-1.73		
NWMN_1077	Ssl14	superantigen-like protein 14	-2.17		
NWMN_1872	Eap/Map	MAP domain-containing protein	-1.58	+	+

NWMN_1876	SCIN	complement inhibitor SCIN	-2.76	+	+
NWMN_1877	CHIPS	chemotaxis-inhibiting protein CHIPS	-2.22	+	+
NWMN_2109	NWMN_2109	toxin	-1.94		
NWMN_2317	Sbi	immunoglobulin-binding protein sbi	-1.79	+	+
NWMN_2318	HlgA	gamma-hemolysin component A	-1.89	+	+
NWMN_2319	HlgC	gamma-hemolysin component C	-1.48	+	+
NWMN_2529	ClfB	clumping factor B	-1.42	+	
Extracellular Enzymes					
NWMN_0262	Geh	lipase	-1.93	+	+
NWMN_1332	CtpA	serine protease	-1.45		
NWMN_1702	SplE	serine protease SplE	-1.86	+	+
NWMN_1703	SplD	serine protease SplD	-1.61	+	+
NWMN_1705	SplB	serine protease SplB	-1.50	+	+
NWMN_1706	SplA	serine protease SplA	-1.60	+	+
NWMN_2308	DsbA	protein disulfide-isomerase	-2.19		
NWMN_2526	PhoB	alkaline phosphatase	-1.48		
Regulatory Proteins					
NWMN_0677	SaeP	Regulatory protein of the SaeRS system	-1.91	+	+
Transport and binding proteins					
NWMN_0022	AdsA	multifunctional 2,3-cyclic-nucleotide	-1.73		
NWMN_0220	EsaA	protein EsaA	-2.07		
NWMN_0428	MetQ2	ABC transporter substrate-binding protein	-1.62		
NWMN_0581	NWMN_0581	ABC transporter substrate-binding protein	-3.00		
NWMN_0782	MetQ1	methionine ABC transporter substrate-binding	-1.62		
NWMN_0860	Opp-3A	peptide ABC transporter substrate-binding	-2.02		
NWMN_1040	IsdB	iron-regulated surface determinant protein B	-1.54	+	
NWMN_1041	IsdA	iron-regulated surface determinant protein A	-1.53		
NWMN_1042	IsdC	iron-regulated surface determinant protein C	-3.49		
NWMN_1044	IsdE	heme uptake system protein IsdE	DOWN		
NWMN_1540	YajC	preprotein translocase subunit YajC	DOWN		
NWMN_1624	IsdH	iron-regulated surface determinant protein H	-1.14		
NWMN_1733	PrsA	foldase	-2.74		+
NWMN_1750	NWMN_1750	ABC transporter permease	-1.66		+
NWMN_2011	AtpF	ATP synthase subunit B	DOWN		

NWMN_2078	HtsA	ABC transporter substrate-binding protein	-1.62		
NWMN_2162	NWMN_2162	multidrug transporter	-1.39		
NWMN_2179	ModA	molybdate ABC transporter substrate-binding	-1.94		
NWMN_2185	FhuD2	ferrichrome ABC transporter substrate-binding	-2.35		
NWMN_2306	NWMN_2306	zinc ABC transporter substrate-binding protein	-1.95		
NWMN_2313	TcyA	amino acid ABC transporter substrate-binding	-1.95		
NWMN_2345	OpuCC	amino acid transporter	-4.45		
NWMN_2364	CntA	nickel ABC transporter, nickel/metallophore	-2.00		
Cell Wall and Membrane					
NWMN_0041	Plc	1-phosphatidylinositol phosphodiesterase	-2.66	+	
NWMN_0429	Sle1	N-acetylmuramoyl-L-alanine amidase	-1.47	+	+
NWMN_0830	GlpQ	glycerophosphoryl diester phosphodiesterase	-1.90	+	+
NWMN_1361	Pbp2	penicillin-binding protein 2	-1.12		
NWMN_1455	Pbp3	penicillin-binding protein 3	-1.05		
NWMN_1534	LytH	cell wall amidase	DOWN		
NWMN_1667	NWMN_1667	mannosyl-glycoprotein endo-beta-N-acetylglucosamidase	-2.00		+
NWMN_1999	SceD	transglycosylase SceD	-1.05		
NWMN_2092	-	alpha/beta hydrolase	-1.69		
NWMN_2392	SasG	accumulation-associated protein	-2.31		+
NWMN_2395	GtaB	UTP--glucose-1-phosphate uridylyltransferase	-1.45		
NWMN_2426	SrtA	class A sortase SrtA	-1.89		
NWMN_2467	OatA	O-acetyltransferase OatA	-2.27		
NWMN_2469	IsaA	transglycosylase IsaA	-1.65		
Hypothetical proteins and other functions					
NWMN_0306	NWMN_0306	hypothetical protein	-1.48		
NWMN_0402	NWMN_0402	hypothetical protein	-3.06	+	+
NWMN_0412	Lpl9	tandem lipoprotein	-1.30		
NWMN_0585	NWMN_0585	hypothetical protein	-2.06		+
NWMN_0646	NWMN_0646	hypothetical protein	-2.20		
NWMN_0665	NWMN_0665	hypothetical protein	-5.34		+
NWMN_0759	NWMN_0759	hypothetical protein	-2.98	+	
NWMN_0931	NWMN_0931	hypothetical protein	-3.02	+	

NWMN_0969	NWMN_0969	hypothetical protein	-2.51		
NWMN_1020	NWMN_1020	hypothetical protein	-3.05		
NWMN_1021	NWMN_1021	phage head-tail adapter protein	-3.10		
NWMN_1033	NWMN_1033	hypothetical protein	-2.20		
NWMN_1037	NWMN_1037	hypothetical protein	-2.70		
NWMN_1476	NWMN_1476	hypothetical protein	DOWN		
NWMN_1552	NWMN_1552	DUF4930 domain-containing protein	-3.42		+
NWMN_1631	NWMN_1631	hypothetical protein	-2.52		
NWMN_1679	NWMN_1679	hypothetical protein	DOWN		
NWMN_1708	NWMN_1708	hypothetical protein	-2.45		+
NWMN_1730	NWMN_1730	hypothetical protein	-2.71		
NWMN_1820	NWMN_1820	hypothetical protein	-4.93		
NWMN_2088	AmaP	hypothetical protein	-2.20		
NWMN_2199	SsaA	secretory antigen precursor SsaA	-1.48	+	+
NWMN_2211	NWMN_2211	LytR family transcriptional regulator	-1.69		
NWMN_2257	TcaA	teicoplanin resistance associated protein A	-2.06		

(a) Locus Tag referring to the *S. aureus* Newman genome sequence annotation

(b) Fold change was determined as the log2 value of the intensity ratio between Δ*pvr* and wild type, negative values indicate a lower amount in the Δ*pvr* mutant strain and positive values indicate a higher amount; DOWN means only identified in the wild type strain. Only fold changes above 1 or below -1 having a p-Value <0.05 were considered

(c) Known SaeRS regulation of the proteins is marked with a + [113] [89] [162] [160] [161] [64]; Known WalKR regulation of the proteins is marked with a + [86]

Table 16 Possible interaction partner of NWMN_0364 from Co-IP

Locus tag [a]	Protein	Function	Relative Intensity[b]	RSD (%)[c]
NWMN_0507	RpsL	30S ribosomal protein S12	0.02137	14
NWMN_0677	SaeP	Regulatory protein of SaeRS	0.08345	29
NWMN_0782	MetQ1	methionine ABC transporter substrate-binding protein	0.03667	32

(a) Locus Tag referring to the *S. aureus* Newman genome sequence annotation.
(b) The relative intensity demonstrates the abundance of the identified protein compared to the bait protein NWMN_0364, where 1 would be equal amounts. Only proteins with a relative abundance >0.02 were considered.
(c) RSD: the relative standard deviation (displayed in percent) determines the reproducibility over three replicates. Only proteins with a maximum RSD of 35% were considered.

Table 17 Possible interaction partner of NWMN_0364 from strep based pull down

Locus tag [a]	Protein	Function	Relative Intensity[b]	RSD (%)[c]
NWMN_0428	MetQ2	Methionine ABC transporter substrate-binding protein	0.0011	22
NWMN_0601	MntC	Metal ABC transporter substrate-binding protein	0.0325	4
NWMN_0753	NWMN_0753	DUF5067 domain-containing protein	0.0011	25
NWMN_0782	MetQ1	Methionine ABC transporter substrate-binding protein	0.0039	23
NWMN_0962	PdhD	dihydrolipoyl dehydrogenase	0.0055	31
NWMN_2147	RplV	50S ribosomal protein L22	0.0011	15
NWMN_2179	ModA	Molybdate ABC transporter substrate-binding protein	0.0019	14
NWMN_2313	TcyA	Amino acid ABC transporter substrate-binding	0.0166	22

(a) Locus Tag referring to the *S. aureus* Newman genome sequence annotation.
(b) The relative intensity demonstrates the abundance of the identified protein compared to the bait protein NWMN_0364, where 1 would be equal amounts. Only proteins with a relative abundance >0.001 were considered.
(c) RSD: the relative standard deviation (displayed in percent) determines the reproducibility over three replicates. Only proteins with a maximum RSD of 35% were considered.

Table 18 Intramolecular cross-links of NWMN_0364

Additive	Cross-linker	Total[a]	w/o tag[b]	<cutoff[c]	satisfaction[d]
buffer	CDI	2	1	1	100%
	DSBU	33	31	24	77.4%
ZnCu	CDI	2	2	2	100%
	DSBU	28	25	24	96%
Zn	CDI	6	5	4	80%
	DSBU	14	14	14	100%
Cu	CDI	2	0	0	-
	DSBU	32	28	25	89.3%

(a) Number identified cross-links

(b) Number identified cross-links, without connecting the strep-tag

(c) Number of cross-links that match within the Euclidian distance below 30Å for DSBU and below 25Å for CDI

(d) Percentage of satisfaction of the cross-links identified without connection to the strep-tag to the monomeric model of NWMN_0364

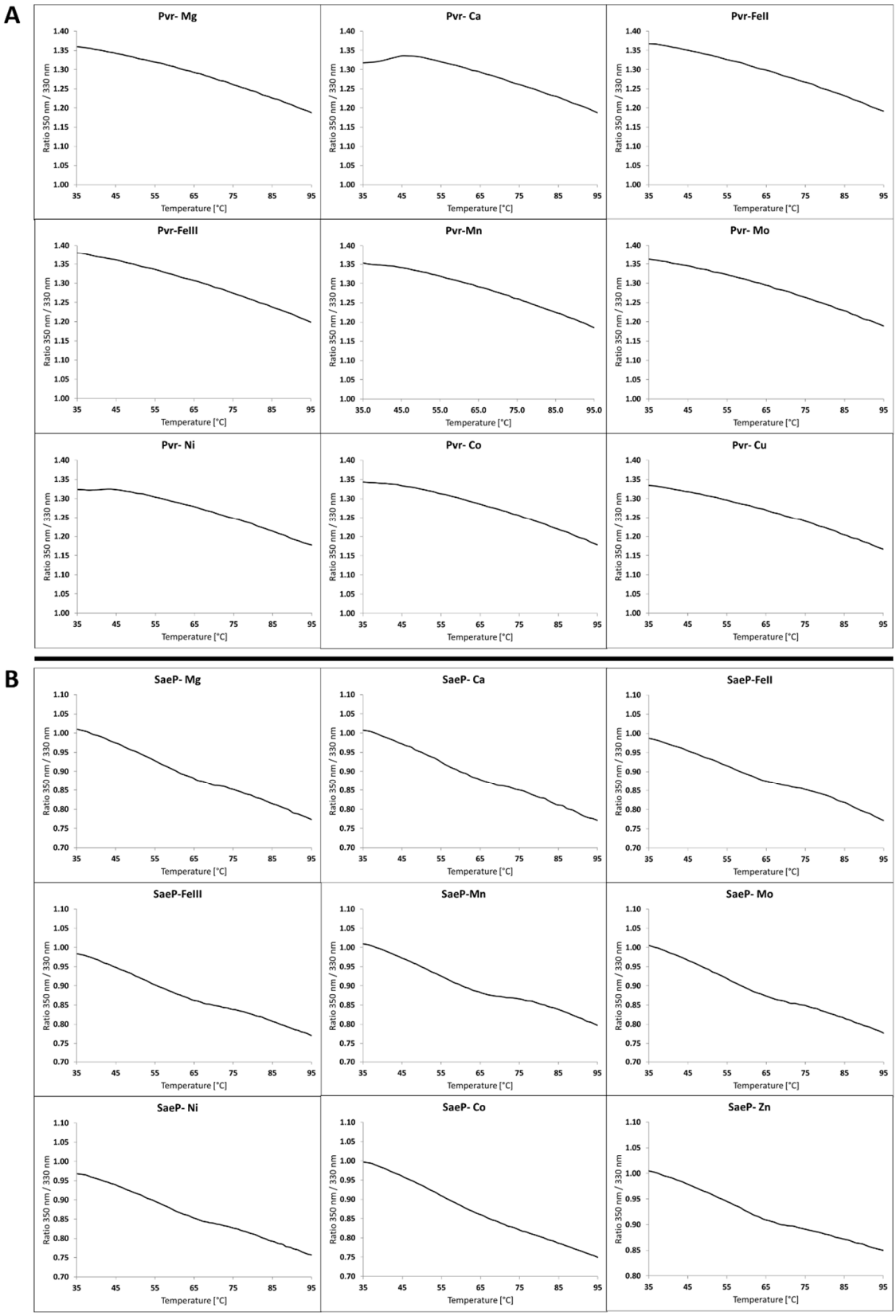

Figure 39 Melting curves SaeP and Pvr with metal ions
Temperature is plotted against the UV-absorption. Shown are the proteins in addition of 1 mM of the following metals: $MgCl_2$, $CaCl_2$, $FeSO_4$, $FeCl_3$, $MnCl_2$, Na_2MoO_4, $NiCl_2$, $CoCl_2$, $ZnCl_2$ and $CuCl_2$ **(A)** melting curves of Pvr **(B)** melting curves of SaeP.

Table 19 all identified extracellular and membrane associated proteins in the TSB proteome

Locus Tag	Mean Intensity WT	Sandard deviation WT	Mean Intensity Δ0364	Standard deviation Δ0364	Log2 Ratio	t-test significant
NWMN_0364	1.13E+08	2.33E+07	0.00E+00	0.00E+00	DOWN	+
NWMN_1066	1.27E+06	5.30E+05	0.00E+00	0.00E+00	DOWN	+
NWMN_1438	5.18E+05	7.93E+04	0.00E+00	0.00E+00	DOWN	+
NWMN_0665	1.19E+06	1.41E+06	0.00E+00	0.00E+00	DOWN	
NWMN_0369	0.00E+00	0.00E+00	2.12E+05	1.45E+05	UP	
NWMN_1091	8.29E+05	9.82E+05	0.00E+00	0.00E+00	DOWN	
NWMN_2283	6.03E+05	2.52E+05	0.00E+00	0.00E+00	DOWN	
NWMN_1090	4.17E+05	5.06E+05	0.00E+00	0.00E+00	DOWN	
NWMN_0930	5.83E+05	9.11E+04	1.83E+06	2.00E+06	1.65	
NWMN_2254	2.02E+07	4.74E+06	4.70E+07	8.13E+06	1.22	+
NWMN_2384	5.23E+05	4.03E+05	9.59E+05	3.15E+05	0.87	
NWMN_0390	3.29E+05	4.53E+04	4.92E+05	1.68E+05	0.58	
NWMN_1631	4.93E+06	9.10E+05	6.47E+06	3.16E+06	0.39	
NWMN_2203	2.32E+08	1.22E+08	2.66E+08	6.26E+06	0.20	
NWMN_1689	9.58E+05	3.61E+05	1.09E+06	9.22E+04	0.19	
NWMN_1924	9.33E+05	3.12E+05	1.01E+06	3.06E+05	0.12	
NWMN_0473	1.29E+06	1.79E+05	1.36E+06	1.46E+05	0.08	
NWMN_2092	7.37E+06	1.28E+06	7.59E+06	1.36E+06	0.04	
NWMN_0524	1.57E+08	2.72E+07	1.55E+08	7.27E+07	-0.03	
NWMN_2466	1.53E+06	5.90E+05	1.50E+06	8.05E+05	-0.03	
NWMN_1645	7.62E+06	3.23E+06	7.04E+06	1.67E+06	-0.11	
NWMN_2078	3.25E+06	2.46E+05	2.98E+06	1.09E+06	-0.12	
NWMN_1040	3.75E+06	1.54E+06	3.40E+06	5.52E+05	-0.14	
NWMN_1624	2.05E+06	1.72E+06	1.85E+06	1.45E+06	-0.15	
NWMN_0782	7.50E+06	1.90E+06	6.60E+06	7.06E+05	-0.19	
NWMN_0055	1.09E+08	2.82E+07	9.40E+07	4.61E+07	-0.21	
NWMN_2061	5.59E+07	5.74E+06	4.79E+07	2.09E+07	-0.22	
NWMN_2106	2.29E+07	1.93E+06	1.97E+07	7.15E+06	-0.22	
NWMN_2392	6.81E+07	5.16E+06	5.80E+07	2.61E+07	-0.23	
NWMN_2467	9.12E+06	1.39E+06	7.69E+06	1.97E+06	-0.25	
NWMN_0922	2.57E+10	3.82E+09	2.15E+10	7.73E+09	-0.26	
NWMN_2569	7.47E+09	1.62E+09	6.14E+09	2.83E+09	-0.28	
NWMN_1551	7.14E+07	1.81E+07	5.86E+07	1.33E+07	-0.29	
NWMN_0917	9.21E+08	1.53E+08	7.55E+08	1.49E+08	-0.29	
NWMN_1712	1.06E+07	1.61E+06	8.64E+06	1.21E+06	-0.29	
NWMN_1455	5.02E+08	6.77E+07	4.01E+08	6.66E+07	-0.33	
NWMN_0428	2.34E+06	3.83E+05	1.86E+06	1.52E+05	-0.33	
NWMN_0146	1.05E+06	8.16E+04	8.36E+05	1.55E+05	-0.33	
NWMN_0059	3.66E+06	8.54E+05	2.90E+06	2.68E+05	-0.34	
NWMN_2537	2.23E+08	3.99E+07	1.76E+08	4.96E+07	-0.35	
NWMN_1332	1.35E+07	4.17E+06	1.06E+07	5.58E+05	-0.36	
NWMN_1361	1.60E+07	1.84E+06	1.24E+07	4.07E+06	-0.36	

NWMN_0220	5.13E+07	6.31E+06	3.97E+07	1.67E+07	-0.37	
NWMN_0753	1.20E+06	4.34E+05	9.17E+05	5.34E+05	-0.39	
NWMN_2109	5.73E+08	5.10E+07	4.35E+08	1.04E+08	-0.40	
NWMN_0396	3.09E+06	4.32E+05	2.34E+06	7.77E+05	-0.40	
NWMN_1038	6.89E+05	1.58E+05	5.20E+05	1.13E+05	-0.41	
NWMN_2063	8.56E+06	5.55E+05	6.40E+06	1.28E+06	-0.42	
NWMN_2270	3.93E+07	1.00E+07	2.94E+07	7.03E+06	-0.42	
NWMN_0394	1.23E+07	2.07E+06	9.14E+06	1.13E+06	-0.43	
NWMN_0523	5.97E+07	4.07E+06	4.42E+07	1.90E+07	-0.43	
NWMN_1043	3.11E+06	4.98E+05	2.27E+06	6.55E+05	-0.45	
NWMN_1730	8.04E+05	4.99E+05	5.86E+05	3.18E+05	-0.46	
NWMN_0210	4.99E+07	7.24E+06	3.61E+07	9.57E+06	-0.47	
NWMN_0705	2.69E+07	3.89E+06	1.94E+07	1.12E+07	-0.47	
NWMN_2179	4.47E+06	1.16E+06	3.22E+06	1.20E+06	-0.48	
NWMN_1041	2.60E+08	2.85E+07	1.86E+08	3.90E+07	-0.48	
NWMN_1847	1.27E+09	2.44E+08	9.05E+08	1.76E+08	-0.48	
NWMN_2345	1.08E+06	3.27E+05	7.71E+05	3.61E+05	-0.49	
NWMN_1236	5.26E+05	3.18E+05	3.69E+05	1.14E+05	-0.51	
NWMN_0525	4.08E+08	1.25E+07	2.85E+08	1.44E+08	-0.52	
NWMN_0925	8.99E+07	2.31E+07	6.25E+07	1.45E+07	-0.52	
NWMN_0851	3.00E+08	7.23E+07	2.06E+08	4.04E+07	-0.54	
NWMN_2211	2.04E+07	4.09E+06	1.40E+07	3.68E+06	-0.54	
NWMN_2543	3.45E+09	3.94E+08	2.31E+09	5.63E+08	-0.58	
NWMN_2185	1.99E+07	2.42E+06	1.32E+07	9.73E+05	-0.59	+
NWMN_0836	7.25E+06	1.51E+06	4.81E+06	1.54E+06	-0.59	
NWMN_1274	5.33E+06	3.97E+05	3.52E+06	1.65E+06	-0.60	
NWMN_2199	4.83E+08	1.18E+08	3.18E+08	8.54E+07	-0.60	
NWMN_0429	1.68E+09	4.60E+08	1.10E+09	1.80E+08	-0.61	
NWMN_1435	1.59E+06	1.00E+06	1.04E+06	2.65E+05	-0.62	
NWMN_0687	4.72E+09	8.82E+08	3.06E+09	4.31E+08	-0.63	
NWMN_0756	3.36E+08	3.22E+07	2.15E+08	8.95E+07	-0.65	
NWMN_1123	3.34E+06	7.03E+05	2.12E+06	6.67E+05	-0.65	
NWMN_1077	1.38E+07	3.45E+06	8.69E+06	5.36E+06	-0.67	
NWMN_1621	6.71E+06	2.53E+05	4.22E+06	1.81E+06	-0.67	
NWMN_0412	1.64E+07	4.35E+06	1.03E+07	1.39E+06	-0.67	
NWMN_0393	1.42E+06	4.19E+05	8.70E+05	3.09E+05	-0.70	
NWMN_1345	5.68E+07	3.62E+06	3.47E+07	2.20E+07	-0.71	
NWMN_0391	4.07E+06	1.84E+05	2.44E+06	1.01E+06	-0.74	
NWMN_1940	6.39E+07	4.38E+06	3.81E+07	2.26E+07	-0.74	
NWMN_0758	1.39E+08	1.72E+07	8.27E+07	9.91E+06	-0.75	+
NWMN_2536	7.39E+07	5.46E+06	4.39E+07	9.89E+06	-0.75	+
NWMN_1042	1.52E+07	4.81E+06	9.03E+06	3.28E+06	-0.75	
NWMN_0612	1.20E+06	8.75E+04	7.13E+05	2.45E+05	-0.76	
NWMN_1733	1.02E+07	1.95E+06	6.06E+06	9.72E+05	-0.76	+
NWMN_0634	4.97E+08	8.63E+07	2.93E+08	6.31E+07	-0.76	+
NWMN_2529	4.33E+08	3.41E+07	2.55E+08	7.95E+07	-0.76	

NWMN_0087	2.27E+07	2.13E+06	1.34E+07	2.87E+06	-0.77	+
NWMN_0388	5.53E+06	1.53E+06	3.19E+06	1.37E+06	-0.80	
NWMN_1540	3.57E+05	7.54E+04	2.05E+05	2.90E+05	-0.80	
NWMN_1883	7.82E+08	1.82E+08	4.44E+08	6.29E+07	-0.81	+
NWMN_0218	9.66E+07	8.11E+06	5.49E+07	1.17E+07	-0.82	+
NWMN_0601	1.61E+08	3.32E+07	9.06E+07	1.23E+07	-0.83	+
NWMN_1061	3.60E+06	6.10E+05	2.01E+06	8.17E+05	-0.84	
NWMN_0173	1.10E+06	4.37E+05	6.10E+05	4.74E+04	-0.85	
NWMN_2313	5.79E+07	2.36E+07	3.20E+07	6.16E+06	-0.85	
NWMN_2306	4.65E+06	7.66E+05	2.55E+06	3.83E+05	-0.87	+
NWMN_0585	9.62E+08	2.25E+08	5.26E+08	1.54E+08	-0.87	
NWMN_1880	6.37E+07	9.61E+06	3.48E+07	7.80E+06	-0.87	+
NWMN_2469	2.88E+09	3.43E+08	1.55E+09	3.49E+08	-0.90	+
NWMN_2526	3.79E+06	5.48E+05	2.02E+06	7.45E+05	-0.91	
NWMN_2088	2.59E+06	3.56E+05	1.37E+06	7.79E+05	-0.92	
NWMN_0724	4.02E+06	7.60E+05	2.11E+06	7.10E+05	-0.93	
NWMN_1750	4.37E+05	1.56E+05	2.27E+05	1.69E+05	-0.95	
NWMN_0760	4.46E+08	1.39E+08	2.27E+08	7.61E+06	-0.97	+
NWMN_0041	1.17E+09	5.02E+08	5.81E+08	9.48E+07	-1.01	
NWMN_0830	5.58E+08	2.11E+08	2.77E+08	4.29E+07	-1.01	
NWMN_1067	7.02E+06	2.97E+06	3.47E+06	1.79E+06	-1.02	
NWMN_0249	7.39E+08	1.90E+08	3.65E+08	3.47E+07	-1.02	+
NWMN_0860	1.99E+06	1.21E+06	9.64E+05	3.50E+05	-1.05	
NWMN_0389	3.65E+06	1.47E+06	1.72E+06	3.97E+05	-1.08	
NWMN_1069	1.96E+08	5.66E+07	9.20E+07	2.94E+07	-1.09	
NWMN_0262	1.09E+09	2.02E+08	5.13E+08	1.27E+08	-1.09	+
NWMN_0392	5.27E+06	3.17E+06	2.46E+06	1.19E+06	-1.10	
NWMN_1841	3.92E+06	8.25E+05	1.82E+06	5.15E+05	-1.11	+
NWMN_1820	6.83E+05	5.44E+04	3.16E+05	2.85E+05	-1.11	
NWMN_1999	3.98E+07	1.47E+07	1.83E+07	1.43E+06	-1.12	+
NWMN_0764	4.93E+06	2.38E+06	2.27E+06	9.53E+05	-1.12	
NWMN_1632	7.84E+05	3.63E+05	3.36E+05	2.99E+05	-1.22	
NWMN_1704	4.89E+07	1.75E+07	2.08E+07	4.63E+06	-1.23	
NWMN_2320	2.31E+09	4.34E+08	9.84E+08	3.41E+08	-1.23	+
NWMN_2317	1.80E+08	2.69E+07	7.53E+07	1.04E+07	-1.26	+
NWMN_1076	3.19E+07	1.21E+07	1.28E+07	6.82E+06	-1.31	
NWMN_1649	1.10E+06	1.66E+05	4.29E+05	3.52E+05	-1.35	
NWMN_1718	1.76E+08	2.55E+07	6.79E+07	3.22E+07	-1.37	+
NWMN_2318	2.00E+09	5.57E+08	7.61E+08	1.06E+08	-1.40	+
NWMN_0166	1.39E+09	1.22E+08	5.25E+08	1.04E+08	-1.41	+
NWMN_0581	2.98E+06	6.99E+05	1.13E+06	1.45E+05	-1.41	+
NWMN_2426	3.81E+06	1.63E+06	1.40E+06	2.91E+05	-1.45	
NWMN_1073	1.30E+10	2.82E+09	4.67E+09	8.92E+08	-1.47	+
NWMN_1708	1.40E+08	1.70E+07	5.02E+07	1.97E+07	-1.48	+
NWMN_1701	9.16E+07	4.30E+07	3.25E+07	7.11E+06	-1.49	
NWMN_0401	3.92E+08	2.01E+07	1.37E+08	4.43E+07	-1.52	+

NWMN_0400	1.70E+08	6.31E+07	5.92E+07	2.36E+07	-1.52	
NWMN_1877	2.67E+08	9.27E+07	9.13E+07	2.33E+07	-1.55	+
NWMN_0931	1.09E+07	5.70E+06	3.71E+06	1.64E+06	-1.56	
NWMN_1928	1.69E+09	4.43E+08	5.68E+08	4.92E+07	-1.58	+
NWMN_1872	6.03E+09	1.71E+09	2.01E+09	5.94E+08	-1.58	+
NWMN_0395	2.19E+06	4.28E+05	7.23E+05	2.62E+05	-1.60	+
NWMN_1980	1.49E+06	1.23E+06	4.84E+05	2.37E+05	-1.62	
NWMN_2319	3.53E+09	9.30E+08	1.13E+09	1.14E+08	-1.64	+
NWMN_1719	2.23E+08	6.36E+07	7.10E+07	5.40E+06	-1.65	+
NWMN_1927	1.22E+09	3.17E+08	3.87E+08	6.00E+07	-1.65	+
NWMN_0677	4.27E+08	1.17E+08	1.36E+08	2.12E+07	-1.65	+
NWMN_1702	1.54E+08	5.96E+07	4.66E+07	1.50E+07	-1.72	+
NWMN_1705	7.93E+08	3.08E+08	2.32E+08	1.72E+07	-1.77	+
NWMN_1075	8.14E+05	1.01E+05	2.29E+05	1.77E+05	-1.83	+
NWMN_1703	4.62E+07	1.26E+07	1.18E+07	3.73E+06	-1.97	+
NWMN_0362	1.52E+08	1.00E+08	3.73E+07	7.78E+06	-2.03	
NWMN_0757	5.02E+07	2.00E+06	1.11E+07	2.62E+06	-2.18	+
NWMN_1706	1.68E+08	7.44E+07	3.59E+07	7.64E+06	-2.23	+
NWMN_2443	3.71E+06	2.91E+06	7.74E+05	5.04E+05	-2.26	
NWMN_0759	2.85E+06	1.31E+06	5.89E+05	2.70E+05	-2.27	+
NWMN_1876	4.54E+07	1.76E+07	8.61E+06	6.78E+06	-2.40	
NWMN_0078	2.79E+07	3.30E+07	3.93E+06	3.68E+05	-2.83	

Table 20 all identified extracellular and membrane associated proteins in the SA proteome

Locus Tag	Mean Intensity WT	Sandard deviation WT	Mean Intensity Δ0364	Standard deviation Δ0364	Log2 Ratio	t-test significant
NWMN_0364	3.77E+08	4.73E+07	0.00E+00	0.00E+00	DOWN	
NWMN_1476	1.17E+07	1.65E+07	0.00E+00	0.00E+00	DOWN	
NWMN_1044	1.52E+06	7.81E+05	0.00E+00	0.00E+00	DOWN	
NWMN_0392	1.36E+06	4.85E+05	0.00E+00	0.00E+00	DOWN	
NWMN_1679	2.99E+05	5.38E+04	0.00E+00	0.00E+00	DOWN	
NWMN_1534	1.40E+06	3.21E+05	0.00E+00	0.00E+00	DOWN	
NWMN_2379	1.01E+06	6.78E+04	0.00E+00	0.00E+00	DOWN	
NWMN_1540	9.11E+05	4.67E+05	0.00E+00	0.00E+00	DOWN	
NWMN_2011	1.83E+05	3.13E+04	0.00E+00	0.00E+00	DOWN	
NWMN_RS01590	9.79E+06	5.52E+06	0.00E+00	0.00E+00	DOWN	
NWMN_RS10960	1.26E+06	3.71E+05	0.00E+00	0.00E+00	DOWN	
NWMN_2254	1.16E+06	3.72E+05	1.32E+06	1.51E+06	0.19	

NWMN_0651	2.49E+06	1.09E+06	2.80E+06	2.17E+06	0.17	
NWMN_0369	6.14E+06	2.93E+06	6.54E+06	2.77E+06	0.09	
NWMN_0918	1.30E+08	3.85E+07	1.35E+08	5.56E+07	0.05	
NWMN_1038	3.48E+05	2.46E+05	3.22E+05	2.42E+05	-0.11	
NWMN_2106	5.48E+06	2.34E+06	4.81E+06	1.61E+06	-0.19	
NWMN_1924	8.26E+06	1.60E+06	6.88E+06	4.10E+06	-0.26	
NWMN_2203	2.35E+09	6.94E+08	1.92E+09	1.99E+09	-0.29	
NWMN_1689	2.08E+07	3.49E+06	1.67E+07	9.88E+06	-0.31	
NWMN_2545	1.50E+07	1.07E+06	1.20E+07	5.15E+06	-0.32	
NWMN_1701	4.63E+06	8.62E+05	3.64E+06	2.55E+06	-0.34	
NWMN_1784	3.60E+05	6.17E+04	2.79E+05	3.95E+05	-0.37	
NWMN_2536	2.54E+07	2.06E+06	1.91E+07	2.79E+06	-0.41	
NWMN_1940	2.87E+08	7.80E+07	1.98E+08	6.40E+07	-0.53	
NWMN_0604	8.94E+05	2.02E+05	6.16E+05	3.92E+05	-0.54	
NWMN_1790	5.24E+06	1.38E+06	3.57E+06	1.50E+06	-0.55	
NWMN_0983	1.28E+06	6.29E+05	8.58E+05	3.67E+05	-0.57	
NWMN_0390	2.70E+07	5.16E+06	1.80E+07	6.57E+06	-0.58	
NWMN_RS01180	9.93E+07	3.57E+07	6.60E+07	1.80E+07	-0.59	
NWMN_1435	1.16E+07	2.78E+06	7.66E+06	6.15E+06	-0.60	
NWMN_1300	1.10E+07	1.22E+06	7.18E+06	3.24E+06	-0.62	
NWMN_0687	6.47E+09	2.56E+09	4.21E+09	8.73E+08	-0.62	
NWMN_0218	4.74E+07	1.49E+07	3.03E+07	2.01E+07	-0.65	
NWMN_1712	4.05E+06	5.09E+05	2.51E+06	1.22E+06	-0.69	
NWMN_0705	1.80E+07	3.52E+06	1.10E+07	3.60E+06	-0.71	
NWMN_2569	1.72E+09	2.26E+08	1.04E+09	1.89E+08	-0.72	+
NWMN_0612	4.52E+06	8.95E+05	2.69E+06	1.09E+06	-0.75	
NWMN_1718	2.58E+08	8.59E+07	1.53E+08	4.90E+07	-0.76	
NWMN_1091	1.59E+07	1.44E+06	9.35E+06	2.03E+06	-0.76	+
NWMN_0601	6.15E+06	1.17E+06	3.62E+06	1.65E+06	-0.76	
NWMN_0473	2.57E+07	7.62E+06	1.51E+07	8.07E+06	-0.77	
NWMN_0482	1.57E+07	3.12E+06	8.91E+06	7.79E+06	-0.82	
NWMN_0481	1.49E+06	2.90E+05	8.39E+05	9.32E+05	-0.82	
NWMN_2542	3.89E+07	4.95E+06	2.20E+07	9.11E+06	-0.82	
NWMN_1274	2.93E+07	2.75E+06	1.65E+07	9.02E+06	-0.83	
NWMN_1847	4.96E+07	5.40E+05	2.77E+07	1.08E+07	-0.84	
NWMN_2320	6.89E+08	2.42E+08	3.81E+08	7.23E+07	-0.86	
NWMN_0917	3.43E+08	8.51E+07	1.86E+08	7.25E+07	-0.88	
NWMN_0922	2.29E+09	2.59E+08	1.23E+09	3.67E+08	-0.89	
NWMN_1398	1.69E+06	1.06E+06	9.07E+05	5.20E+05	-0.90	
NWMN_0525	1.18E+09	4.44E+08	6.24E+08	1.82E+08	-0.92	
NWMN_0173	2.47E+07	7.48E+06	1.28E+07	3.83E+06	-0.95	
NWMN_2466	2.83E+07	1.03E+07	1.46E+07	5.34E+06	-0.95	
NWMN_0019	1.16E+06	2.50E+05	5.94E+05	2.17E+05	-0.96	
NWMN_0756	2.72E+08	7.13E+07	1.39E+08	8.78E+07	-0.96	

NWMN_2543	2.03E+09	6.23E+08	1.01E+09	2.69E+08	-1.01	
NWMN_0925	4.66E+08	1.43E+08	2.29E+08	6.62E+07	-1.02	
NWMN_1719	2.79E+08	6.41E+07	1.37E+08	8.65E+07	-1.03	
NWMN_0087	9.15E+07	3.63E+07	4.46E+07	1.20E+07	-1.03	
NWMN_0958	2.25E+07	3.44E+06	1.09E+07	4.43E+06	-1.04	
NWMN_1455	5.61E+08	7.67E+07	2.71E+08	4.92E+07	-1.05	+
NWMN_1999	1.34E+08	2.78E+07	6.47E+07	1.28E+07	-1.05	+
NWMN_1043	9.06E+06	1.30E+06	4.35E+06	2.01E+06	-1.06	
NWMN_1927	1.18E+09	3.06E+08	5.52E+08	1.98E+08	-1.10	
NWMN_2063	3.24E+07	7.20E+06	1.50E+07	7.37E+06	-1.11	
NWMN_1361	5.90E+07	1.07E+07	2.71E+07	6.95E+06	-1.12	+
NWMN_1624	8.00E+05	7.37E+04	3.63E+05	1.30E+05	-1.14	+
NWMN_1551	5.75E+08	4.15E+07	2.54E+08	1.24E+08	-1.18	
NWMN_0861	1.24E+06	8.81E+05	5.48E+05	4.02E+05	-1.18	
NWMN_0760	8.41E+08	5.74E+07	3.57E+08	1.36E+08	-1.24	+
NWMN_0249	2.14E+07	5.69E+06	8.98E+06	8.21E+06	-1.25	
NWMN_1704	4.09E+06	6.86E+05	1.69E+06	8.23E+05	-1.27	
NWMN_1841	5.18E+07	1.88E+07	2.14E+07	6.68E+06	-1.27	
NWMN_0634	1.15E+09	2.77E+08	4.70E+08	1.86E+08	-1.29	
NWMN_1980	1.45E+06	6.59E+05	5.92E+05	5.83E+05	-1.29	
NWMN_1066	3.55E+06	4.89E+05	1.44E+06	1.24E+06	-1.30	
NWMN_1632	8.54E+07	1.89E+07	3.46E+07	2.50E+07	-1.30	
NWMN_0412	5.94E+07	1.13E+07	2.40E+07	7.40E+06	-1.30	+
NWMN_1928	2.39E+09	1.81E+08	9.63E+08	4.72E+08	-1.31	
NWMN_2537	9.51E+05	2.73E+05	3.76E+05	3.62E+05	-1.34	
NWMN_2162	1.64E+07	3.04E+06	6.27E+06	2.30E+06	-1.39	+
NWMN_2207	1.92E+06	2.01E+05	7.31E+05	3.97E+05	-1.39	
NWMN_1883	4.06E+08	6.59E+07	1.54E+08	9.60E+07	-1.40	
NWMN_2283	5.57E+06	1.31E+06	2.10E+06	1.52E+06	-1.40	
NWMN_0836	8.36E+07	2.79E+06	3.15E+07	2.08E+07	-1.41	
NWMN_0401	9.34E+06	2.51E+06	3.52E+06	2.07E+06	-1.41	
NWMN_2529	5.60E+07	6.56E+06	2.10E+07	4.19E+06	-1.42	+
NWMN_0851	2.92E+08	9.87E+07	1.08E+08	5.46E+07	-1.43	
NWMN_2395	3.34E+06	5.34E+05	1.22E+06	4.70E+05	-1.45	+
NWMN_1332	7.24E+07	1.15E+07	2.65E+07	1.03E+07	-1.45	+
NWMN_1123	2.65E+06	7.72E+05	9.62E+05	5.58E+05	-1.46	
NWMN_0429	2.78E+08	7.33E+07	1.00E+08	3.20E+07	-1.47	+
NWMN_2526	2.00E+07	6.53E+06	7.17E+06	3.03E+06	-1.48	+
NWMN_0306	2.80E+06	5.86E+05	1.00E+06	4.16E+05	-1.48	+
NWMN_2319	4.87E+08	1.12E+08	1.74E+08	7.86E+07	-1.48	+
NWMN_2199	2.34E+09	5.54E+08	8.37E+08	3.02E+08	-1.48	+
NWMN_1705	8.96E+07	2.14E+07	3.17E+07	1.06E+07	-1.50	+
NWMN_1041	2.38E+08	4.34E+07	8.28E+07	2.31E+07	-1.53	+
NWMN_1040	2.76E+06	3.90E+05	9.53E+05	2.21E+05	-1.54	+
NWMN_1645	2.77E+08	3.89E+07	9.47E+07	7.92E+07	-1.55	
NWMN_1872	7.61E+09	8.28E+08	2.54E+09	9.11E+08	-1.58	+

NWMN_1706	2.19E+07	2.07E+06	7.25E+06	1.83E+06	-1.60	+
NWMN_1703	2.31E+06	3.69E+05	7.59E+05	3.56E+05	-1.61	+
NWMN_2061	1.43E+06	1.20E+06	4.67E+05	1.28E+05	-1.61	
NWMN_0782	3.59E+09	7.25E+08	1.17E+09	4.16E+08	-1.62	+
NWMN_2078	1.26E+08	2.73E+07	4.11E+07	1.83E+07	-1.62	+
NWMN_0428	2.62E+07	5.20E+06	8.49E+06	3.61E+06	-1.62	+
NWMN_0396	3.92E+07	4.69E+06	1.26E+07	5.65E+06	-1.64	+
NWMN_2469	9.57E+09	2.18E+09	3.05E+09	1.71E+09	-1.65	+
NWMN_1750	1.37E+07	1.30E+06	4.35E+06	1.64E+06	-1.66	+
NWMN_1621	2.62E+07	8.23E+06	8.30E+06	4.31E+06	-1.66	
NWMN_0020	3.24E+06	3.07E+05	1.01E+06	5.45E+05	-1.67	
NWMN_1069	1.24E+09	6.14E+08	3.88E+08	1.20E+08	-1.68	
NWMN_2211	2.10E+08	6.05E+07	6.53E+07	1.68E+07	-1.69	+
NWMN_2092	6.73E+07	1.15E+07	2.08E+07	6.13E+06	-1.69	+
NWMN_0022	2.03E+08	3.28E+07	6.12E+07	1.17E+07	-1.73	+
NWMN_1076	5.09E+08	5.89E+07	1.53E+08	6.26E+07	-1.73	+
NWMN_0391	1.10E+08	2.79E+07	3.30E+07	1.32E+07	-1.73	+
NWMN_1880	1.57E+07	8.18E+06	4.66E+06	1.72E+06	-1.75	
NWMN_0362	7.66E+08	4.26E+08	2.27E+08	1.37E+08	-1.75	
NWMN_1019	5.25E+06	1.50E+06	1.56E+06	1.34E+06	-1.75	
NWMN_2317	2.64E+09	3.70E+08	7.65E+08	2.97E+08	-1.79	+
NWMN_1702	1.28E+07	1.25E+06	3.53E+06	2.48E+06	-1.86	+
NWMN_0394	8.97E+07	1.54E+07	2.47E+07	1.18E+07	-1.86	+
NWMN_2426	1.83E+07	1.39E+06	4.93E+06	2.36E+06	-1.89	+
NWMN_2318	2.23E+09	7.10E+08	6.01E+08	1.90E+08	-1.89	+
NWMN_0830	2.89E+08	5.26E+07	7.75E+07	3.24E+07	-1.90	+
NWMN_0677	4.94E+09	1.41E+09	1.31E+09	7.79E+08	-1.91	+
NWMN_0262	4.03E+08	9.98E+07	1.06E+08	8.83E+06	-1.93	+
NWMN_2109	3.64E+08	1.67E+08	9.49E+07	3.11E+07	-1.94	+
NWMN_2179	2.34E+07	1.53E+06	6.07E+06	1.50E+06	-1.94	+
NWMN_2313	1.47E+08	1.78E+07	3.81E+07	1.02E+07	-1.95	+
NWMN_2306	7.21E+07	1.35E+07	1.87E+07	7.91E+06	-1.95	+
NWMN_2364	1.21E+07	2.76E+06	3.02E+06	7.49E+05	-2.00	+
NWMN_1667	1.96E+06	2.47E+05	4.90E+05	3.80E+05	-2.00	+
NWMN_0860	3.85E+06	4.68E+05	9.49E+05	2.96E+05	-2.02	+
NWMN_0930	4.77E+06	1.90E+06	1.17E+06	6.74E+05	-2.02	
NWMN_1539	1.73E+06	8.38E+05	4.25E+05	3.69E+05	-2.03	
NWMN_2270	3.41E+08	5.59E+07	8.31E+07	1.99E+07	-2.04	+
NWMN_1236	8.60E+05	4.22E+05	2.08E+05	2.00E+05	-2.05	
NWMN_0585	1.26E+09	3.49E+08	3.04E+08	1.09E+08	-2.06	+
NWMN_2257	4.90E+06	1.62E+06	1.17E+06	3.21E+05	-2.06	+
NWMN_0220	5.16E+06	7.70E+05	1.23E+06	2.44E+05	-2.07	+
NWMN_0059	8.38E+06	1.81E+06	1.99E+06	1.12E+06	-2.08	
NWMN_1090	7.57E+05	1.49E+05	1.77E+05	1.92E+05	-2.10	
NWMN_0709	1.53E+06	1.93E+05	3.53E+05	3.29E+05	-2.11	
NWMN_1077	6.39E+08	4.97E+07	1.42E+08	5.57E+07	-2.17	+

NWMN_0006	2.87E+07	2.14E+06	6.35E+06	1.69E+06	-2.18	+
NWMN_2308	3.18E+06	9.52E+05	7.00E+05	4.74E+05	-2.19	+
NWMN_2088	5.07E+06	7.10E+05	1.11E+06	8.92E+05	-2.20	+
NWMN_0646	1.57E+06	1.59E+05	3.42E+05	2.72E+05	-2.20	+
NWMN_1033	3.24E+06	4.06E+05	7.03E+05	2.86E+05	-2.20	+
NWMN_1877	6.77E+08	4.23E+07	1.45E+08	1.14E+08	-2.22	+
NWMN_2467	5.16E+07	7.84E+06	1.07E+07	4.22E+06	-2.27	+
NWMN_2392	1.15E+07	2.17E+06	2.32E+06	1.00E+06	-2.31	+
NWMN_1073	7.41E+08	2.16E+08	1.49E+08	6.58E+07	-2.32	+
NWMN_0395	4.73E+07	5.42E+06	9.41E+06	3.84E+06	-2.33	+
NWMN_0388	1.64E+08	3.82E+07	3.25E+07	1.75E+07	-2.33	+
NWMN_0397	2.60E+06	1.33E+06	5.14E+05	2.62E+05	-2.34	
NWMN_2185	3.15E+08	6.29E+07	6.20E+07	1.58E+07	-2.35	+
NWMN_0400	2.09E+07	5.39E+06	4.07E+06	3.25E+06	-2.36	
NWMN_0758	3.62E+09	7.94E+08	6.94E+08	2.17E+08	-2.38	+
NWMN_0389	7.57E+07	3.70E+06	1.45E+07	7.85E+06	-2.39	+
NWMN_1075	6.75E+07	5.52E+06	1.28E+07	7.14E+06	-2.40	+
NWMN_1708	1.69E+08	6.02E+07	3.10E+07	1.77E+07	-2.45	+
NWMN_0969	6.84E+06	2.09E+06	1.20E+06	6.28E+05	-2.51	+
NWMN_1631	6.69E+07	2.45E+07	1.16E+07	3.26E+06	-2.52	+
NWMN_0166	2.84E+09	3.09E+08	4.76E+08	1.61E+08	-2.58	+
NWMN_0764	2.44E+06	1.43E+06	3.95E+05	2.80E+05	-2.63	
NWMN_0041	1.85E+07	5.30E+06	2.93E+06	1.71E+06	-2.66	+
NWMN_1037	6.05E+06	1.69E+06	9.31E+05	4.14E+05	-2.70	+
NWMN_1730	1.50E+07	4.30E+06	2.28E+06	6.58E+05	-2.71	+
NWMN_1733	1.49E+08	3.20E+07	2.23E+07	5.36E+06	-2.74	+
NWMN_1876	6.21E+08	1.56E+08	9.17E+07	2.31E+07	-2.76	+
NWMN_0759	5.85E+07	9.90E+06	7.42E+06	4.52E+06	-2.98	+
NWMN_0581	1.68E+07	3.98E+06	2.09E+06	9.35E+05	-3.00	+
NWMN_0931	5.79E+07	1.62E+07	7.14E+06	1.69E+06	-3.02	+
NWMN_1020	3.87E+07	1.10E+07	4.66E+06	8.85E+05	-3.05	+
NWMN_0402	3.40E+06	3.52E+06	4.08E+05	6.67E+04	-3.06	+
NWMN_1021	4.51E+06	9.50E+05	5.26E+05	1.44E+05	-3.10	+
NWMN_0393	1.23E+08	2.84E+07	1.38E+07	5.89E+06	-3.15	+
NWMN_0055	6.59E+06	1.50E+06	6.39E+05	1.71E+05	-3.37	+
NWMN_1552	1.19E+07	2.96E+06	1.11E+06	2.34E+05	-3.42	+
NWMN_1042	1.73E+07	2.07E+06	1.54E+06	4.16E+05	-3.49	+
NWMN_1067	1.29E+08	4.01E+07	1.05E+07	4.40E+06	-3.63	+
NWMN_1070	5.08E+06	9.32E+05	3.06E+05	1.58E+05	-4.05	+
NWMN_2345	9.45E+06	2.77E+06	4.31E+05	2.20E+05	-4.45	+
NWMN_1820	5.41E+06	3.33E+06	1.78E+05	1.84E+05	-4.93	+
NWMN_0757	1.01E+08	2.16E+07	3.06E+06	1.22E+06	-5.05	+
NWMN_0665	5.45E+07	1.47E+07	1.34E+06	6.77E+05	-5.34	+